

ANALYSIS OF THE ROLE OF LIPIDS IN RETROVIRUS TRANSDUCTION

A Dissertation
Presented to
The Academic Faculty

By

Nimisha Gupta Mukherjee

In Partial Fulfillment
Of the Requirements for the Degree
Doctor of Philosophy in Biomedical Engineering

Georgia Institute of Technology

DECEMBER 2008

ANALYSIS OF THE ROLE OF LIPIDS IN RETROVIRUS TRANSDUCTION

Approved by:

Dr. Joseph M. Le Doux, Advisor
Department of Biomedical Engineering
*Georgia Institute of Technology and Emory
University*

Dr. Mark R. Prausnitz
Department of Chemical Engineering
Georgia Institute of Technology

Dr. Ravi V. Bellamkonda
Department of Biomedical Engineering
*Georgia Institute of Technology and Emory
University*

Dr. Trent Spencer
Department of Pediatrics
Emory University, School of Medicine

Dr. Andrew L. Lyon
Department of Chemistry and Biochemistry
Georgia Institute of Technology

Date Approved: October 20 2008

To my wonderful family:

Mom, Dad and my brother, Abhishek

For my loving husband, Neil

ACKNOWLEDGMENTS

During my time at Georgia Tech, I have had the opportunity to interact with some very talented people. One such person has been my advisor, Joe Le Doux. From the time I stepped into his lab, he has guided me and encouraged me to think independently. Over the past few years, he has taught me how to critically analyze my data and present it accurately. In the process, I have had the chance to see the dedication and commitment Joe has to science and research, and I was and always will be motivated by him. Working with Joe has taught me that research can be a creative process and it is never as 'straight-forward' as you think it is!

I would also like to thank my committee members, Dr. Bellamkonda, Dr. Prausnitz, Dr. Spencer and Dr. Lyon. They have taken a personal interest in many different components of my research and I thank you for your guidance and support. I would also like to thank IBB staff: Allen, Tracie, Chris R., Steve W., for always being kind and generous with their time and helping me especially this past year.

Over the years, I have had the chance to interact with many wonderful people, and they really have made my experience at Georgia Tech unforgettable. I could not have had a better group of lab mates to learn and laugh with on many occasions: Natalia, Delfi, Jamie and Cindy. Thank you Natalia for being so kind, Delfi for your audible laughter, Jamie for always being there and Cindy for being my 'work spouse' (Nindy). Hours of FCS and confocal microscopy and battle for the lab temperature control could not have been accomplished (or won) without you. I have learned so much from all of you and something tells me that the good times are not over yet!

Research is a dynamic process, and I would like to thank some very important people for helping me enjoy life when times were good and also when times got tough. I would like to thank Sarah, Richard, Marcus, Maxine, Heather P., Gustavo, John, Mary, C-Dub, Hillary, Allison, Jesse, Andrea, Brian, Jeff, Diane, Stacey, Adam, Heather B. and

George. Thank you for being such wonderful friends and I hope we find many excuses to see each other – MLK weekend style! You all have been an integral part of my life and I am so thankful to have built life long friendships with you.

Last but not least, I would like to thank my family. I really can't put into words what they mean to me or the magnitude of their contribution, but I will try. Their unwavering love and support was the foundation that allowed me to pursue my goals and follow my dreams. I have turned to them in my times of need, whatever it may be, and they have always patiently listened and supported me. My Father is my inspiration. He has not only encouraged me to pursue my goals in life but also set an example and showed me that the path is never easy. My Mom is my greatest guide and I could not have come this far in life without her love and support (and her care packages that were many a time sent to the package cage!). Abhishek, thank you for being my number #1 cheerleader. You continually amaze me with your hard work and dedication and, I sometimes forget who is older and wiser! Also, thank you for filling my life with unforgettable memories, especially ones surrounding a particular quesadilla maker and mom's growth-stunted cactus plant. I am thankful to my new family, the Mukherjees who have been a constant source of love and support. They have shared in all my victories (big and small) and have supported me throughout the years.

Finally, I would like to thank my husband, Neil. He has been my anchor, my best-friend and I could not have done any of this without him. He has made me laugh in my most serious times and I can't thank him enough for always believing in me. I am one lucky girl to have him in my life!

TABLE OF CONTENTS

LIST OF TABLES	VIII
LIST OF FIGURES	IX
SUMMARY	XII
CHAPTER 1: BACKGROUND AND OBJECTIVES	1
1.1 Gene Therapy	1
1.2 Recombinant Retroviruses as Gene Delivery Vectors	2
1.3 Retrovirus Production.....	4
1.4 Retrovirus Infection	6
1.5 Insertional Mutagenesis Concerns in Retrovirus and Lentivirus Vectors	7
1.6 Lipid Composition of Virus Particles.....	10
1.7 Approaches to Retrovirus Targeting	12
1.8 Thesis Objectives.....	18
1.9 Organization of the Thesis	19
1.10 Outcomes and Contributions.....	20
1.11 References.....	21
CHAPTER 2: RAPID MODIFICATION OF BIOLOGICAL NANOPARTICLES USING LIPID CONJUGATES.....	28
2.1 Abstract.....	28
2.2 Introduction	28
2.3 Materials and methods.....	31
2.4 Results	37
2.5 Discussion.....	48
2.6 References.....	51
CHAPTER 3: ALTERATION OF VIRAL LIPID COMPOSITION BY MYRIOCIN REDUCES RETROVIRUS INFECTIVITY	55
3.1 Abstract.....	55
3.2 Introduction	55
3.3 Materials and methods.....	57
3.4 Results	65
3.5 Discussion.....	92
3.6 References.....	96

CHAPTER 4: ALTERATION OF VIRAL COMPOSITION BY FUMONISIN B-1 INCREASES RETROVIRAL INFECTIVITY AND REDUCES VIRUS BUDDING	98
4.1 Abstract.....	98
4.2 Introduction	98
4.3 Materials and methods.....	100
4.4 Results	108
4.5 Discussion.....	132
4.6 References.....	135
 CHAPTER 5: CONCLUSIONS AND FUTURE RESEARCH	137
5.1 Summary of Results.....	137
5.2 Conclusions.....	138
5.3 Future Considerations.....	139
 APPENDIX.....	145
A.1 Experimental Protocol: Development of Biotin ELISA assay	145
A.2 Radius of Gyration Approximation using Asymmetrical Field-Flow Fractionation..	146
B.1 Technological Innovation: Generating Economic Results (TI:GER)	148

LIST OF TABLES

TABLE

1.1 Key Features of Recombinant Retroviruses and Lentiviruses	5
1.2 Strategies for Targeting Retroviruses	17

LIST OF FIGURES

FIGURE

CHAPTER 1

1.1 Production of recombinant retroviruses	8
1.2 Transduction of target cells by recombinant retroviruses.....	9
1.3 Fusion between virus and cell lipid membrane	13
1.4 Lipid raft composition in cell lipid bilayer	15

CHAPTER 2

2.1 Structure of DSPE-PEG-biotin	38
2.2 (A) The DSPE-PEG-biotin lipid conjugate co-purifies with retroviruses.	39
2.2 (B) The DSPE-PEG-biotin lipid conjugate co-purifies with retroviruses.	40
2.3 (A-D) The DSPE-PEG-biotin lipid conjugate co-localizes with lentiviruses	42
2.3 (E) Modified virus particles co-localize with streptavidin.	43
2.4 Lipid conjugates rapidly associate with retroviruses	44
2.5 Lipid conjugates stably associate with retroviruses	45
2.6 Retroviruses modified with the DSPE-PEG-biotin lipid conjugate bind to streptavidin-coated plates	47

CHAPTER 3

3.1 The pathway of <i>de novo</i> sphingolipid biosynthesis and sites of action of myriocin, a serine palmitoyl-transferase inhibitor	66
3.2 (A) Mass spectroscopy analysis of ceramide present in virus producer cells	67
3.2 (B) Mass spectroscopy analysis of glucosylsphingolipid present in virus producer cells	68
3.2 (C) Mass spectroscopy analysis of sphingomyelin present in virus producer cells..	69
3.2 (D) Mass spectroscopy analysis of ceramide present in virus particles.....	70
3.2 (E) Mass spectroscopy analysis of glucosylsphingolipid present in virus particles..	71
3.2 (F) Mass spectroscopy analysis of sphingomyelin present in virus particles	72
3.3 (A) Myriocin treatment does not affect virus production.....	74
3.3 (B) Treatment of virus producer cells with ISP-1 decreases the titer of the virus produced from those cells	75
3.4 Effect of ISP-1 treatment on cell viability.....	76

3.5 (A) Myriocin treatment does not affect amount of gp70 incorporation into virus particles.....	78
3.5 (B) Myriocin treatment of virus producer cells does not affect structure of gp70 incorporated into virus particles	79
3.6 (A) Treating virus producer cells with ISP-1 does not decrease the amount of gp70 incorporated into the virus particles.	80
3.6 (B) Treating virus producer cells with ISP-1 does not decrease the amount of gp70 incorporated into the virus particles	81
3.7 Stability of virus particles is not affected by myriocin treatment	82
3.8 Binding of myriocin treated virus to target cells is not adversely affected	84
3.9 Virus particles produced by ISP-1 treated cells fuses less efficiently to target cells membrane	85
3.10 (A) Mass spectroscopy analysis of ceramide present in target cell membrane before and after myriocin treatment	86
3.10 (B) Mass spectroscopy analysis of glucosylceramide present in target cell membrane before and after myriocin treatment	87
3.10 (C) Mass spectroscopy analysis of sphingomyelin present in target cell membrane before and after myriocin treatment	88
3.11 (A) Treatment of NIH 3T3 cells with ISP-1 decreases virus infection.....	90
3.11 (B) Treatment of HeLa cells with ISP-1 decreases virus infection	91

CHAPTER 4

4.1 The pathway of <i>de novo</i> sphingolipid biosynthesis and sites of action of FB-1	109
4.2 (A) Mass spectroscopy analysis of ceramide present in virus producer cells	110
4.2 (B) Mass spectroscopy analysis of glucosylceramide present in virus producer cells	111
4.2 (C) Mass spectroscopy analysis of sphingomyelin present in virus producer cells	112
4.2 (D) Mass spectroscopy analysis of ceramide present in virus particles.....	113
4.2 (E) Mass spectroscopy analysis of glucosylceramide present in virus particles ...	114
4.2 (F) Mass spectroscopy analysis of sphingomyelin present in virus particles	115
4.3 Effect of varying doses of FB-1 treatment on cell viability	117
4.4 (A) Fumonisin treatment affects virus production.....	118
4.4 (B) Effect of fumonisin treatment on gp70 production.....	119
4.4 (C) Amount of gp70 proteins per p30 virus capsid protein.....	120
4.5 Fumonisin treatment affects the ability of virus to bud from target cell membranes	121

4.6 (A) Effect on virus production and infection after treating virus producer cells with FB-1	123
4.6 (B) Treatment of virus producer cells with FB-1 increases the titer of the virus produced from those cells	124
4.7 Stability of virus particles is not affected by fumonisin treatment	125
4.8 (A) Binding of virus particles to NIH 3T3 cells is not saturated at high concentrations of virus	126
4.8 (B) Binding of virus particles produced from myriocin treated virus producer cells is not adversely affected	128
4.9 Virus particles produced by FB-1 treated cells fuse more efficiently with target cells ..	129
4.10 (A) Effect of virus infection after FB-1 treatment of NIH 3T3 cells	130
4.10 (B) Effect of virus infection after FB-1 treatment of HeLa cells	131

SUMMARY

The most common gene transfer vehicle used in gene therapy protocols are mammalian virus vectors. Specifically, retroviruses are one of the most common viral vectors used since they are able to permanently integrate their transgene into the host cell genome, providing, in principal, to a long-term cure. The potential applications of gene therapies are vast, ranging from monogenic disorders such as cystic fibrosis to complex gene disorders such as cancer. However, the application of such therapies in clinical settings has been limited partially because of inefficient gene delivery of the therapeutic gene to diseased cells. Furthermore, safety concerns of accidentally altering the genetic expression in healthy bystander cells or nearby tissue has increased the interest in creating targeted viral vectors which infect only the diseased cells without infecting others. Thus, the success of gene therapy will depend on identifying and understanding the parameters critical for virus entry into cells, including factors that facilitate virus absorption onto the cell surface, virus binding, and fusion. The objective of this thesis was to understand the role of lipids in binding and infection, and to investigate the use of lipid-based conjugates to alter the surface of virus particles.

In this thesis, we described a novel method for modifying the surfaces of retrovirus particles using lipid conjugates. We developed a method for rapidly modifying the surface properties of retroviruses using conjugates that are composed of a hydrophobic lipid anchor, 1,2-Distearoyl-*sn*-Glycero-3-phosphoethanolamine (DSPE), attached to a polymer linker, poly (ethylene glycol) chain which is covalently attached to the targeting functional group, biotin. These constructs, when mixed with a virus stock, rapidly associate with the virus surface. We used model replication-incompetent amphotropic retroviruses that encoded *lacZ* gene to investigate the characteristics of

lipid conjugate modification containing biotin as a model cell-targeting group. We found that in less than 2 hours, the number of constructs that were associated with the particles reached a maximum. Even though the lipid conjugates were not covalently bound to the viruses, less than 30% dissociated from the viruses after 8 hours of incubation at 37^o C in medium that contained 10% serum. Viruses modified with biotin conjugates bound to streptavidin-coated plates three-fold more than unmodified viruses. Importantly, virus titer experiments showed that the conjugates did not reduce the ability of the viruses to transduce cells. The implication of this work for improving the characteristics of retroviruses in gene therapy and vaccination protocols is discussed.

In chapter 3 we investigated the use of fungal endotoxin, myriocin (ISP-1) to inhibit *de novo* sphingolipid synthesis in virus producer cells. We investigated the effect on the lipid composition of the virus producing cells as well as the virus produced after treatment. Sphingolipids have been implicated in a variety of pathogens to help facilitate the entry process. Here we studied the effect of altering the lipid composition of virus particles on virus function. Our results suggest that the virus lipid composition can be significantly altered by treating cells with ISP-1 and that these particles exhibit reduced infectivity in a cell-type dependant manner. Furthermore, the lipids of enveloped viruses play an important role in virus viral morphogenesis and infectivity, therefore we investigated different steps involved in the virus infection pathway and found that virus particles produced from ISP-1 treated cells are less fusogenic as compared to untreated cells. The implications of these results to improve gene therapy vectors and anti-retroviral therapies are discussed.

In chapter 4 we determined the effect of blocking sphingolipid synthesis by using fumonisin B-1 (FB-1) of virus producing cells and examined the effect on virus function.

We found culturing virus producer cells in the presence of FB-1 causes drastic decrease in the levels of ceramide, sphingomyelin and glucosyphingolipids. Viruses produced with 50 μ M FB-1 treatment were observed to be as stable as, and bind to the same extent as viruses produced from untreated cells. Interestingly, virus from FB-1 treatment was 4 to 6-fold more infectious at doses of 100 μ M than controls virus particles. Interestingly, we found that FB-1 treatment interferes with virus budding and release from virus producing cells.

CHAPTER 1

BACKGROUND AND OBJECTIVES

1.1 Gene Therapy

Gene therapy is an important approach to the treatment of diseases, which involves the delivery of genetic material into cells to produce a therapeutic effect. Initial efforts in the 1970's and 1980's in developing recombinant DNA technologies were aimed at treating monogenic disorders, where a 'normal' gene was inserted into diseased cells to replace an 'abnormal' gene (17). Since this time gene therapy has been expanded to a broad range of applications to include complex acquired genetic disorders such as cancer, infectious diseases such as human immunodeficiency virus (HIV) and has many applications in tissue and stem cell engineering (1, 2, 11, 12, 17). Currently almost 70% of the gene therapy clinical trials use viral vectors, in the hopes of exploiting the ability of viruses to efficiently infect and express their transgene in host cells (2, 22, 79). Non-viral gene delivery methods, such as those involving delivery of plasmid DNA by mechanical or electrical stimulation or by complexing with charged polymers, are currently limited by low gene transfer efficiencies (61, 82). Building on the advantage that viruses have had millions of years to evolve their ability to efficiently bind, fuse and infect cells, most research efforts have focused on identifying and overcoming major limitations with retroviral vectors.

Gene therapy can be clinically applied in two settings: *ex vivo* or *in vivo*. In *ex vivo* gene therapy, cells are harvested from the patient, expanded outside of the body, genetically modified using a gene-delivery vector, then cells are cultured under selective pressure to obtain only the cells with the gene modification and finally, the cells are implanted back into the patient to elicit the desired therapeutic effect (2, 17). Although

in this setting gene delivery occurs under controlled conditions and the vector can be targeted and optimized for gene transfer, this method is not always feasible. Frequently, *ex vivo* gene therapy is not possible because the diseased cells/tissues cannot be excised from the patient, such as in diseases afflicting the heart, lungs or brain. In these cases, *in vivo* gene therapy is used and the gene-delivery vector carrying the therapeutic gene is directly injected into the patient's body (47, 84, 89). For this method to be effective however, the viral vector should be specifically targeted to the cells of interest such that it does not genetically alter nearby healthy cells. Clinical trials have highlighted some limitations with viral gene therapies and one main limitation has been the lack of transductional targeting, that is, the efficient delivery of genes to a desired cell type, without harming nearby bystander cells (3, 29, 79). In either setting used for gene therapy, a targeted gene delivery vector would be advantageous because it would reduce the need to select and expand the targeted cell type in *ex vivo* protocols and provide a more suitable delivery vector for *in vivo* gene therapy.

To date there more than 1,000 gene therapy clinical trials have been completed, and one of the main obstacles has been the inability to control the retroviral tropism; that is, the types of cells that retroviruses can and cannot, transduce (37, 43, 87). In certain applications, virus tropism needs to be narrowed in order to deliver genes to only diseased cells without damaging surrounding tissue such as in the case of delivering apoptotic genes to cancer cells (2). In other applications, such as for cystic fibrosis, the retroviral tropism may need to be broadened such that the retroviruses can transduce the lung epithelial cells (14, 29).

1.2 Recombinant Retroviruses as Gene Delivery Vectors

Retroviruses are the most common viral vector used for gene therapy protocols because they can permanently integrate a therapeutic gene into the DNA of target cells,

resulting theoretically in a long-term cure (2, 16). Specifically, Moloney murine leukemia viruses (MLV) are the class of retroviruses most often used for human gene transfer (43). These retroviruses consist of two copies of genomic RNA packaged in a protein capsid, which is surrounded by a lipid bilayer composed of virus and host cell proteins and lipids (Table 1.1). This lipid envelope contains polypeptide chains including receptor binding proteins (i.e. envelope proteins) which interact with cell specific receptors and initiate the process of fusion and hence, infection. The recombinant viral particles are structurally identical to the wild type virus but carry a genetically engineered genome that encodes for the therapeutic gene of interest. These recombinant viruses are incapable of self-replication but can infect and insert their genomes into the cellular genome of a target cell (2).

Recombinant retroviruses can be manipulated altered in a number of ways. For instance, wild type MLV virus particles consist of ecotropic envelope proteins that bind to the mouse cationic amino acid transporter -1 (mCAT-1) (28, 66). Since this receptor is only found on rodent cells, infection of ecotropic MLV can only infect murine cells. To make this vector clinically relevant for human cell lines, a different envelope protein is expressed in virus producing cells, in a process called pseudotyping (32, 38). Amphotropic retroviruses are of primary interest in human gene therapy protocols because they can infect human cells. These proteins interact with cell surface receptors, sodium-dependant phosphate transporter protein (pit2), found on many different types of human cells (28). Furthermore, lentivirus vectors are a subclass of retroviruses and have been pseudotyped with different envelope proteins for a wide range of applications (36, 78). Lentiviruses are an interesting vector type also because they have an added benefit in that they can infect and integrate their genome into non-dividing cells (Table 1.1) (8, 19, 32, 78). In contrast to retroviruses, which can only infect dividing cells,

lentivirus vectors can be used for a broad range of applications to treat cells that have slow rates of division.

1.3 Retrovirus Production

Recombinant retroviruses are similar to the wild-type virus from which they were derived, however they are engineered to encode therapeutic genes or other genes of interest, and do not contain viral genes necessary for replication (2, 48). For the production of recombinant retroviruses, packaging cell lines are transfected with more than one plasmid encoding for viral proteins (*gag*, *pol*, *env*) and the therapeutic gene (Figure 1.1) (2, 51). *Gag* encodes the capsid proteins and is necessary for encapsidation of the viral particle. *Pol* encodes the enzymatic activities of the virus including reverse transcriptase. *Env* encodes the surface proteins that bind to cell surface receptors on the target cell. Many times cell lines are stably transfected with the viral genes to create derivative cell lines that permanently produce virus particles in their cell culture medium. For instance, for the studies conducted in this dissertation, we used a stably transfected cell line called Telceb6, derived from stable transfection of TE671 cells (neuron-derived medulloblastoma human line) with the E.coli lacZ gene (without a nuclear localization sequence), MLV *gag* and *pol* genes and the amphotropic envelope glycoprotein (15, 45).

Transfection with these plasmids provides the packaging cell line with the genetic information needed to express all the structural viral genes necessary to form an infectious virus particle. The therapeutic vector encodes the transgene(s) and the regulatory sequences necessary for their expression as well as a special packaging sequence (ψ) which is required for encapsidation of the genome into an infectious viral particle (51). The structural proteins of the virus and the RNA genome self-assemble inside the transfected cell and bud from the plasma membrane of the cell into the culture

Table 1.1 Key Features of Recombinant Retroviruses and Lentivirus

Feature	Units	Retrovirus	Lentivirus	Reference
Particle Diameter	nm	90-147	110-128	(21, 68)
Mass	g	3.6×10^{-16}	3.15×10^{-16}	(30, 74)
Genome size	kb	8.3	9.2	(50, 74)
Typical titers	(units/mL)	10^8	10^6	(39, 54)
Shape of capsid		Hexamer	Conical	(6, 49)
Chromosomal integration		Yes	Yes	(36, 79)
Infects quiescent cells		No	Yes	(32)
Risk by activation of oncogene		++	+	(3, 39, 65)
Composition				
RNA	%	2		(67)
Protein	%	62		(67)
Lipid	%	36		(67)

HIV-1 Lipid Composition (7)

Lipid molecule	Molecules per average RV particle	% mol
Phosphatidylcholine	26,000	9.0
Sphingomyelin	37,000	13.0
Dyhydro sphingomyelin	17,000	5.9
Phosphatidylethanolamine	13,000	4.5
Plasmogen Phosphatidylethanolamine	44,000	15.3
Phosphatidylserine	25,000	8.7
Cholesterol	134,000	46.7
Ceramide	160	0.05
Glucosylceramide	600	0.21

media. The conditioned medium, which contains infectious recombinant viruses, is harvested and used to transduce target cells.

1.4 Retrovirus Infection

A retrovirus must complete several steps for the therapeutic gene to be successfully inserted into the genome of a target cell. First the virus must reach the cell surface by convection or diffusion where it attaches to components of the glycocalyx on the target cell surface (24). Initially, the virus binds to the cell surface through nonspecific interactions between the proteins on the cell surface and on the virus (Figure 1.2) (18, 57, 58). These initial binding events between virus particles to the host cell membrane have been shown to occur by receptor – envelope independent interactions (4, 57). For example recent studies by Pizzato et al found that virus particles bind to cells even when the cells did not express the virus receptor (57). Furthermore, virus binding was observed even when envelope-defective virus particles were used, suggesting that the virus encoded envelope proteins do not control virus binding. Altogether, the results from these studies indicate that the initial interaction between virus particles and the cell surface is partially mediated by non envelope-receptor interactions. Therefore current strategies used to target viruses by altering virus envelope proteins do little to mitigate receptor-envelope independent interactions (4, 57, 71, 88).

After the initial binding of virus particles to the cell surface, the virus envelope proteins (fusion proteins) bind to their cognate cell receptors (if present), bringing the two membranes in close apposition with each other (76). This initial apposition forms a stalk or hemifusion intermediate which allows for fusion of the outer leaflets of the membranes (Figure 1.3). At this stage, the outer leaflet of the virus and cell lipid bilayers are merged but the inner leaflets and the aqueous compartments, remain separate (83). The virus

fusion proteins, which remain anchored within one bilayer, undergo conformational changes that reveal a hydrophobic fusion peptide (10, 83). This peptide inserts into the apposed host cell membrane and oligomerizes, thus stressing the apposed bilayers causing the formation of a fusion pore (83). This early pore formation enlarges to give rise to the late fusion pore, at which point the virus protein-RNA complex is released into the cytoplasm of the cell (25). The naked RNA genome of the retrovirus is reverse transcribed into DNA by a virus associated enzyme (reverse transcriptase) and the protein-DNA complex is transported to the nucleus where it is integrated into the host cell genome by the virus associated enzyme integrase. During and after integration, the therapeutic gene is transcribed and translated to elicit the desired effect.

1.5 Insertion Mutagenesis Concerns in Retrovirus and Lentivirus Vectors

In an ideal setting, a vector would integrate its genome into the host genome of long-term repopulating cells and express the 'corrective' gene for the life span of the infected cells as well as their progeny without significant toxic or immunogenic effects. However, gene therapy clinical trials worldwide have helped highlight many limitations still present with gene therapy vectors. Using model systems, researchers have known for many years that onco-retroviruses have the potential to induce cancers (41, 44, 75). Cancer development requires a series of DNA changes which lead to disruption in cell division and apoptosis, hence it was believed that multiple retrovirus integration events in a cell evolve into tumorigenesis. Interestingly, studies conducted with experimental tumors resulting from retrovirus infection suggest that oncogenesis is usually caused by only one insert (73). Furthermore, two patients treated for X-linked severe combined immunodeficiency (X-SCID) in 2002 using retroviral gene therapy were diagnosed with monoclonal T-cell leukemia (5, 62). The cause of both these independent leukemic

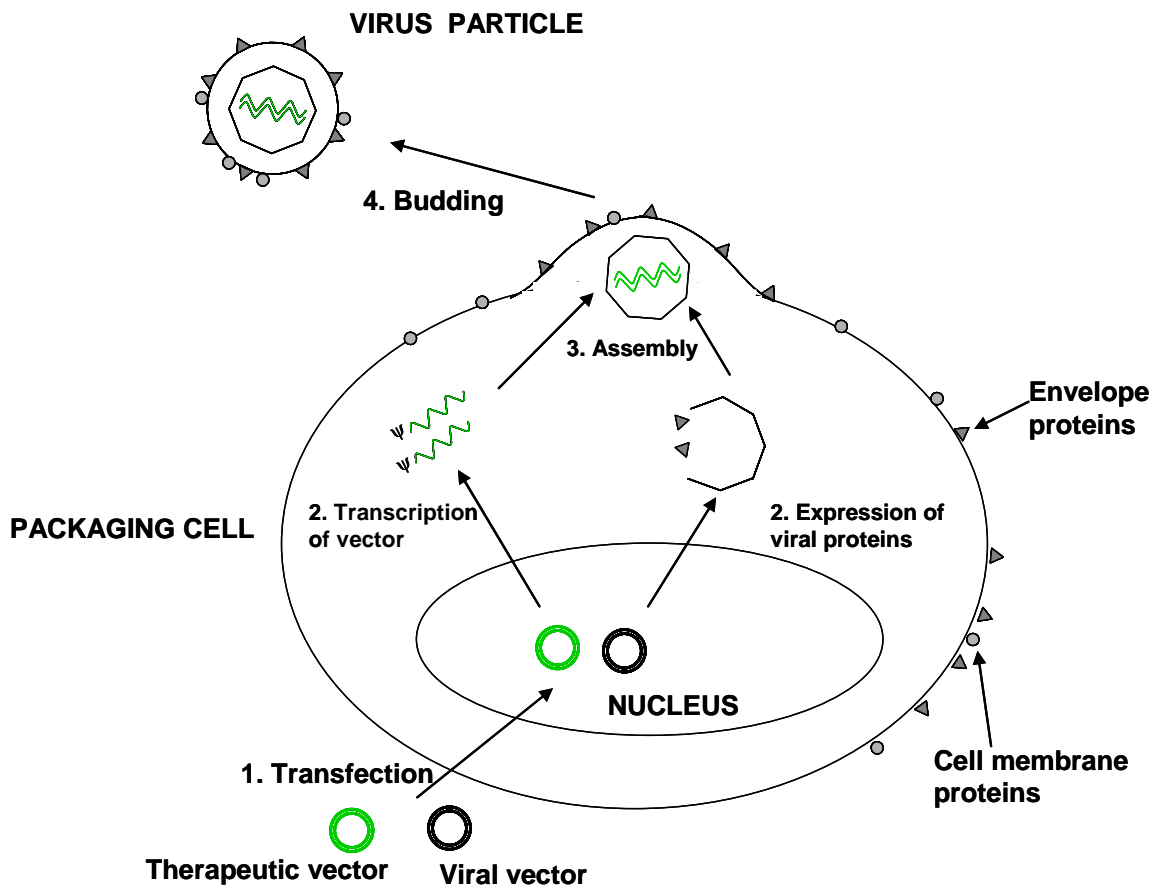


Figure 1.1 Production of recombinant retroviruses. Recombinant retroviruses are produced by transfecting packaging cells with plasmids carrying the therapeutic vector and other plasmids encoding structural proteins of a retrovirus particle. Viral proteins expressed from the viral vector self-assemble with the therapeutic gene near the cell membrane. The therapeutic gene contains a packaging sequence (ψ) that allows for efficient incorporation of the therapeutic gene into the budding virus particles. The assembled virus particle buds from the cell membrane, acquiring viral envelope proteins as well as host cell proteins in its lipid bilayer.

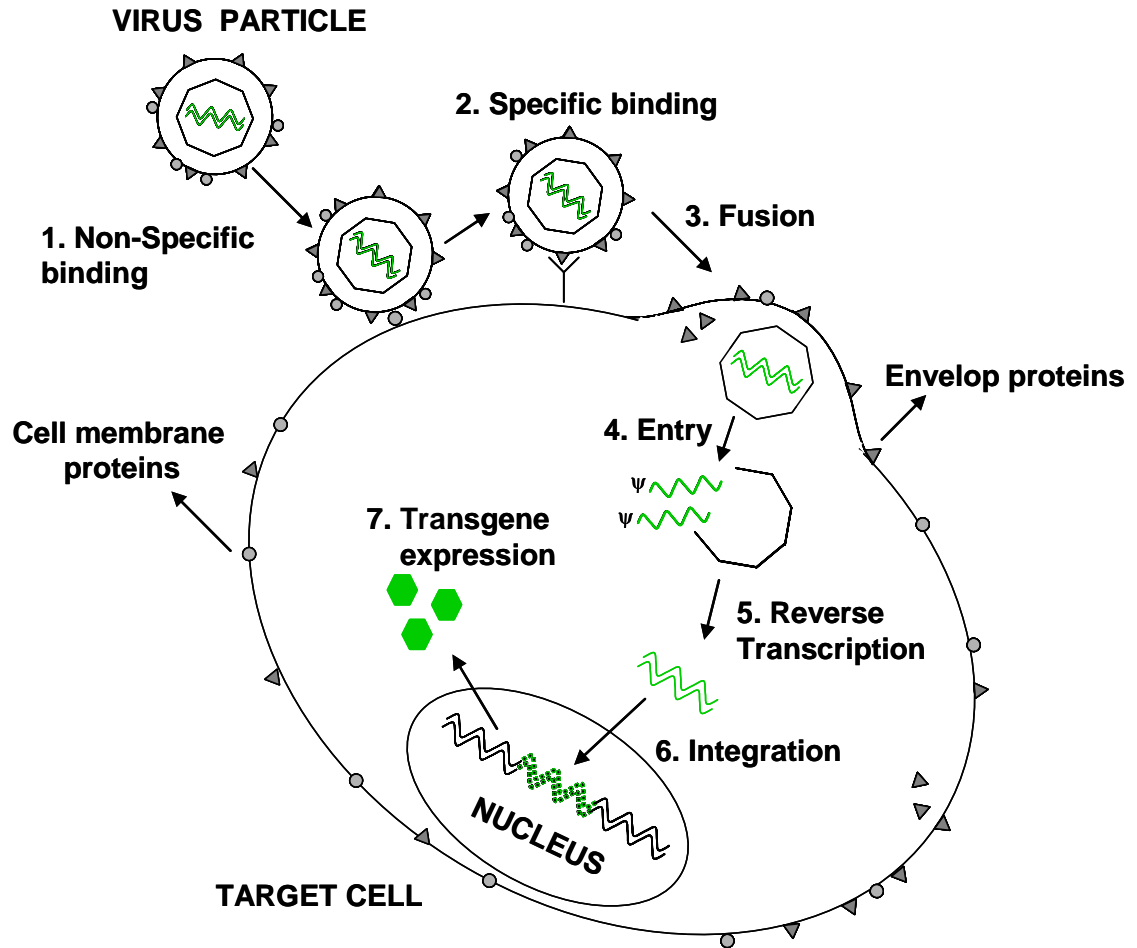


Figure 1.2 Transduction of target cells by recombinant retroviruses. Retroviruses first diffuse to the cell and bind to the cell surface via nonspecific interactions. The virus envelope proteins then bind irreversibly to specific cell receptors, initiating conformational changes that facilitate fusion between the virus lipid bilayer and the cell membrane. After fusion, the internal components of the virus are released into the cell cytoplasm and the RNA genome is reverse transcribed to DNA. This DNA is integrated into the host cell genome and now can be transcribed and translated to express the therapeutic gene of interest.

events have been linked to the aberrant expression of the same gene, LMO-2 locus, and therefore suggests that oncogenesis related with retroviral gene therapy is not random and may share a common mechanism. For this reason many efforts have been made to predict the sites of integration preferred by viral vectors.

Many studies suggest that the site of viral vector integration is dependant on the virus vector used to deliver the gene. Recent studies have revealed that the human immunodeficiency virus (HIV-1) integration occurs along the length of transcriptionally active genes (46, 69). Several HIV-1 hotspots have been identified, including a 2.5 kb region which contained nearly 1% of the integration events. The Moloney murine leukemia virus (MLV) integration events however, have been shown to largely occur near transcription start regions and CpG islands (54). Specifically, 17% of the MLV-vector integration was near transcription start regions and another 17% was seen to occur near CpG islands (86). This preference for retrovirus vector insertion near transcriptionally active genes may directly affect nearby gene enhancer and promoter regions, thereby influencing gene expression. Also, vector promoter may itself give rise to functional gene transcript, thereby giving rise to a full-length functional gene transcript. Thus, because of the preference retrovirus vectors exhibit to integrate their genes near promoters or transcriptionally active genes, they are thought to be more prone to inducing insertional mutagenesis than lentivirus vectors (77).

1.6 Lipid Composition of Virus Particles

Interestingly, recent studies suggest that retrovirus binding is controlled by factors other than their viral envelope proteins and that these proteins are not, as previously thought, required for virus binding, but are primarily for mediating fusion and entry of the virus particle after it binds to the cell. Research studies on the lipid composition of the retroviral bilayer revealed that the proteins responsible for mediating

viral fusion are derived from specific sites within the plasma membrane of virus producing cells, called lipid rafts (42). Lipid rafts are specialized membrane domains enriched in certain lipids, mainly cholesterol (CH), and sphingolipids. More recently, it was shown that retroviral membranes contain dihydrosphingomyelin (DHSM), an uncommon subspecies of SM (7, 59). These researchers showed that inhibition of the DHSM backbone significantly reduces HIV-1 infectivity and provided proof of concept that particular subcategories of lipids can be viewed as targets for the modulation of retroviral infection (59, 81). These discoveries suggest that a comprehensive understanding of the role of lipids in retrovirus production and infectivity is necessary for the successful construction of an effective targeted retrovirus for gene therapy.

Furthermore, lipids and proteins on the surface of enveloped viruses are known to play a key role in the infection of host cells by inducing fusion of the viral and target cell membrane (59, 80). For efficient fusion of virus particles to the target cell, both the virus envelope proteins and lipid constituents in the viral lipid bilayer must work cooperatively (59). It is known that lipids within the viral membrane are not incorporated randomly, and are heavily enriched in cholesterol (CH), sphingolipids (SL), sphingomyelin (SM) and glycolipids, possibly because retroviruses bud from specialized sites within the plasma membrane, called lipid rafts (Table 1.1, Figure 1.4) (53). It is suggested that viruses acquire signaling proteins and lipids during the budding process and that these proteins and lipids play a significant role in virus attachment, fusion and entry (9).

Interestingly, recent studies show that, indeed, altering the lipid composition of virus particles or the target cell membrane significantly reduces the ability of the viruses to infect cells (7, 63). Recently, several studies have demonstrated that depletion of lipids from the target cell inhibits virus fusion and subsequent infection (26, 27). Furthermore, Hug et al found that blocking the sphingolipid (SL) biosynthesis in cells

reduced their susceptibility for retrovirus infection, thus implying that retroviruses utilize SL in their fusion process. Interestingly, reconstituting the SL restored virus fusion and its subsequent infection. Therefore, modulating lipid content of virus particles or viral producer cells can have critical implications in altering the viral fusion properties. It is also important to note that not all enveloped viruses have specific lipid requirements (such as influenza virus) probably because these viruses enter host cells through pH-dependant pathway and thus have a considerably different mechanism of entry into the host cell (76). The most recent studies show that viruses that use the cell membrane as platforms to gain entry are most affected by lipid composition, possibly because lipids are involved in the physicochemical and mechanical properties of the virus and host membrane as they relate to fusion (25, 76).

1.7 Approaches to Retrovirus Targeting

Clinical trials have helped to highlight some major limitations of *in vivo* gene therapy. One such limitation is the inability to transfer genes to a specific targeted cell type without affecting the surrounding non-targeted cells. The types of cells a virus can infect is dictated in large part by its envelope proteins. Many viral vectors commonly used for gene therapy are pseudotyped with the amphotropic envelope protein (17, 43). Amphotropic envelope proteins specifically interact with pit2 on the cell surface to facilitate infection (33, 66). This protein is found on many different types of cells in the human body, and therefore amphotropic viruses are not useful for transferring genes to a single targeted cell type or tissue (65). Therefore, to achieve targeted gene transfer to diseased cells there is a need to narrow the tropism of virus vectors.

Most attempts to develop targeted viral vectors have for the most part focused on controlling or altering the interactions between the envelope proteins of the viruses and

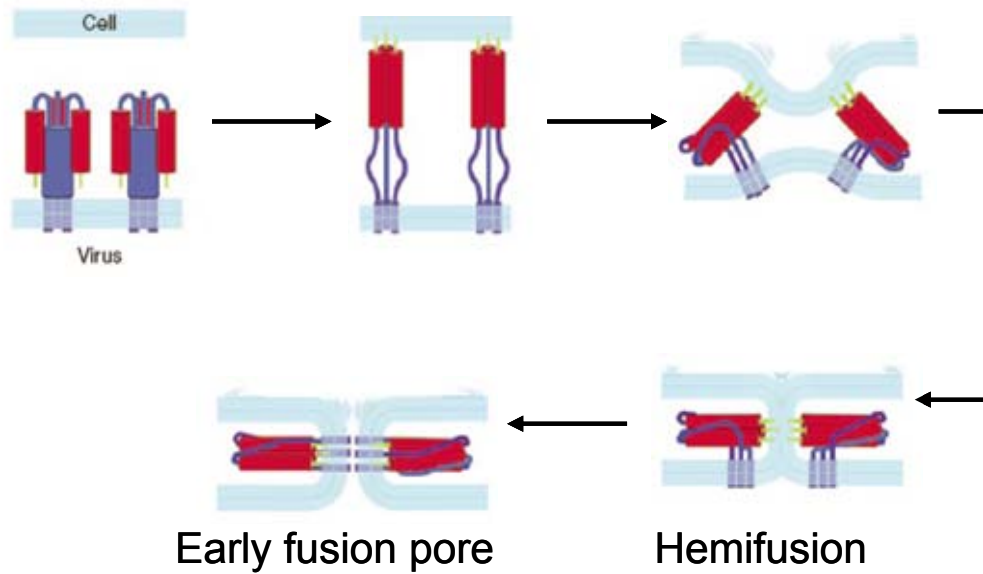


Figure 1.3 Fusion between virus and cell lipid membrane is mediated by viral fusion proteins (Adapted from Harrison et al 2008). Schematic of virus fusion pathway. Virus and cell membranes initially come into close apposition that leads to irreversible binding between virus fusion membranes and their cognate cell receptors (not shown). The virus fusion protein undergoes conformational changes, facilitating first the fusion of the outer leaflets of the membranes, then subsequently the inner leaflets. The mixing of the inner lipid leaflets gives rise to the formation of the early fusion pore, which enlarges to form the late fusion pore. At that stage, the viral protein-RNA capsid is delivered to the cell cytoplasm.

their cognate cell surface receptors (Table 1.2). It has been thought that since the interaction between viral envelope proteins and its cognate receptor is absolutely required for virus infection to occur, changing the properties of these proteins would alter virus infection (55, 72). Perhaps the most common approach taken to alter the types of cells a virus binds to is by pseudotyping (i.e. replacing the viral envelope proteins with envelope proteins from another virus) (32, 38). The tropism of most viruses is relatively broad however, and so this strategy does not allow specific targeting of viruses to one desired cell type (22, 32).

Therefore, to create targeted viruses, most efforts have focused on modifying the structure of the viral envelope proteins, either chemically or genetically, to enable them to bind to receptors that are expressed only by the cell type that is being targeted and no others (22). Initial strategies to construct targeted virus vectors involved genetic incorporation of sequences for cell-specific ligands into the native virus envelope protein to enable virus binding to specific cell types (23, 40, 60). Although these methods increased specific binding of the targeted virus, the altered envelope proteins lacked full activity (3, 79). In a recent study, Qi et al showed that insertion of the PreS1 domain (108 amino acids in length) from hepatitis B virus envelope protein, into the receptor binding domain of the murine leukemia virus envelope (MLV) causes defects in protein processing of the chimeric envelope protein and results in inactive virus particles (60). Interestingly, virus particles constructed from inserting a small segment of the PreS1 domain (26 amino acids) into their envelope protein sequence selectively bound and infected target cells (60). Additionally, a systematic approach to examine the effect of ligand insertion into murine leukemia virus envelope protein on virus infection, showed

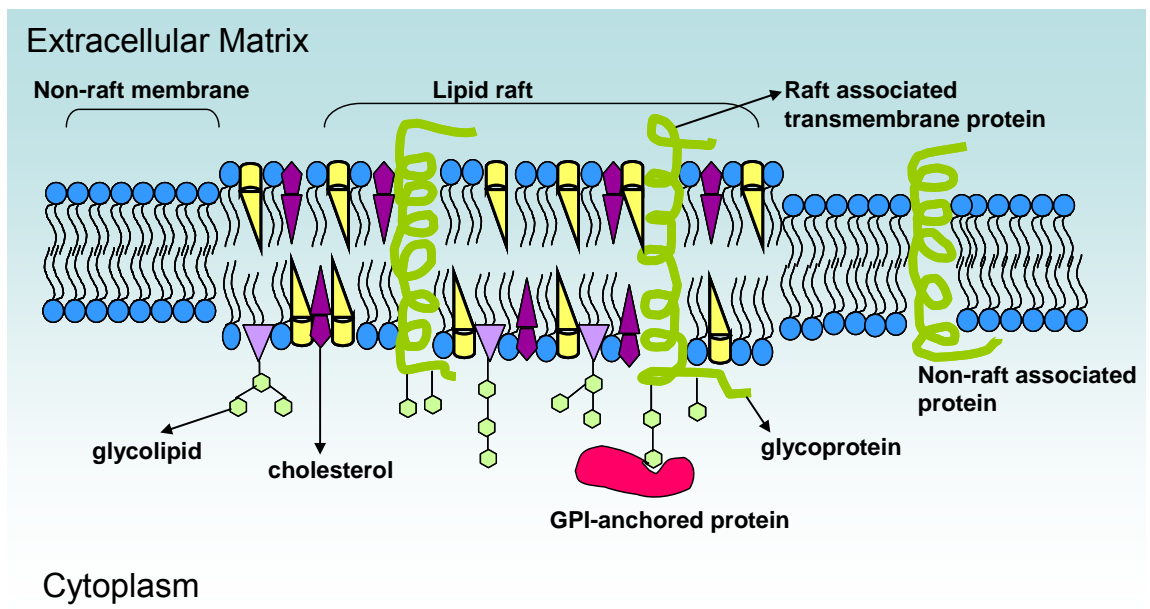


Figure 1.4 Lipid Raft Composition in Cell Lipid Bilayer

that even insertion of short peptide ligands (such as the RGD peptide, 6 amino acids in length) had deleterious effects on virus infectivity. Furthermore, the insertion of the peptides was shown to depend on the location of ligand insertion, size of the ligand, and the sequences flanking the ligand (23, 85). Therefore, genetic engineering based strategies take time to develop, provide variable results and often fail to produce targeted viral vectors.

In an alternate approach, virus surfaces can be modified by covalently linking virus envelope proteins to binding motifs such as cell-specific growth factors, biotin-streptavidin complexes, or targeting ligands attached to polymers chains for targeted cell transduction (79). For instance, Reddy chemically conjugated activated folic acid to the surface of ecotropic retroviruses (64). These studies indicated that the chemical conjugation process reduced virus infectivity by 3-fold. In addition, when the same strategy was used to chemically conjugate folic acid on the surface of amphotropic adenoviruses, it was found that again, modified virus was significantly less efficient in transducing the folate expressing KB cells (64). Data from this study and previous other studies implies that covalent modification of virus envelope proteins compromise the ability of envelope proteins to initiate fusion by inhibiting post-binding conformational changes necessary for membrane fusion (78, 88).

Interestingly, researchers have attempted to use small molecules that did not interfere with virus envelope structure and function, and have shown that virus binding and infection can be successfully redirected towards a desired cell-type (52). Neda et al chemically coupled lactose (360 MW) residues to the surface of ecotropic retroviruses and showed that the modified virus could efficiently bind and transduce human hepatocytes via the asialoglycoprotein receptor (52). Although, the results from this study indicate that envelope proteins have some tolerance

Table 1.2 Strategies for Targeting Retroviruses

Approach	Methodology	Advantages	Disadvantages	Reference
Pseudotyping	Incorporation of envelope proteins from one virus strain or family into lipid bilayer of another virus	Technically feasible and easy to do when vector is permissive for incorporation of heterologous glycoprotein	Variable gene transfer efficiency; Modified virus still has broad tropism	(31, 34, 38, 56)
Genetic Modification	A small peptide or protein is incorporated into virus membrane by genetic means (Examples: small targeting motifs, single-chain antibody, mosaic viral attachment proteins)	Some strategies allows for high-titer vector production; Single-component system;	Can be deleterious to virus functionality, may affect virus	(13, 40, 60)
Adaptor-coupled Modifications	Utilizes a molecule which binds to both the viral vector and the receptor of a desired cell-type, facilitating binding and transduction;	Limited knowledge of envelope protein structure and binding is sufficient; minimal change to vector structure; different targeting ligands can be easily tested;	Usually involves multiple components; variability of adaptor attachment between batches; adaptor system more likely to dissociate <i>in vivo</i> ; clinical applicability is limited; many issues with regulatory agencies;	(20, 65, 70)

for covalent attachment of ligands, there have been limited successes applying this strategy to target infection to other cell-types (35, 79). Altogether, covalent modification strategies engineer the virus envelope protein with the intention that virus binding and fusion will be triggered by the interaction between displayed targeting ligand and its cognate cell receptor, however most of the time, these modifications have deleterious effects on envelope protein function (78, 79).

1.8 Thesis Objectives

The overall objective of this thesis was to determine the effect of modifying the composition of viral lipid bilayer on retrovirus transduction. To accomplish these objectives we pursued the following aims:

- 1. Determine if lipid conjugates can be used to alter the lipid bilayer of retrovirus particles.** We hypothesize that the surface of retrovirus particles can be non-covalently modified using lipid-polyethyleneglycol (PEG) conjugates to increase virus binding to a targeted receptor without adversely altering the function of native viral envelope proteins.
- 2. Investigate the extent to which altering the lipid composition of the bilayer of retroviruses affects their ability to transduce cells.** We hypothesize that treating virus producer cells with a lipid inhibitor will decrease sphingolipid levels in the virus lipid bilayer and affect the virus' ability to transduce cells.
- 3. Examine the mechanism by which changes in the lipid composition of retrovirus bilayers affects their ability to transduce cells.** We hypothesize that lipid inhibitors affect the fusiogenicity of the virus particles produced from treated cells.

1.9 Organization of the Thesis

In chapter 1 we provide an overview of gene therapy and specifically the use of recombinant retroviruses in gene therapy protocols. We discuss the main approaches taken to construct targeted retroviral vectors and also, the role that lipids play in virus targeting. We also discuss the motivation and significance of the thesis project. We identify some of the main limitations with current gene transfer methods and discuss the goals we have formulated to address them.

In chapter 2, we examine a new method for rapidly modifying retroviruses by using lipid conjugates composed of a lipid anchor, a polymer chain and a targeting moiety. We characterize the rate of adsorption and desorption of the lipid conjugate to the virus surface, and the affect of this modification on virus binding. Finally, we test the ability of the modified viruses to infect cells.

In chapter 3, we alter the lipid composition of retrovirus particles by using the fungal endotoxin, myriocin, to inhibit serine palmitoyltransferase in the *de novo* sphingolipid pathway of the virus producer cells. We characterize the changes in lipid composition of the virus membrane, examine the affect of these changes on virus infectivity, and determine if changes in the transduction efficiency of the altered virus particles is cell-type dependant.

In chapter 4, we examine the mechanism by which changes in the lipid composition, caused by treatment of virus producer cells with endotoxin, fumonisin B-1, affects virus infection. We examine the effect of fumonisin B-1 treatment of virus producer cells on the rate of virus production, the incorporation of viral envelope proteins into the viruses they produce, and the ability of these viruses to bind and fuse with cells.

In chapter 5, we summarize our major conclusions and present some suggestions for future work.

1.10 Outcome & Contribution

One outcome of these studies has been the establishment of a rapid and flexible method for modifying the surfaces of retroviruses. The approach taken is fundamentally different from previous virus modification methods because it employs a novel lipid-polymer targeting strategy that non-covalently modifies the virus surface without altering virus infectivity, and because it has the potential to block non-receptor mediated binding of retroviruses to cells. Furthermore we manipulated the lipid content of retroviruses and examined the effect on virus binding, fusion and infection. The results of these studies helped elucidate the role of viral lipids in infection and provided insights into how the lipid content of viral vectors might be manipulated in the future to improve their function for use in human gene therapy protocols. Finally, the concept of virus targeting using the lipid-polymer method may have potentially broad reaching applications in virus detection, diagnosis and vaccine construction. This work is significant because 1) it utilizes a novel lipid-polymer targeting strategy that confers upon retroviruses the ability to bind to specific receptors while maintaining their ability to efficiently transfer genes to cells, and 2) attempts to control the lipid composition of retroviruses as a means to alter the selectivity of their fusogenicity, which has been the major challenge in previous virus targeting studies.

1.11 References

1. **Aloia, R. C., H. Tian, and F. C. Jensen.** 1993. Lipid composition and fluidity of the human immunodeficiency virus envelope and host cell plasma membranes. *Proc Natl Acad Sci U S A* **90**:5181-5185.
2. **Anderson, W. F.** 1998. Human gene therapy. *Nature* **392**:25-30.
3. **Bartosch, B., and F. L. Cosset.** 2004. Strategies for retargeted gene delivery using vectors derived from lentiviruses. *Curr Gene Ther* **4**:427-43.
4. **Benedict, C. A., R. Y. Tun, D. B. Rubinstein, T. Guillaume, P. M. Cannon, and W. F. Anderson.** 1999. Targeting retroviral vectors to CD34-expressing cells: binding to CD34 does not catalyze virus-cell fusion. *Hum Gene Ther* **10**:545-557.
5. **Blaese, R. M., K. W. Culver, A. D. Miller, C. S. Carter, T. Fleisher, M. Clerici, G. Shearer, L. Chang, Y. Chiang, P. Tolstoshev, J. J. Greenblatt, S. A. Rosenberg, H. Klein, M. Berger, C. A. Mullen, W. J. Ramsey, L. Muul, R. A. Morgan, and W. F. Anderson.** 1995. T lymphocyte-directed gene therapy for ADA- SCID: initial trial results after 4 years. *Science* **270**:475-80.
6. **Briggs, J. A., T. Wilk, R. Welker, H. G. Krausslich, and S. D. Fuller.** 2003. Structural organization of authentic, mature HIV-1 virions and cores. *Embo J* **22**:1707-15.
7. **Brugger, B., B. Glass, P. Haberkant, I. Leibrecht, F. T. Wieland, and H. G. Krausslich.** 2006. The HIV lipidome: a raft with an unusual composition. *Proc Natl Acad Sci U S A* **103**:2641-6.
8. **Bukrinsky, M. I., N. Sharova, M. P. Dempsey, T. L. Stanwick, A. G. Bukrinskaya, S. Haggerty, and M. Stevenson.** 1992. Active nuclear import of human immunodeficiency virus type 1 preintegration complexes. *Proc Natl Acad Sci U S A* **89**:6580-4.
9. **Campbell, S. M., S. M. Crowe, and J. Mak.** 2001. Lipid rafts and HIV-1: from viral entry to assembly of progeny virions. *J Clin Virol* **22**:217-27.
10. **Chazal, N., G. Singer, C. Aiken, M. L. Hammariskjold, and D. Rekosh.** 2001. Human immunodeficiency virus type 1 particles pseudotyped with envelope proteins that fuse at low pH no longer require Nef for optimal infectivity. *J Virol* **75**:4014-8.
11. **Chen, S. T., A. Lida, L. Guo, T. Friedmann, and J. K. Yee.** 1996. Generation of packaging cell lines for pseudotyped retroviral vectors of the G protein of vesicular stomatitis virus by using a modified tetracycline inducible system. *Proc Natl Acad Sci U S A* **93**:10057-10062.
12. **Collins, M., and Y. Ikeda.** 2003. Continuous high-titer HIV-1 vector production. *Nature biotechnology* **21**:569.

13. **Collins, S. A., B. A. Guinn, P. T. Harrison, M. F. Scallan, G. C. O'Sullivan, and M. Tangney.** 2008. Viral vectors in cancer immunotherapy: which vector for which strategy? *Curr Gene Ther* **8**:66-78.
14. **Copreni, E., M. Penzo, S. Carrabino, and M. Conese.** 2004. Lentivirus-mediated gene transfer to the respiratory epithelium: a promising approach to gene therapy of cystic fibrosis. *Gene Ther* **11, Suppl 1S**:67-75.
15. **Cosset, F. L., Y. Takeuchi, J. L. Battini, R. A. Weiss, and M. K. Collins.** 1995. High-titer packaging cells producing recombinant retroviruses resistant to human serum. *J Virol* **69**:7430-6.
16. **Cosset, F. L., Y. Takeuchi, J. L. Battini, R. A. Weiss, and M. K. Collins.** 1995b. High-titer packaging cells producing recombinant retroviruses resistant to human serum. *J Virol* **69**:7430-7436.
17. **Cotrim, A. P., and B. J. Baum.** 2008. Gene therapy: some history, applications, problems, and prospects. *Toxicol Pathol* **36**:97-103.
18. **Croyle, M. A., S. M. Callahan, A. Auricchio, G. Schumer, K. D. Linse, J. M. Wilson, L. J. Brunner, and G. P. Kobinger.** 2004. PEGylation of a vesicular stomatitis virus G pseudotyped lentivirus vector prevents inactivation in serum. *J Virol* **78**:912-21.
19. **Dvorin, J. D., P. Bell, G. G. Maul, M. Yamashita, M. Emerman, and M. H. Malim.** 2002. Reassessment of the roles of integrase and the central DNA flap in human immunodeficiency virus type 1 nuclear import. *J Virol* **76**:12087-96.
20. **Etienne-Julan, M., P. Roux, S. Carillo, P. Jeanteur, and M. Piechaczyk.** 1992. The efficiency of cell targeting by recombinant retroviruses depends on the nature of the receptor and the composition of the artificial cell-virus linker. *J Gen Virol* **73 (Pt 12)**:3251-5.
21. **Gentile, M., T. Adrian, A. Scheidler, M. Ewald, F. Dianzani, G. Pauli, and H. R. Gelderblom.** 1994. Determination of the size of HIV using adenovirus type 2 as an internal length marker. *J Virol Methods* **48**:43-52.
22. **Goff, S. P.** 2007. Host factors exploited by retroviruses. *Nat Rev Microbiol* **5**:253-63.
23. **Gollan, T. J., and M. R. Green.** 2002. Redirecting retroviral tropism by insertion of short, nondisruptive peptide ligands into envelope. *J Virol* **76**:3558-3563.
24. **Guibinga, G. H., A. Miyanochara, J. D. Esko, and T. Friedmann.** 2002. Cell surface heparan sulfate is a receptor for attachment of envelope protein-free retrovirus-like particles and VSV-G pseudotyped MLV-derived retrovirus vectors to target cells. *Mol Ther* **5**:538-46.
25. **Harrison, S. C.** 2008. Viral membrane fusion. *Nat Struct Mol Biol* **15**:690-8.

26. **Hildreth, J. E., and Z. Liao.** 2001. Lipid rafts and HIV pathogenesis: Host membrane cholesterol is required for infection by HIV type-1. *AIDS Res Hum Retroviruses* **17**:1009.
27. **Hug, P., H. M. Lin, and J. M. Wang.** 2000. Glycosphingolipids promote entry of a broad range of human immunodeficiency virus type 1 isolates into cell lines expressing CD4, CXCR4, and/or CCR5. *Journal of virology* **74**:6377.
28. **Jobbagy, Z., S. Garfield, L. Baptiste, M. V. Eiden, and W. B. Anderson.** 2000. Subcellular redistribution of Pit-2 P(i) transporter/amphotropic leukemia virus (A-MuLV) receptor in A-MuLV-infected NIH 3T3 fibroblasts: involvement in superinfection interference. *J Virol* **74**:2847-54.
29. **Johnson, L. G., J. C. Olsen, L. Naldini, and R. C. Boucher.** 2000. Pseudotyped human lentiviral vector-mediated gene transfer to airway epithelia in vivo. *Gene Ther* **7**:568-574.
30. **Johnson MC, B. J., Fuller SD, Simon M, Vogt VM.** 2003. Presented at the 10th Conf Retrovir Oppor Infect Boston Mass, Feb 10-14.
31. **Jung, C., B. N. Grzybowski, S. Tong, L. Cheng, R. W. Compans, and J. M. Le Doux.** 2004. Lentiviral vectors pseudotyped with envelope glycoproteins derived from human parainfluenza virus type 3. *Biotechnol Prog* **20**:1810-1816.
32. **Kafri, T.** 2004. Gene delivery by lentivirus vectors an overview. *Methods Mol Biol* **246**:367-90.
33. **Kavanaugh, M. P., D. G. Miller, W. Zhang, W. Law, S. L. Kozak, D. Kabat, and A. D. Miller.** 1994. Cell-surface receptors for gibbon ape leukemia virus and amphotropic murine retrovirus are inducible sodium-dependent phosphate symporters. *Proc Natl Acad Sci U S A* **91**:7071-7075.
34. **Kobinger, G. P., D. J. Weiner, Q. C. Yu, and J. M. Wilson.** 2001. Filovirus-pseudotyped lentiviral vector can efficiently and stably transduce airway epithelia in vivo. *Nat Biotechnol* **19**:225-230.
35. **Kuroki, M., F. Arakawa, P. D. Khare, M. Kuroki, S. Liao, H. Matsumoto, H. Abe, and T. Imakiire.** 2000. Specific targeting strategies of cancer gene therapy using a single-chain variable fragment (scFv) with a high affinity for CEA. *Anticancer Res* **20**:4067-71.
36. **Larochelle, A., K. W. Peng, and S. J. Russell.** 2002. Lentiviral vector targeting. *Curr Top Microbiol Immunol* **261**:143-63.
37. **Lavillette, D., S. J. Russell, and F. L. Cosset.** 2001. Retargeting gene delivery using surface-engineered retroviral vector particles. *Curr Opin Biotechnol* **12**:461-466.
38. **Lo, H. L., and J. K. Yee.** 2007. Production of vesicular stomatitis virus G glycoprotein (VSV-G) pseudotyped retroviral vectors. *Curr Protoc Hum Genet Chapter 12*:Unit 12 7.

39. **Logan, A. C., S. J. Nightingale, D. L. Haas, G. J. Cho, K. A. Pepper, and D. B. Kohn.** 2004. Factors influencing the titer and infectivity of lentiviral vectors. *Hum Gene Ther* **15**:976-88.
40. **Lorimer, I. A., and S. J. Lavictoire.** 2000. Targeting retrovirus to cancer cells expressing a mutant EGF receptor by insertion of a single chain antibody variable domain in the envelope glycoprotein receptor binding lobe. *J Immunol Methods* **237**:147-57.
41. **Lund, A. H., G. Turner, A. Trubetskoy, E. Verhoeven, E. Wientjens, D. Hulsman, R. Russell, R. A. DePinho, J. Lenz, and M. van Lohuizen.** 2002. Genome-wide retroviral insertional tagging of genes involved in cancer in *Cdkn2a*-deficient mice. *Nat Genet* **32**:160-5.
42. **Marchant, J. S., V. S. Subramanian, I. Parker, and H. M. Said.** 2002. Intracellular trafficking and membrane targeting mechanisms of the human reduced folate carrier in Mammalian epithelial cells. *J Biol Chem* **277**:33325-33333.
43. **Medicine, J. o. G.** 2008. *Gene Therapy Clinical Trials Worldwide.*
44. **Mikkers, H., J. Allen, P. Knipscheer, L. Romeijn, A. Hart, E. Vink, and A. Berns.** 2002. High-throughput retroviral tagging to identify components of specific signaling pathways in cancer. *Nat Genet* **32**:153-9.
45. **Miller, D. G., R. H. Edwards, and A. D. Miller.** 1994. Cloning of the cellular receptor for amphotropic murine retroviruses reveals homology to that for gibbon ape leukemia virus. *Proc Natl Acad Sci U S A* **91**:78-82.
46. **Mitchell, R. S., B. F. Beitzel, A. R. Schroder, P. Shinn, H. Chen, C. C. Berry, J. R. Ecker, and F. D. Bushman.** 2004. Retroviral DNA integration: ASLV, HIV, and MLV show distinct target site preferences. *PLoS Biol* **2**:E234.
47. **Mok, H., D. J. Palmer, P. Ng, and M. A. Barry.** 2005. Evaluation of polyethylene glycol modification of first-generation and helper-dependent adenoviral vectors to reduce innate immune responses. *Mol Ther* **11**:66-79.
48. **Morgan, J. R., J. M. LeDoux, R. G. Snow, R. G. Tompkins, and M. L. Yarmush.** 1995. Retrovirus infection: effect of time and target cell number. *J Virol* **69**:6994-7000.
49. **Mortuza, G. B., L. F. Haire, A. Stevens, S. J. Smerdon, J. P. Stoye, and I. A. Taylor.** 2004. High-resolution structure of a retroviral capsid hexameric amino-terminal domain. *Nature* **431**:481-5.
50. **Muesing MA, S. D., Cabradilla CD, Benton CV, Lasky LA, Capoon DJ.** 1985. Nucleic acid structure and expression of the human AIDS/lymphadenopathy retrovirus. *Nature* **131**:405-8.
51. **Mulligan, R. C.** 1993. The basic science of gene therapy. *Science* **260**:926-32.

52. **Neda, H., C. H. Wu, and G. Y. Wu.** 1991. Chemical modification of an ecotropic murine leukemia virus results in redirection of its target cell specificity. *J Biol Chem* **266**:14143-14146.
53. **Ono, A., and E. O. Freed.** 2005. Role of lipid rafts in virus replication. *Adv Virus Res* **64**:311-58.
54. **Ory, D. S., B. A. Neugeboren, and R. C. Mulligan.** 1996. A stable human-derived packaging cell line for production of high titer retrovirus/vesicular stomatitis virus G pseudotypes. *Proc Natl Acad Sci U S A* **93**:11400-11406.
55. **Overbaugh, J., A. D. Miller, and M. V. Eiden.** 2001. Receptors and entry cofactors for retroviruses include single and multiple transmembrane-spanning proteins as well as newly described glycoposphatidylinositol-anchored and secreted proteins. *Microbiol Mol Biol Rev* **65**:371-89, table of contents.
56. **Pickl, W. F., F. X. Pimentel-Muinos, and B. Seed.** 2001. Lipid rafts and pseudotyping. *J Virol* **75**:7175-83.
57. **Pizzato, M., E. D. Blair, M. Fling, J. Kopf, A. Tomassetti, R. A. Weiss, and Y. Takeuchi.** 2001. Evidence for nonspecific adsorption of targeted retrovirus vector particles to cells. *Gene Ther* **8**:1088-1096.
58. **Pizzato, M., S. A. Marlow, E. D. Blair, and Y. Takeuchi.** 1999. Initial binding of murine leukemia virus particles to cells does not require specific Env-receptor interaction. *J Virol* **73**:8599-611.
59. **Puri, A., R. Blumenthal, and A. Rein.** 2003. Modulation of entry of enveloped viruses by cholesterol and sphingolipids (review). *Molecular membrane Biology* **20**:243-254.
60. **Qi, P., J. X. Han, Y. Q. Lu, and C. X. Wang.** 2007. Redirecting retroviral tropism by insertion of hepatitis B virus PreS1 core peptide into the envelope. *Arch Virol* **152**:1721-30.
61. **R, P., and E. Burckheimer.** 2004. In vivo efficacy of folate-targeted lipid-protamine-DNA (LPD-PEG-Folate) complexes in an immunocompetent syngeneic model for breast adenocarcinoma. *Cancer gene therapy* **11**:128.
62. **Rabbits, T. H., K. Bucher, G. Chung, G. Grutz, A. Warren, and Y. Yamada.** 1999. The effect of chromosomal translocations in acute leukemias: the LMO2 paradigm in transcription and development. *Cancer Res* **59**:1794s-1798s.
63. **Rawat, S. S., B. T. Johnson, and A. Puri.** 2005. Sphingolipids: modulators of HIV-1 infection and pathogenesis. *Biosci Rep* **25**:329-43.
64. **Reddy, J. A., D. W. Clapp, and P. S. Low.** 2001. Retargeting of viral vectors to the folate receptor endocytic pathway. *J Control Release* **74**:77-82.

65. **Roux, P., P. Jeanteur, and M. Piechaczyk.** 1989. A versatile and potentially general approach to the targeting of specific cell types by retroviruses: application to the infection of human cells by means of major histocompatibility complex class I and class II antigens by mouse ecotropic murine leukemia virus-derived viruses. *Proc Natl Acad Sci U S A* **86**:9079-83.
66. **Sabatino, D. E., B. Q. Do, L. C. Pyle, N. E. Seidel, L. J. Girard, S. K. Spratt, D. Orlic, and D. M. Bodine.** 1997. Amphotropic or gibbon ape leukemia virus retrovirus binding and transduction correlates with the level of receptor mRNA in human hematopoietic cell lines. *Blood Cells Mol Dis* **23**:422-33.
67. **Salmeen, I., L. Rimai, L. Liebes, M. A. Rich, and J. J. McCormick.** 1975. Hydrodynamic diameters of RNA tumor viruses. Studies by laser beat frequency light scattering spectroscopy of avian myeloblastosis and Rauscher murine leukemia viruses. *Biochemistry* **14**:134-41.
68. **Salmeen, I., L. Rimai, R. B. Luftig, L. Libes, E. Retzel, M. Rich, and J. J. McCormick.** 1976. Hydrodynamic diameters of murine mammary, Rous sarcoma, and feline leukemia RNA tumor viruses: studies by laser beat frequency light-scattering spectroscopy and electron microscopy. *J Virol* **17**:584-96.
69. **Schroder, A. R., P. Shinn, H. Chen, C. Berry, J. R. Ecker, and F. Bushman.** 2002. HIV-1 integration in the human genome favors active genes and local hotspots. *Cell* **110**:521-9.
70. **Snitkovsky, S., and J. A. Young.** 2002. Targeting retroviral vector infection to cells that express heregulin receptors using a TVA-heregulin bridge protein. *Virology* **292**:150-5.
71. **Somia, N. V., M. Zoppe, and I. M. Verma.** 1995. Generation of targeted retroviral vectors by using single-chain variable fragment: an approach to in vivo gene delivery. *Proc Natl Acad Sci U S A* **92**:7570-7574.
72. **Sommerfelt, M. A.** 1999. Retrovirus receptors. *J Gen Virol* **80 (Pt 12)**:3049-64.
73. **Stocking, C., U. Bergholz, J. Friel, K. Klingler, T. Wagener, C. Starke, T. Kitamura, A. Miyajima, and W. Ostertag.** 1993. Distinct classes of factor-independent mutants can be isolated after retroviral mutagenesis of a human myeloid stem cell line. *Growth Factors* **8**:197-209.
74. **Strand, M., and J. T. August.** 1976. Structural proteins of ribonucleic acid tumor viruses. Purification of envelope, core, and internal components. *J Biol Chem* **251**:559-64.
75. **Suzuki, T., H. Shen, K. Akagi, H. C. Morse, J. D. Malley, D. Q. Naiman, N. A. Jenkins, and N. G. Copeland.** 2002. New genes involved in cancer identified by retroviral tagging. *Nat Genet* **32**:166-74.
76. **Teissier, E., and E. I. Pecheur.** 2007. Lipids as modulators of membrane fusion mediated by viral fusion proteins. *Eur Biophys J* **36**:887-99.

77. **Trono, D.** 2003. Virology. Picking the right spot. *Science* **300**:1670-1.
78. **Verhoeven, E., and F. L. Cosset.** 2004. Surface-engineering of lentiviral vectors. *J Gene Med* **6 Suppl 1**:S83-94.
79. **Waehler, R., S. J. Russell, and D. T. Curiel.** 2007. Engineering targeted viral vectors for gene therapy. *Nat Rev Genet* **8**:573-87.
80. **Wang, E., and A. Merrill.** 2005. Sphingolipidomics: high-throughput, structure-specific, and quantitative analysis of sphingolipids by lipid chromatography tandem mass spectrometry. *Methods* **36**:207.
81. **Wang, E., W. P. Norred, C. W. Bacon, R. T. Riley, and A. H. Merrill, Jr.** 1991. Inhibition of sphingolipid biosynthesis by fumonisins. Implications for diseases associated with *Fusarium moniliforme*. *J Biol Chem* **266**:14486-90.
82. **Ward, C. M.** 2000. Folate-targeted non-viral DNA vectors for cancer gene therapy. *Curr Opin Mol Ther* **2**:182-187.
83. **Wickner, W., and R. Schekman.** 2008. Membrane fusion. *Nat Struct Mol Biol* **15**:658-64.
84. **Wils, P., H. Hofland, and C. Masson.** 2002. Folate-Targeted Gene Transfer In vivo. *Molecular Therapy* **5**:739.
85. **Wu, B. W., J. Lu, T. K. Gallaher, W. F. Anderson, and P. M. Cannon.** 2000. Identification of regions in the Moloney murine leukemia virus SU protein that tolerate the insertion of an integrin-binding peptide. *Virology* **269**:7-17.
86. **Wu, X., Y. Li, B. Crise, and S. M. Burgess.** 2003. Transcription start regions in the human genome are favored targets for MLV integration. *Science* **300**:1749-51.
87. **Yi, Y., S. H. Hahm, and K. H. Lee.** 2005. Retroviral gene therapy: safety issues and possible solutions. *Curr Gene Ther* **5**:25-35.
88. **Zhao, Y., L. Zhu, S. Lee, L. Li, E. Chang, N. W. Soong, D. Douer, and W. F. Anderson.** 1999. Identification of the block in targeted retroviral-mediated gene transfer. *Proc Natl Acad Sci U S A* **96**:4005-4010.
89. **Zufferey, R., D. Nagy, R. J. Mandel, L. Naldini, and D. Trono.** 1997. Multiply attenuated lentiviral vector achieves efficient gene delivery in vivo. *Nat Biotechnol* **15**: 871-875.

CHAPTER 2

RAPID MODIFICATION OF RETROVIRUSES USING LIPID CONJUGATES

2.1 Abstract

Methods are needed to manipulate natural nanoparticles. Viruses are particularly interesting because they can act as therapeutic cellular delivery agents. Here we examine a new method for rapidly modifying retroviruses that uses lipid conjugates composed of a lipid anchor (1,2-distearoyl-*sn*-glycero-3-phosphoethanolamine), a polyethylene glycol chain, and biotin. The conjugates rapidly and stably modified retroviruses and enabled them to bind streptavidin. The implication of this work for modifying viruses for gene therapy and vaccination protocols is discussed.

2.2 Introduction

As the use of nanostructures in a wide range of fields grows, the development of methods by which nanoparticles of natural origin (e.g. viruses) can be manipulated is becoming increasingly important (43, 49, 51). For example, the range of jobs for which viruses have evolved (carrying cargo, cell binding and entry, gene delivery) makes such natural nanoparticles intrinsically interesting for cellular delivery applications. Specifically, there is significant interest in engineering recombinant enveloped viruses that bind to a specific targeted cell type for gene therapy and vaccine applications (8, 17, 29). Strategies to develop targeted viral vectors have for the most part focused on controlling or altering the interactions between the envelope proteins of the viruses and their cognate cell surface receptors, since these interactions are absolutely required for virus infection to occur (33, 45). Perhaps the most common approach taken to alter the

types of cells a virus binds to is to replace its envelope proteins with envelope proteins from another virus in a process called 'pseudotyping' (23, 35). The cell types that a virus is able to infect (that is, its tropism) is dictated in large part by its envelope proteins, so pseudotyping viruses with envelope proteins from a different virus can significantly change, and potentially enhance the infectivity of the virus with respect to certain cells (17, 23). Unfortunately the tropism of most pseudotyped viruses is relatively broad and rarely directly corresponds with what is required for targeted gene delivery (48).

As a result, most efforts to create targeted viruses have focused on chemically or genetically altering the viral envelope proteins to include a binding motif for the targeted receptor (17). Early studies frequently modified the ecotropic envelope protein because human cells do not express the ecotropic receptor. The hypothesis central to this approach was that viruses pseudotyped with modified ecotropic envelope proteins would only be able to bind to and fuse with human cells that expressed the targeted receptor. There were some notable early successes using this approach. For example, retroviruses pseudotyped with ecotropic envelope proteins that were genetically modified to contain erythropoietin were able to infect human cells bearing the erythropoietin receptor (24), and ecotropic retroviruses chemically modified with galactose were able to infect human HepG2 cells via the asialoglycoprotein receptor (32). Unfortunately, this approach has proven difficult to generalize, primarily because the modified envelope proteins are usually not able to initiate fusion of the virus via interactions with the targeted receptor (52). Viral envelope proteins, in general, must interact with their cognate cellular receptors in order to induce fusion, because binding to these receptors triggers cross-talk between the envelope glycoproteins and a series of conformational changes that are required to promote virus-cell fusion (47).

Recently, alternative approaches have been explored that do not directly alter the structure of the viral envelope protein. In one such approach, Snitkovsky et al. created

an adaptor protein, composed of the extracellular domain of the avian sarcoma and leukemia virus (ASLV) receptor and heregulin- β 1, that served as a bridge between ASLV pseudotyped retroviruses and cells that expressed heregulin receptors (44). A key advantage of this approach is that it does not require changes to the structure of the retroviral envelope protein, changes that often impair virus production or function. Most adaptors tested to date, however, bind to the retroviral envelope proteins (39, 44), which often ablates the native tropism of the virus, and redirects the virus towards the targeted receptor. A drawback of this approach is that adaptor – envelope protein pairs must be identified that will not only bind to the targeted receptor, but that also promote the conformational changes necessary to induce virus fusion (15). It is not yet clear if this approach can be generalized to the targeting of other types of receptors or how readily it can be used with other retroviral envelope proteins.

These previous studies showed that it is difficult to target retroviruses by manipulating their retroviral envelope proteins and prompted us to consider an alternative approach. In particular, the variety of “plug-and-play” self-assembled monolayer methods for the non-covalent modification of inorganic nanoparticles was extremely attractive; such self-assembly approaches permit rapid, non-covalent, and reconfigurable modification of the nanoparticle surface with a wide range of potential functionalities (2, 4, 13, 38). We postulated that the problem of enveloped virus particle modification could be solved if cell-specific binding motifs could be attached to viruses non-covalently, and without altering or otherwise influencing the structure and function of their envelope proteins. The obvious locus for such self-assembly is the lipid bilayers of such viruses, which should permit dynamic exchange between lipids in the envelope and those in the surrounding medium. Replacement of native envelope lipids with ones presenting the desired functionality would thereby result in a semi-synthetic, self-assembled virus coat. An approach similar to this has been used to target mammalian

cells to specific binding sites. Dennis et al. showed that chondrogenic progenitor cells, coated with lipidated protein G and bound to antibodies specific for cartilage matrix proteins, were able to home to the site of injured cartilage (12). The lipidated protein G efficiently (in 2 hours at 37 °C) intercalated into the cellular lipid bilayer thereby providing an anchor for the targeting antibody. Similar approaches are also common in the creation of targeted liposomes. For example, Saul et al. incorporated lipid-PEG-folate conjugates into liposomes, and showed that the folate-modified liposomes were preferentially taken up by C6 glioma cells that expressed high levels of the folate receptor as compared to terminally differentiated primary cortical neurons derived from chick embryos, which do not express the folate receptor (41).

Based on these findings with cells and liposomes, we hypothesized that lipid conjugates could be used to modify the surfaces of retroviruses without altering or compromising the structure or function of their envelope proteins. To test this strategy, we modified the surfaces of amphotropic murine leukemia retroviruses with lipid conjugates composed of a double chain saturated lipid, a polyethylene glycol chain, and a biotin molecule. We then measured the effect of the modification on their infectivity, and examined their ability to bind to streptavidin, the native protein binding partner of biotin. The results of these studies clearly show the potential power of this approach, which should enable a versatile toolbox for non-covalent viral nanoparticle modification.

2.3 Materials and Methods

Chemicals and Antibodies. The lipid conjugate, 1,2-distearoyl-sn-glycero-3-phosphoethanolamine-N-[biotinyl(polyethylene glycol)2000] (DSPE-PEG₂₀₀₀-biotin), was obtained from Avanti Polar Lipids (Alabaster, AL). Rhodamine redTM-streptavidin was from Molecular Probes (Eugene OR). Gluteraldehyde, and 1,5-dimethyl-1,5-diazaundecamethylene polymethobromide (Polybrene, PB) were from Sigma Chemical

Co. (St. Louis, MO). Hydrogen peroxide 30%, and polyoxyethylene 20-sorbitan monolaurate (Tween 20) were from Fisher Scientific (Fair Lawn, NJ). Non-fat dry milk (blotting grade) was from Bio-Rad Laboratories (Hercules, CA). o-phenylenediamine dihydrochloride (OPD) was from Pierce (Rockford, IL). 5-bromo-4-chloro-3-indolyl- β -D-galactopyranoside (X-Gal) was from Denville Scientific, Inc. (Metuchen, NJ). Mouse anti-p30 was purified from the supernatant of the CRL-1219 (ATCC, Rockville, MD) hybridoma cell lines following standard procedures (18). The biotin ELISA was from MD Biosciences (St. Paul, MN). Poly-L-lysine was purchased from Sigma (St. Louis, MO).

Cell Culture. HeLa cells (human cervical kidney) and 293T/17 cells (human embryonic kidney epithelial) were cultured in Dulbecco's modified Eagle's medium (DMEM; Hyclone Labs Inc., Logan, UT) with 10% fetal bovine serum (FBS; Hyclone Labs Inc.), 100 U/mL of penicillin and 100 μ g/mL of streptomycin (Hyclone Labs Inc.). TELCeB6-A (TE671 cells stably transfected to express lacZ, Mo-MLVgagpol (28) and the amphotropic envelope glycoprotein (26)) were cultured in DMEM, 10% fetal bovine serum (Hyclone Labs, Inc.), 100 U/mL of penicillin, and 100 mg/mL of streptomycin (DMEM/FBS).

Virus Production. To generate retrovirus stocks, TELCeB6-A cells were grown to confluence in T175 tissue culture flasks, and then incubated for 24 h with 30 mL of cell culture medium (26). The virus-laden tissue culture medium was harvested, filter sterilized (0.45 μ m), then frozen (80 °C) for later use. To produce lentivirus pseudotyped with the amphotropic envelope protein, 293 cells were plated in 12-well plates coated with poly-L-lysine (2×10^6 per well), then cotransfected the next day with a mixture of Lipofectamine 2000 (Invitrogen; Carlsbad, CA), 8 μ g of the packaging construct pCMV Δ R8.91 (9), 8 μ g of lentivirus vector pTYEFnlacZ (AIDS Research and Reference Reagent Program, Bethesda, MD), and 8 μ g of the amphotropic envelope protein

expression plasmid pFB4070ASALF (53). Virus supernatants were harvested after 36 h, filter sterilized (0.45 μm), and frozen (-80 °C) for later use.

Retrovirus Modification. Amphotropic retrovirus produced from TELCEB6-2A was pelleted using overnight centrifugation at 4 °C at 6000 $\times g$, then concentrated 10-fold by resuspending them in 1/10th their original volume in tris buffered saline (TBS) that contained 6 $\mu\text{g}/\text{mL}$ solution of DSPE-PEG(2000)-biotin. Samples were gently agitated on a rotating platform for 2 h at 4 °C, and then brought to 320 $\mu\text{g}/\text{mL}$ of PB. The resulting solution was incubated for 30 min at 37 °C, centrifuged at 10,000 $\times g$ for 20 min, and then the pellet resuspended to the original volume with TBS and analyzed using an enzyme-linked immunosorbent assay (ELISA) for p30 and biotin.

ELISA for p30 and Biotin. The concentration of virus capsid protein (p30) was quantified using a previously described enzyme-linked immunosorbent assay (ELISA) (26). Briefly, ELISA plates (Nunc immuno Maxisorp 96-well plates, Nalgen Nunc International, Rochester, NY) were coated overnight at 4 °C with 10 $\mu\text{g}/\text{mL}$ of mouse anti-p30 antibody (100 $\mu\text{L}/\text{well}$) in PBS. The next day, the antibody solution was removed and blocking buffer (PBS, 0.05% Tween-20, 5% non-fat milk) added (200 $\mu\text{L}/\text{well}$) for 2 h at 37°C to block non-specific binding sites. Virus particles were lysed using 0.5% Triton-X to expose the p30 antigen, then added to the ELISA plate (100 $\mu\text{L}/\text{well}$) and incubated for 1 h at 37 °C. Bound p30 was sandwiched by the addition of the goat polyclonal anti-p30 antibody for 1 h at 37 °C (26). The horseradish peroxidase conjugated polyclonal rabbit anti-goat immunoglobulin G was then added in blocking buffer to the ELISA plate (100 $\mu\text{L}/\text{well}$) for 1 h at 37 °C to enable detection and quantitation of the sandwiched p30 antigen. The plates were developed for 5 min using hydrogen peroxide (H_2O_2) and OPD (100 $\mu\text{g}/\text{well}$) from a solution of 3 mg of OPD and 3 μL H_2O_2 in 7.5 mL of substrate buffer (24 mM citric acid-monohydrate, 51 mM $\text{Na}_2\text{HPO}_4^-$

7H₂O, pH 5.0). Sulfuric acid (8 N, 50 µL/well) was used to stop the reaction, the optical density at 490 nm was measured using an absorbance plate reader, and the non-specific background at 650 nm was subtracted. Values for replicate wells without virus were subtracted as background.

To quantify biotin levels, we used a commercially available ELISA kit according to the manufacturer's instructions (MD Biosciences). Briefly, samples were incubated on streptavidin coated plates for 30 min at room temperature. The wells were then incubated with enzyme-labeled biotin for 30 min, washed, and developed using the manufacturer's substrate (urea peroxide) and chromogen (tetramethylbenzidine). The plates were developed for 30 min. Sulfuric acid (2 N) was used to stop the reaction and the optical density at 450 nm measured using an absorbance plate reader. Values for replicate wells without virus were subtracted as background.

Fluorescence Microscopy Co-localization Assay. To determine if the lipid conjugates were directly associated with the virus particles, we modified GFP-labeled lentiviruses with DSPE-PEG₂₀₀₀-biotin and then subsequently labeled them with rhodamine-streptavidin. The lentivirus was first concentrated 10-fold using overnight centrifugation at 4 °C at 6000 × *g*. Then it was resuspended in a 6 µg/mL solution of DSPE-PEG(2000)-biotin in TBS or in TBS alone (control). After agitation on a rotating platform (2 h, 4 °C), a small aliquot of the solution was mixed at 1:1 ratio of 10 µg/mL rhodamine-streptavidin. After labeling for 5 min at 37 °C, 10µl of the mixture was visualized by epifluorescence microscopy using the 60 x lens of an inverted microscope (Olympus IX50; Melville, NY). As a control GFP-labeled lentivirus was not reacted with functionalized PEG lipid but allowed to incubate with rhodamine-streptavidin. The number of GFP-labeled virus particles co-localized with rhodamine-streptavidin and the number of GFP-labeled virus particles alone were counted and averaged over ten random fields of view.

Measurement of Lipid Conjugate Association and Dissociation Rates. To determine the rate at which DSPE-PEG₂₀₀₀-biotin modifies retrovirus, frozen *lacZ* virus stocks in culture medium were thawed, centrifuged (6000 × *g*, 4 °C) overnight, after which the pelleted virus was modified with DSPE-PEG₂₀₀₀-biotin or, as a control, mock-modified with TBS only. Samples were incubated at 37 °C or 4 °C. At intervals (after 0.5, 1, 2, and 5 h) virus particles were separated from unbound DSPE-PEG₂₀₀₀-biotin by flocculation with Polybrene (320 µg/mL) for 30 min at 37 °C, the flocculated virus pelleted by (10,000 × *g*, 20 min), the pelleted virus resuspended in TBS to its original volume, and analyzed for p30 and biotin content by ELISA.

To determine the rate at which DSPE-PEG₂₀₀₀-biotin dissociates from retrovirus, retrovirus (100 µL) was brought to 6 µg/mL of DSPE-PEG-biotin, incubated 2 h at 4 °C, flocculated with Polybrene (320 µg/mL) for 30 min at 37 °C, pelleted by centrifugation (10,000 × *g*, 30 min), resuspended in 100 µL of TBS, or TBS with 10% fetal bovine serum, and incubated for 8 hours at 37 °C or 4 °C. Next, the retroviruses were flocculated with Polybrene (320 µg/mL) for 30 min at 37 °C and pelleted by centrifugation (10,000 × *g*, 30 min) to separate them from newly dissociated DSPE-PEG₂₀₀₀-biotin, and then resuspended to their original volume in TBS and the amount of DSPE-PEG-biotin still associated with them quantified by ELISA.

Streptavidin Binding Assay. To examine the effect of the lipid conjugates on the ability of the viruses to bind to streptavidin, amphotropic virus stocks were concentrated 10-fold by centrifuging (6000 × *g*, 4 °C) them overnight and then resuspending the pelleted virus in TBS to 1/10th their original volume. The concentrated virus was incubated (2 h, 4 °C) with DSPE-PEG₂₀₀₀-biotin (6 µg/mL) in TBS. The virus particles, now modified DSPE-PEG₂₀₀₀-biotin, were separated from unbound DSPE-PEG₂₀₀₀-biotin by flocculation with Polybrene (320 µg/mL) for 30 min at

37 °C, the flocculated virus pelleted by (10,000 × *g*, 20 min), the pelleted virus resuspended in NaCl (1 M) and applied to a streptavidin coated plate. A small aliquot of each sample was taken, before it was applied to the coated plate, and the amount of p30 quantified by ELISA. To accelerate virus binding, the plate was centrifuged (3000 × *g*) for 30 min at room temperature. The wells were then washed (3 times, 200 μL) with the biotin ELISA wash buffer (10 mM PBS salt, pH7.4 and tween 20; MD Bioscience) to remove unbound virus. To quantify the amount of bound virus, the wells were incubated (30 min at 37 °C) with lysis buffer (100 μl) and the amount of p30 in the lysis buffer quantified by ELISA. The amount of p30 that bound to the wells, as a fraction of the total amount that was added to the wells, was calculated.

Diluted Titer Assay. Ten-fold serial dilutions of *lacZ* virus stock were made in DMEM/BCS and Polybrene (8 μg/mL). A 1-mL amount per well was used to transduce HeLa cells that had been seeded (8 × 10⁴ per well) the previous day in a 12-well plate. Two days after the start of the transduction, the cells were fixed and stained for β-galactosidase activity with X-Gal. Colonies of *lacZ*⁺ cells (typically in clusters of 2, 4, or 8 blue cells) were counted with the aid of a dissecting microscope. At appropriate dilutions of the virus stock, the clusters of blue cells were sufficiently spread over the dish such that each cluster arose from a single transduction event. From triplicate wells, the number of *lacZ*⁺ CFU per milliliter of virus produced from TELCeB6-A cell line was approximately 2.5 ± 0.1 × 10⁶. The titer of the virus after it was modified with DSPE-PEG₂₀₀₀-biotin was 5.6 ± 0.4 × 10⁶ CFU/mL.

Statistical Analysis. Data are summarized as the mean ± one standard deviation for triplicate samples. Statistical analysis was performed using one-way analysis of variance for repeated measurements of the same variable. The Tukey

multiple comparison test was used to conduct pairwise comparisons between means. Differences at $p < 0.05$ were considered statistically significant.

2.4 Results

As a first step to determine if lipid conjugates can modify the surfaces of retroviruses, we incubated (2 h, 4 °C) *lacZ* amphotropic retrovirus with DSPE-PEG-biotin (6 µg/mL, Figure 2.1). Next, to separate the retroviruses from unincorporated lipid conjugate, we flocculated them with Polybrene (PB; 320 µg/mL), pelleted the resultant flocs of virus by low speed centrifugation (4 °C, 30 min, 10,000 x g), and then resuspended them to their original volume in tris-buffered saline (TBS). As a control, we processed lipid conjugate solutions that did not contain any virus using the same procedure. The amount of virus (i.e., virus capsid protein, p30) and biotin in the samples were quantified by ELISA. As expected, we found that most of the virus particles (about 80%) were in the pellet (Figure 2.2A). Significant amounts of biotin were detected in the pellet, but only when virus particles were present in the sample (Figure 2.2B), which suggests that the lipid conjugates were physically associated with the virus particles.

To determine if the lipid conjugates were directly associated with the retrovirus particles, we incubated (2 h, 4 °C) stocks of GFP-labeled amphotropic lentivirus with DSPE-PEG-biotin (6 µg/mL), or in TBS as a control, added rhodamine-streptavidin (10 mM) to the stocks, and then visualized the samples by epifluorescence microscopy (Figure 2.3 A-D). Several random fields of view were observed, and the fraction of viruses that were colocalized with the red fluorophore (rhodamine) was determined (Figure 2.3 E). Most of the GFP-labeled viruses co-localized with rhodamine (94% ± 4%), which suggests that the lipid conjugates directly associate with, and physically modify the surfaces of, retroviruses and lentiviruses.

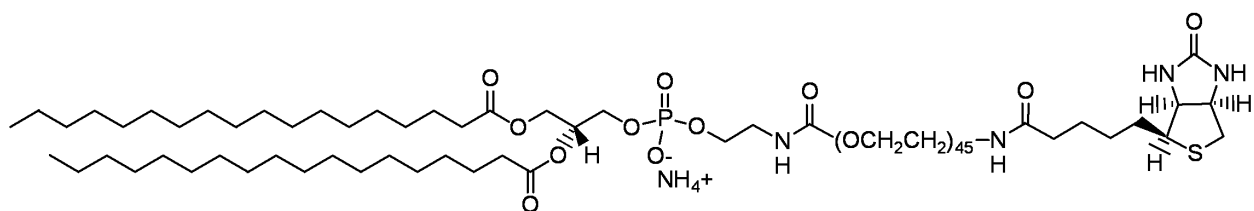


Figure 2.1 Structure of the DSPE-PEG-biotin (1,2-distearoyl-*sn*-glycero-3-phosphoethanolamine-N-[biotinyl(polyethylene glycol)2000]) lipid conjugate used to modify the retrovirus particles.

A.

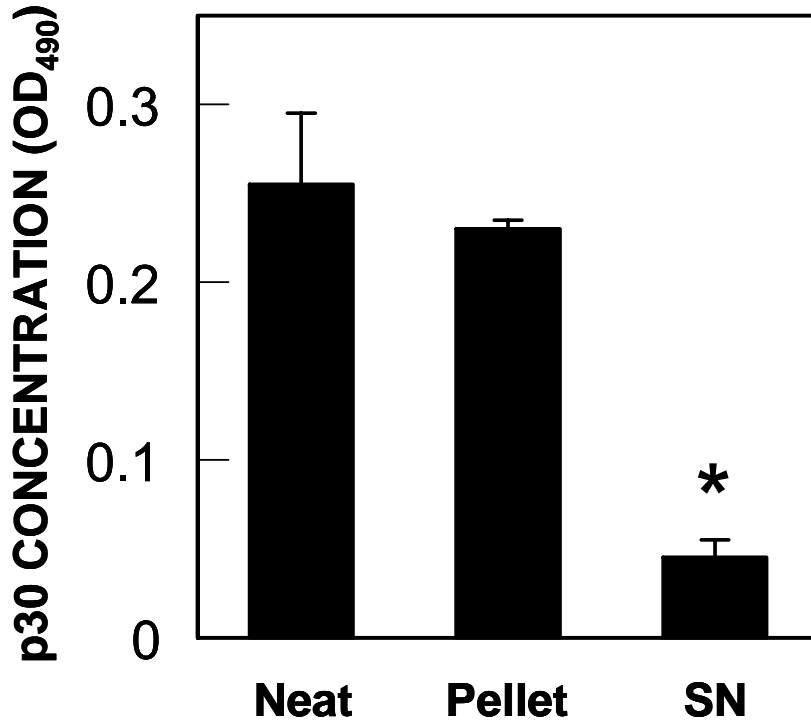


Figure 2.2 (A). The DSPE-PEG-biotin lipid conjugate co-purifies with retroviruses. Retrovirus stock (100 μ L), or tris buffered saline (TBS) as a control, was brought to 6 μ g/mL of DSPE-PEG-biotin, incubated for 2 h at 4 $^{\circ}$ C, and then flocculated with Polybrene (320 μ g/mL) for 30 min at 37 $^{\circ}$ C. The flocculated virus was pelleted by centrifugation (10,000 \times g, 30 min), the supernatant decanted, and the pelleted virus resuspended to its original volume (100 μ L) in TBS. The concentration of (a) virus capsid protein (p30) in the original virus stock (NEAT), resuspended pellet (Pellet), and the decanted supernatant (SN) was quantified using an ELISA for p30. Statistically significant differences ($p < 0.05$) from the original virus stock (NEAT) are denoted with an asterisk.

B.

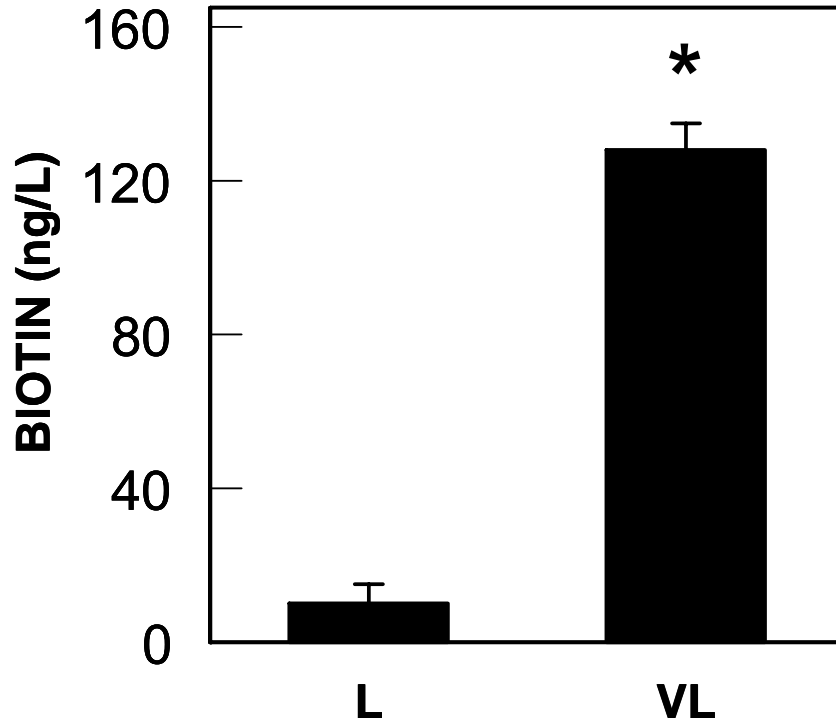


Figure 2.2 (B). The DSPE-PEG-biotin lipid conjugate co-purifies with retroviruses. Retrovirus stock (100 μ L), or tris buffered saline (TBS) as a control, was brought to 6 μ g/mL of DSPE-PEG-biotin, incubated for 2 h at 4 $^{\circ}$ C, and then flocculated with Polybrene (320 μ g/mL) for 30 min at 37 $^{\circ}$ C. The flocculated virus was pelleted by centrifugation (10,000 \times g , 30 min), the supernatant decanted, and the pelleted virus resuspended to its original volume (100 μ L) in TBS. The concentration of (b) biotin in the resuspended virus pellet (VL) and control pellet (L) was quantified using an ELISA for biotin. Statistically significant differences ($p < 0.05$) from the control pellet (L) are denoted with an asterisk. Each point shows the mean and standard deviation of at least three replicate experiments.

Next we wanted to determine the rate at which the lipid conjugates modified the viruses since, to be of practical use, modification would need to take place more rapidly than the rate at which viruses spontaneously decay and lose their activity. To determine if the lipid conjugates modify retrovirus particles on a time scale significantly shorter than the decay rate of the viruses, we incubated retrovirus stocks with DSPE-PEG-biotin (6 $\mu\text{g/mL}$) at 4 °C for up to 5 hours, after which we flocculated and centrifuged the viruses to separate them from unincorporated lipid conjugates. The amount of virus and lipid conjugate in the pellet was then quantified by ELISA (Figure 2.4). No significant differences ($p > 0.05$) in the amount of biotin that was incorporated into the virus particles were observed, even when the virus was incubated with the conjugate for only 30 minutes. These results indicate that the modification reaction occurs rapidly (i.e., in less than 30 minutes) and on a much shorter time scale than virus decay, which occurs with a half-life of about 7.5 hours at 37 °C and 14 days at 4 °C (27).

Next, to determine if the lipid conjugates remain stably associated with the virus particles, we incubated retrovirus, which had been previously modified with DSPE-PEG-biotin as described above, in TBS or in TBS and 10% fetal bovine serum (FBS) for 8 hours at 4 °C or 37 °C. We separated the retroviruses from unincorporated lipid conjugate by flocculation and centrifugation, and then quantified the amount of virus and lipid conjugate in the pellet by p30 and biotin ELISA. We found that after 8 hours, 75 to 90% of the lipid conjugates remained associated with the virus particles (Figure 2.5). The results suggest that more lipid conjugate disassociated from virus in the presence of serum (25%) than in its absence (10%), but the differences were not statistically significant ($p > 0.05$).

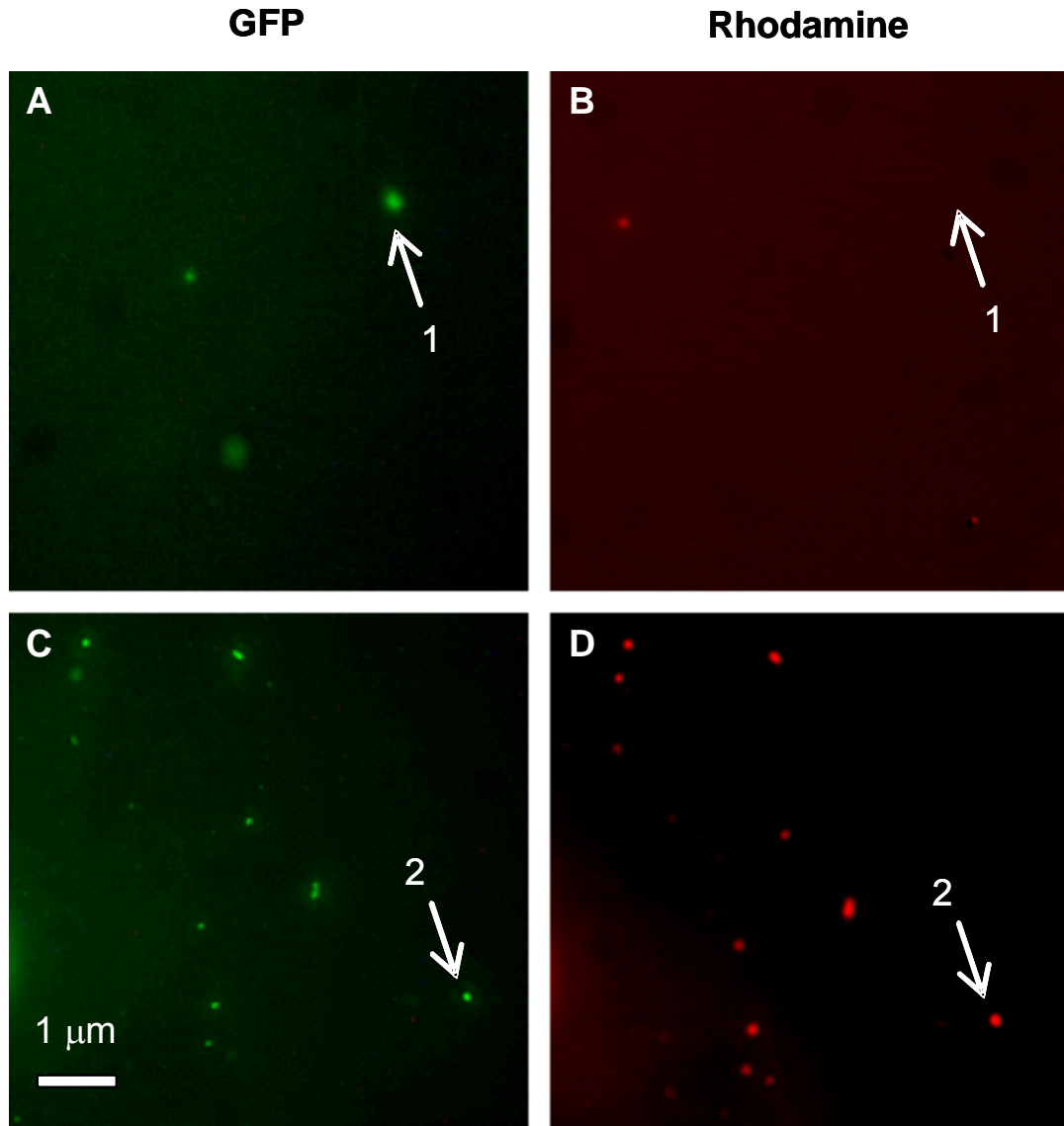


Figure 2.3 (A-D). The DSPE-PEG-biotin lipid conjugate co-localizes with lentiviruses. GFP-labeled lentivirus (100 μ L) (1×10^6 cfu/mL) was incubated (2 h at 4 $^{\circ}$ C) with DSPE-PEG(2000)-biotin (2 μ M) in TBS (modified) or with TBS only as a control (unmodified). Next, the samples were flocculated with Polybrene (320 μ g/mL) for 30 min at 37 $^{\circ}$ C, pelleted by centrifugation (10,000 \times g , 30 min) to separate the virus particles from excess unbound DSPE-PEG-biotin, and 10 μ L of this sample was incubated (5 min at 37 $^{\circ}$ C) with 10 μ L solution of 5 μ g/mL rhodamine-streptavidin in TBS. After incubation, 10 μ L of the sample was visualized by epifluorescence microscopy (60 \times). Arrow 1 shows that, in samples of unmodified virus, (a) GFP fluorescence does not colocalize with (b) rhodamine fluorescence. Arrow 2 shows that, in samples of viruses modified with lipid conjugate, (c) GFP fluorescence colocalizes with (d) rhodamine fluorescence. The scale bar is 1 μ m long.

Figure 2.3 (continued)

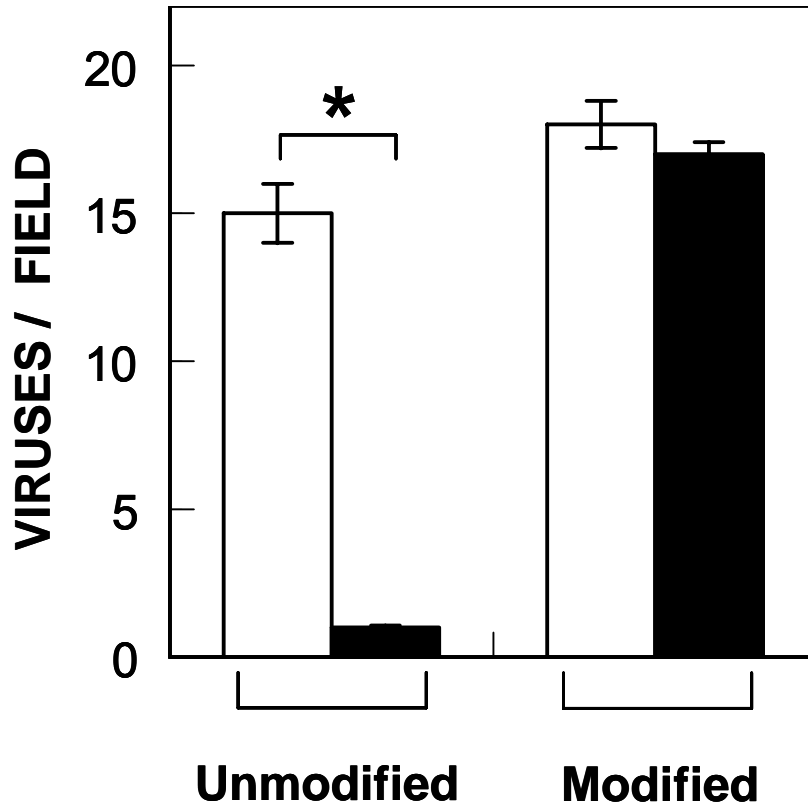


Figure 2.3 (E) Modified virus particles co-localize with streptavidin. The total number of particles (open bars) and the number of particles that colocalized with rhodamine-streptavidin (closed bars) were counted in the modified and unmodified virus samples. Ten random fields of view were observed. Statistically significant differences ($p < 0.05$) from the total number of virus particles counted are denoted with an asterisk. Each point shows the mean and standard deviation.

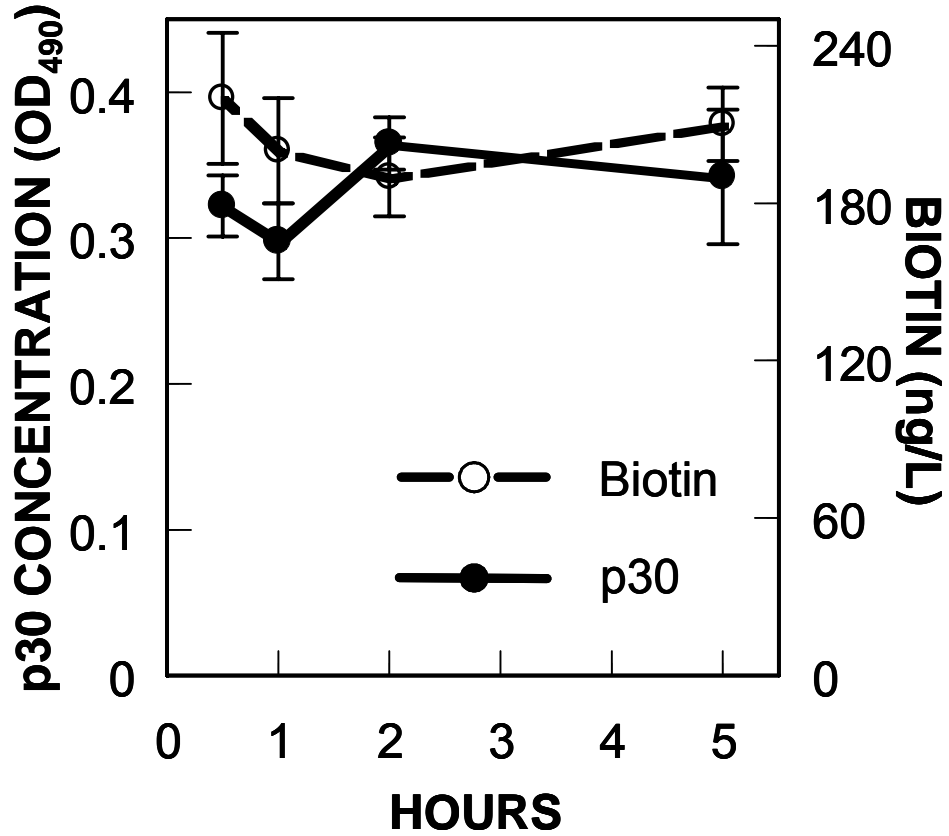


Figure 2.4 Lipid conjugates rapidly associate with retroviruses. Retrovirus stock (100 μL) was brought to 6 $\mu\text{g}/\text{mL}$ of DSPE-PEG-biotin and incubated at 4 $^{\circ}\text{C}$ for 0.5, 1, 2, 5 hours. Next, to separate the virus particles from excess unbound DSPE-PEG-biotin, the samples were flocculated with Polybrene (320 $\mu\text{g}/\text{mL}$) for 30 min at 37 $^{\circ}\text{C}$, pelleted by centrifugation (10,000 $\times g$, 30 min), and resuspended in TBS (100 μL). The amount of p30 (\bullet) and biotin (\circ) in the resuspended pellets were quantified by ELISA. No statistical differences were observed in the amount of biotin at different time points ($p < 0.05$). Each point shows the mean and standard deviation of at least three replicate experiments.

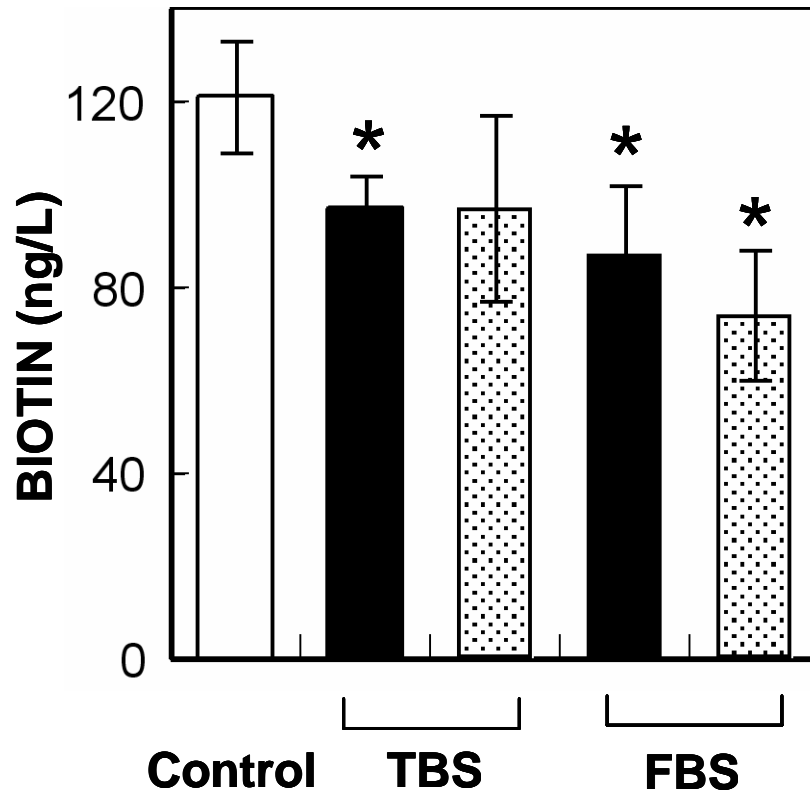


Figure 2.5 Lipid conjugates stably associate with retroviruses. Retrovirus stock (100 μ L) was brought to 6 μ g/mL of DSPE-PEG-biotin, incubated for 2 h at 4 $^{\circ}$ C, flocculated with Polybrene (320 μ g/mL) for 30 min at 37 $^{\circ}$ C, pelleted by centrifugation (10,000 \times g , 30 min), resuspended in 100 μ L of TBS (TBS) or TBS with 10% fetal bovine serum (FBS), and incubated for 8 hours at 37 $^{\circ}$ C or 4 $^{\circ}$ C. To separate the retroviruses from excess unbound DSPE-PEG-biotin, the samples were flocculated with Polybrene (320 μ g/mL) for 30 min at 37 $^{\circ}$ C, pelleted by centrifugation (10,000 \times g , 30 min), and resuspended to their original volume in TBS. Biotin in the virus samples before incubation (Control; open bar) and in the virus samples that were incubated for 8 hours at 37 $^{\circ}$ C (closed bars) and at 4 $^{\circ}$ C (stippled bars) were quantified by ELISA. Statistically significant differences ($p < 0.05$) from the Control were denoted with an asterisk. Each point shows the mean and standard deviation of at least three replicate experiments.

To determine if the modification of the viruses changed their binding properties, we incubated (30 min, 25 °C) modified retroviruses, or unmodified retroviruses as a control, in streptavidin-coated plates (70 $\mu\text{L}/\text{well}$), washed the plates three times (200 $\mu\text{L}/\text{well}$) to remove unbound or loosely bound virus, and then quantified the amount of bound virus by ELISA (Figure 2.6). The wells that had been incubated with modified virus contained 3-fold more virus than the wells that had been incubated with unmodified virus, which indicates that modification of the retroviruses with the biotinylated lipid conjugates increased their ability to bind streptavidin. Finally, to determine if lipid-modification altered the infectivity of the viruses, we measured the titer of modified and unmodified *lacZ* amphotropic retrovirus. Interestingly, titers of the modified viruses were more than two fold higher ($5.6 \pm 0.4 \times 10^6$) than the unmodified viruses ($2.5 \pm 0.1 \times 10^6$) ($p < 0.05$). To summarize the above results, we have found that the DSPE-PEG-biotin conjugates rapidly and stably modified the retrovirus particles, do not reduce their ability to infect cells, and increased by more than three-fold the number of viruses that bound to streptavidin-coated plates, illustrating a dramatic change in their surface properties.

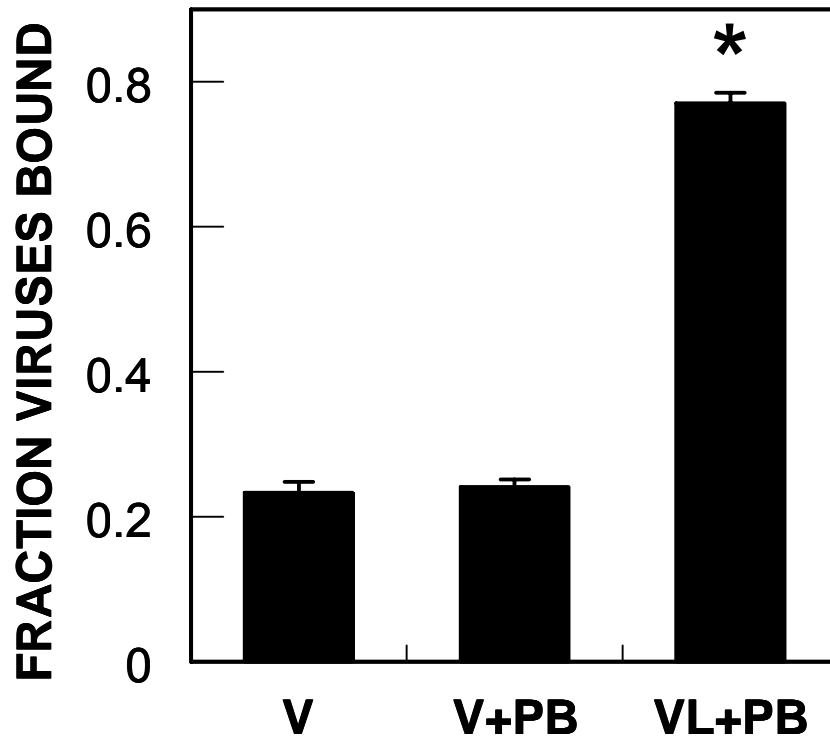


Figure 2.6 Retroviruses modified with the DSPE-PEG-biotin lipid conjugate bind to streptavidin-coated plates. Overnight centrifuged (4 °C at 6000 × *g*) virus stock was concentrated 10-fold in TBS and incubated (2 h at 4 °C) with DSPE-PEG-biotin (6 μg/mL) in TBS (VL+PB), or, as a control, with TBS only (V+PB). Next, the virus was flocculated with Polybrene (320 μg/mL), pelleted by centrifugation (10,000 × *g*, 30 min), resuspended to its original volume (100 μL) in 1 M NaCl, added to a well of a streptavidin coated plate, and centrifuged (3000 × *g*) for 30 min at room temperature. Wash buffer (3 times, 200 μL) was used to remove unbound virus, after which bound virus was resuspended with lysis buffer (100 μL), incubated for 30 min, and quantified by p30 ELISA. We also incubated unmodified virus, in the absence of any Polybrene (V), with streptavidin coated plates as a negative control. The amount of p30 that bound to the wells, as a fraction of the total amount that was added to the wells, is shown. Statistically significant differences ($p < 0.05$) from unmodified virus (V) are denoted with an asterisk. Each point shows the mean and standard deviation of at least three replicate experiments.

2.5 Discussion

Lipids and lipid conjugates have been previously used to label viruses or to create virus-like particles, but this is the first study, to our knowledge, to use lipid conjugates to modify the binding properties of retroviruses. Hoekstra et al. used octadecyl-rhodamine B, an amphiphilic fluorescent lipid dye, to label the lipid bilayers of influenza and Sendai virus particles (20). The dye spontaneously incorporated into the lipid bilayer of the viruses in just one hour at room temperature, and incorporation of the dye did not adversely affect the ability of the viruses to fuse with target cells (3, 20, 46). The work by Hoekstra et al showed that it is possible to insert lipids into the viral membrane without affecting their function. Lipid conjugates have also been used to confer new functions to lipid bilayers derived from viruses. For example, Mastrobattista et al. generated virus-like particles by using detergent to solubilize the lipid bilayers of intact influenza viruses, which were then incubated with PEGylated lipid conjugates (30). The lipid conjugates were coupled to anti-epithelial glycoprotein-2 antibodies, which enabled the virus-like particles to efficiently bind to ovarian carcinoma cells (30, 46). The experiments of Mastrobattista et al showed that lipid conjugates can be used to alter the binding properties of virus-like particles, but the method used is not suitable for retroviruses since detergent solubilization would inactivate them. In this study, we showed that lipid conjugates can be used to modify the binding properties of retrovirus particles without adversely affecting their ability to infect cells.

The model lipid conjugate we used consisted of three components: a lipid anchor (DSPE), a flexible linker (PEG), and a binding moiety (biotin). In principle, it should be possible to fine tune the physico-chemical characteristics of each of these components to optimize the effect the conjugate has on retrovirus binding and infection. The lipid anchor is expected to control the extent and stability with which the conjugates are

incorporated into the viruses, the flexible linker is likely to influence the extent to which the viruses bind to cells via non-specific interactions, and the binding moiety will dictate which receptor and cell types the viruses bind to. For example, several previous studies with liposomes suggest that the stability of lipid conjugates in phospholipid bilayers depends to a large extent on the structure and length of their lipid anchor and the lipids that compose the bilayer into which they are being inserted (11, 21, 40). Pownall et al. found that lipid conjugates constructed with short alkyl chains (C_6 and C_{12}), transfer quickly out of lipid membranes because of their higher solubility in water as compared to conjugates with long alkyl chains (i.e., C_{16}) which have stronger lipid-lipid hydrophobic interactions (21, 36). Schutz et al. found that DMPE (1,2-dimyristoyl-*sn*-glycero-3-phosphoethanolamine), a lipid probe composed of long saturated lipid alkyl chains, preferentially partitioned into detergent resistant regions of cellular membranes, which are largely composed of saturated alkyl chains with structures similar to that of DMPE (21, 42). This and other studies suggest that lipid conjugates incorporate most efficiently into target membranes composed of lipids with similar structures (25, 37, 42). In addition, several investigators have found that lipid conjugates composed of long saturated double-chain anchors remain incorporated in cellular lipid membranes longer than their monounsaturated double chain counterparts (7, 21, 25, 42). Based on these findings, we used DSPE for the lipid anchor of our lipid conjugates because it is long (C_{18}), saturated, double chained, and contains alkyl groups that are similar in structure to phosphatidylethanolamine (PE), a lipid that is present in abundance in the lipid bilayer of retroviruses (6).

It is also interesting to consider how the physical characteristics of the flexible linker will affect the function of the lipid conjugates. The flexible linker, if appropriately designed, could be used to shield the virus particles from binding to non-targeted molecules or surfaces (5, 10, 19, 31). For example, Croyle et al. covalently linked PEG chains to free lysine residues on the surfaces of VSV-G pseudotyped lentiviruses, which protected the viruses from being bound to and inactivated by antibodies and

complement in human and mouse sera (10). The extent to which PEG chains are able to shield surfaces is primarily controlled by their length and number density (34). We estimate, based on our measurements of virus-associated biotin (see Figure 2b), and assuming that the number of particles in our virus stocks was about 100-fold higher than their infectious titers (1, 27), that our modified virus particles contained about 500 biotinylated lipid conjugates, or less than 2 mol% PEGylated lipid (14, 22). Previous work showed that PEG chains of similar molecular weight as ours, when present at similarly low concentrations, protrude only about 7 nm from the surface of the lipid bilayer to which they are anchored (50). In contrast, retroviral envelope proteins extend about 10 nm from the virus surface, which may explain why the lipid conjugates used in our study did not reduce virus titers (16). In the future, it will be interesting to examine how changes in the length and density of the PEG chains affect virus binding and transduction, and to optimize the design of the lipid conjugates so that they are able to reduce the extent to which retroviruses bind to non-targeted cell types while still retaining their ability to efficiently bind to and transduce cells that express the targeted receptor.

In conclusion, we have developed a novel method for modifying the surfaces of retrovirus particles with lipid conjugates. The lipid conjugate used in this study, DSPE-PEG-biotin, was composed of three distinct elements, each of which can be modified as needed to achieve the desired effect on retrovirus binding and infection. We envision that lipid conjugates, similar to those used in this study, may prove useful for protecting viral vectors from complement inactivation, or for targeting them to specific cell types, or for improving their performance in vaccination protocols, such as by targeting them to specific types of immune system cells, or by using the lipid conjugates as adjuvants to alter the immunogenicity of the virus particles.

2.6 References

1. Andreadis, S., T. Lavery, H. E. Davis, J. M. Le Doux, M. L. Yarmush, and J. R. Morgan. 2000. Toward a more accurate quantitation of the activity of recombinant retroviruses: alternatives to titer and multiplicity of infection. *J Virol* 74:3431-9.
2. Bethell, D., M. Brust, D. J. Schiffrin, and C. Kiely. 1996. From monolayers to nanostructured materials: An organic chemist's view of self-assembly. *Journal of Electroanalytical Chemistry* 409:137-143.
3. Blumenthal, R., S. A. Gallo, M. Viard, Y. Raviv, and A. Puri. 2002. Fluorescent lipid probes in the study of viral membrane fusion. *Chem Phys Lipids* 116:39-55.
4. Boal, A. K., and V. M. Rotello. 2000. Fabrication and self-optimization of multivalent receptors on nanoparticle scaffolds. *J. Am. Chem. Soc.* 122:734-735.
5. Boeckle, S., and E. Wagner. 2006. Optimizing targeted gene delivery: chemical modification of viral vectors and synthesis of artificial virus vector systems. *Aaps J* 8:E731-42.
6. Brugger, B., B. Glass, P. Haberkant, I. Leibrecht, F. T. Wieland, and H. G. Krausslich. 2006. The HIV lipidome: a raft with an unusual composition. *Proc Natl Acad Sci U S A* 103:2641-6.
7. Chung, H. A., K. Kato, C. Itoh, S. Ohhashi, and T. Nagamune. 2004. Casual cell surface remodeling using biocompatible lipid-poly(ethylene glycol)(n): development of stealth cells and monitoring of cell membrane behavior in serum-supplemented conditions. *J Biomed Mater Res A* 70:179-85.
8. Collins, S. A., B. A. Guinn, P. T. Harrison, M. F. Scallan, G. C. O'Sullivan, and M. Tangney. 2008. Viral vectors in cancer immunotherapy: which vector for which strategy? *Curr Gene Ther* 8:66-78.
9. Cosset, F. L., Y. Takeuchi, J. L. Battini, R. A. Weiss, and M. K. Collins. 1995. High-titer packaging cells producing recombinant retroviruses resistant to human serum. *J Virol* 69:7430-6.
10. Croyle, M. A., S. M. Callahan, A. Auricchio, G. Schumer, K. D. Linse, J. M. Wilson, L. J. Brunner, and G. P. Kobinger. 2004. PEGylation of a vesicular stomatitis virus G pseudotyped lentivirus vector prevents inactivation in serum. *J Virol* 78:912-21.
11. Cullis, P. R., and A. Chonn. 1998. Recent advances in liposome technologies and their applications for systemic gene delivery. *Adv Drug Deliv Rev* 30:73-83.
12. Dennis, J. E., N. Cohen, V. M. Goldberg, and A. I. Caplan. 2004. Targeted delivery of progenitor cells for cartilage repair. *J Orthop Res* 22:735-41.

13. Elghanian, R., J. J. Storhoff, R. C. Mucic, R. L. Letsinger, and C. A. Mirkin. 1997. Selective colorimetric detection of polynucleotides based on the distance-dependent optical properties of gold nanoparticles. *Science* 277:1078-81.
14. Enoch, H. G., and P. Strittmatter. 1979. Formation and properties of 1000-Å-diameter, single-bilayer phospholipid vesicles. *Proc Natl Acad Sci U S A* 76:145-9.
15. Etienne-Julan, M., P. Roux, S. Carillo, P. Jeanteur, and M. Piechaczyk. 1992. The efficiency of cell targeting by recombinant retroviruses depends on the nature of the receptor and the composition of the artificial cell-virus linker. *J Gen Virol* 73 (Pt 12):3251-5.
16. Forster, F., O. Medalia, N. Zauberman, W. Baumeister, and D. Fass. 2005. Retrovirus envelope protein complex structure in situ studied by cryo-electron tomography. *Proc Natl Acad Sci U S A* 102:4729-34.
17. Goff, S. P. 2007. Host factors exploited by retroviruses. *Nat Rev Microbiol* 5:253-63.
18. H. Harlow, and D. Lane. 1998. *Antibodies: A Laboratory Manual*. Cold Spring Harbor Laboratory Press, Cold Spring Harbor
19. Heyes, J., K. Hall, V. Taylor, R. Lenz, and I. MacLachlan. 2006. Synthesis and characterization of novel poly(ethylene glycol)-lipid conjugates suitable for use in drug delivery. *J Control Release* 112:280-90.
20. Hoekstra, D., T. de Boer, K. Klappe, and J. Wilschut. 1984. Fluorescence method for measuring the kinetics of fusion between biological membranes. *Biochemistry* 23:5675-81.
21. Hoekstra, D., and N. Duzgunes. 1993. Lipid mixing assays to determine fusion in liposome systems. *Methods Enzymol* 220:15-32.
22. Huang, C., and J. T. Mason. 1978. Geometric packing constraints in egg phosphatidylcholine vesicles. *Proc Natl Acad Sci U S A* 75:308-10.
23. Kafri, T. 2004. Gene delivery by lentivirus vectors an overview. *Methods Mol Biol* 246:367-90.
24. Kasahara, N., A. M. Dozy, and Y. W. Kan. 1994. Tissue-specific targeting of retroviral vectors through ligand-receptor interactions. *Science* 266:1373-6.
25. Kato, K., C. Itoh, T. Yasukouchi, and T. Nagamune. 2004. Rapid protein anchoring into the membranes of Mammalian cells using oleyl chain and poly(ethylene glycol) derivatives. *Biotechnol Prog* 20:897-904.
26. Landazuri, N., and J. M. Le Doux. 2004. Complexation of retroviruses with charged polymers enhances gene transfer by increasing the rate that viruses are delivered to cells. *J Gene Med* 6:1304-19.

27. Le Doux, J. M., H. E. Davis, J. R. Morgan, and M. L. Yarmush. 1999. Kinetics of retrovirus production and decay. *Biotechnol Bioeng* 63:654-62.
28. Marandin, A., A. Dubart, F. Pflumio, F. L. Cosset, V. Cordette, S. Chapel-Fernandes, L. Coulombel, W. Vainchenker, and F. Louache. 1998. Retrovirus-mediated gene transfer into human CD34+38low primitive cells capable of reconstituting long-term cultures in vitro and nonobese diabetic-severe combined immunodeficiency mice in vivo. *Hum Gene Ther* 9:1497-511.
29. Marsh, M., and A. Helenius. 2006. Virus entry: open sesame. *Cell* 124:729-40.
30. Mastrobattista, E., P. Schoen, J. Wilschut, D. J. Crommelin, and G. Storm. 2001. Targeting influenza virosomes to ovarian carcinoma cells. *FEBS Lett* 509:71-6.
31. Mok, H., D. J. Palmer, P. Ng, and M. A. Barry. 2005. Evaluation of polyethylene glycol modification of first-generation and helper-dependent adenoviral vectors to reduce innate immune responses. *Mol Ther* 11:66-79.
32. Neda, H., C. H. Wu, and G. Y. Wu. 1991. Chemical modification of an ecotropic murine leukemia virus results in redirection of its target cell specificity. *J Biol Chem* 266:14143-6.
33. Overbaugh, J., A. D. Miller, and M. V. Eiden. 2001. Receptors and entry cofactors for retroviruses include single and multiple transmembrane-spanning proteins as well as newly described glycoposphatidylinositol-anchored and secreted proteins. *Microbiol Mol Biol Rev* 65:371-89, table of contents.
34. Papisov, M. I. 1998. Theoretical considerations of RES-avoiding liposomes: Molecular mechanics and chemistry of liposome interactions. *Adv Drug Deliv Rev* 32:119-138.
35. Pickl, W. F., F. X. Pimentel-Muinos, and B. Seed. 2001. Lipid rafts and pseudotyping. *J Virol* 75:7175-83.
36. Pownall, H. J., and L. C. Smith. 1989. Pyrene-labeled lipids: versatile probes of membrane dynamics in vitro and in living cells. *Chem Phys Lipids* 50:191-211.
37. Rabuka, D., M. B. Forstner, J. T. Groves, and C. R. Bertozzi. 2008. Noncovalent cell surface engineering: incorporation of bioactive synthetic glycopolymers into cellular membranes. *J Am Chem Soc* 130:5947-53.
38. Raschke, G., S. Kowarik, T. Franzl, C. Sonnichsen, T. A. Klar, J. Feldmann, A. Nichtl, and L. Kurzinger. 2003. Biomolecular recognition based on single gold nanoparticle light scattering. *Nano Lett* 3:935-938.
39. Roux, P., P. Jeanteur, and M. Piechaczyk. 1989. A versatile and potentially general approach to the targeting of specific cell types by retroviruses: application to the infection of human cells by means of major histocompatibility complex class I and class II antigens by mouse ecotropic murine leukemia virus-derived viruses. *Proc Natl Acad Sci U S A* 86:9079-83.

40. Rovira-Bru, M., D. H. Thompson, and I. Szleifer. 2002. Size and structure of spontaneously forming liposomes in lipid/PEG-lipid mixtures. *Biophys J* 83:2419-39.
41. Saul, J. M., A. Annapragada, J. V. Natarajan, and R. V. Bellamkonda. 2003. Controlled targeting of liposomal doxorubicin via the folate receptor in vitro. *J Control Release* 92:49-67.
42. Schutz, G. J., G. Kada, V. P. Pastushenko, and H. Schindler. 2000. Properties of lipid microdomains in a muscle cell membrane visualized by single molecule microscopy. *Embo J* 19:892-901.
43. Smith, J. C., K. B. Lee, Q. Wang, M. G. Finn, J. E. Johnson, M. Mrksich, and C. A. Mirkin. 2003. Nanopatterning the chemospecific immobilization of cowpea mosaic virus capsid. *Nano Lett* 3:883-886.
44. Snitkovsky, S., and J. A. Young. 2002. Targeting retroviral vector infection to cells that express heregulin receptors using a TVA-heregulin bridge protein. *Virology* 292:150-5.
45. Sommerfelt, M. A. 1999. Retrovirus receptors. *J Gen Virol* 80 (Pt 12):3049-64.
46. Stegmann, T., H. W. Morselt, F. P. Booy, J. F. van Breemen, G. Scherphof, and J. Wilschut. 1987. Functional reconstitution of influenza virus envelopes. *Embo J* 6:2651-9.
47. Taylor, C. S., D. Lavillette, M. Marin, and D. Kabat. 2003. Cell surface receptors for gammaretroviruses. *Curr Top Microbiol Immunol* 281:29-106.
48. Waehler, R., S. J. Russell, and D. T. Curiel. 2007. Engineering targeted viral vectors for gene therapy. *Nat Rev Genet* 8:573-87.
49. Wang, Q., T. Lin, L. Tang, J. E. Johnson, and M. G. Finn. 2002. Icosahedral virus particles as addressable nanoscale building blocks. *Angew Chem Int Ed Engl* 41:459-62.
50. Woodle, M. C., L. R. Collins, E. Sponsler, N. Kossovsky, D. Papahadjopoulos, and F. J. Martin. 1992. Sterically stabilized liposomes. Reduction in electrophoretic mobility but not electrostatic surface potential. *Biophys J* 61:902-10.
51. Yamada, T., Y. Iwasaki, H. Tada, H. Iwabuki, M. K. Chuah, T. VandenDriessche, H. Fukuda, A. Kondo, M. Ueda, M. Seno, K. Tanizawa, and S. Kuroda. 2003. Nanoparticles for the delivery of genes and drugs to human hepatocytes. *Nat Biotechnol* 21:885-90.
52. Zhao, Y., L. Zhu, S. Lee, L. Li, E. Chang, N. W. Soong, D. Douer, and W. F. Anderson. 1999. Identification of the block in targeted retroviral-mediated gene transfer. *Proc Natl Acad Sci U S A* 96:4005-10.
53. Zufferey, R., D. Nagy, R. J. Mandel, L. Naldini, and D. Trono. 1997. Multiply attenuated lentiviral vector achieves efficient gene delivery in vivo. *Nat Biotechnol* 15:871-5.

CHAPTER 3

ALTERATION OF VIRAL LIPID COMPOSITION BY MYRIOCIN REDUCES RETROVIRAL INFECTIVITY

3.1 Abstract

The lipids of enveloped viruses play an important role in virus morphogenesis and infectivity. These lipids are derived from host cell membranes during virus budding, which has been shown to occur in regions of the host cell that are enriched in cholesterol and sphingomyelin. Sphingolipids have been implicated in a variety of pathogens to help facilitate the process by which viruses enter cells. In this study, we used the fungal endotoxin myriocin (ISP-1) to inhibit *de novo* sphingolipid synthesis in virus producer cells. We examined the effect on the lipid composition of virus producing cells and the virus particles produced from them. Our results suggest that treating virus producer cells with ISP-1 can significantly alter the lipid composition of the viruses that they produce, and that these particles exhibit reduced infectivity in a cell-type dependant manner. We investigated different steps involved in the virus infection pathway and found that virus particles produced from ISP-1 treated cells are less fusogenic as compared to viruses produced from untreated cells. The implications of these results to improve gene therapy vectors and anti-retroviral therapies are discussed.

3.2 Introduction

Enveloped retrovirus vectors are one of the most commonly used viral vectors in clinical human gene therapy protocols (Wiley 2008). Generally, the nucleic acid and protein content of amphotropic murine leukemia virus (A-MLV) are manipulated to enhance and control gene transfer (Wiley 2008). The lipid composition of the viral vector is almost never altered in these protocols, mainly because the role of lipids in

virus fusion and infection, and the means to manipulate lipid composition, are less well established.

Retroviral entry into host cells is mediated by specific interactions between the virus envelope proteins and their cognate cellular receptors (1, 3). Specifically, A-MLV surface glycoprotein gp70 initiates infection by binding to Pit2, which is a sodium-dependant phosphate transporter that resides on the cell surface (8, 18). This interaction triggers irreversible conformational changes in the envelope protein which allow the outer leaflets of the virus and cell lipid bilayers to mix and fuse in a process called hemifusion (1, 23). Subsequently, the inner lipid bilayer leaflets complete the fusion process by inducing the formation of a pore, which allows the delivery of the virus capsid into the cytoplasm of the host cell (2, 23). Although the impact of altering the composition of the virus lipid bilayer is unclear, there is increasing evidence that the lipid composition of virus particles plays a key role in virus function and may potentially be an important means to control gene transfer.

Accumulating evidence suggests that lipids within the viral membrane are not incorporated randomly, and are heavily enriched in cholesterol and sphingomyelin (SM), possibly because retroviruses bud from specialized sites within the plasma membrane, called lipid rafts (15). Previous studies have shown that cholesterol is important in retroviral membrane integrity and function. Treatment of retroviruses with beta-cyclodextrin, a cyclic oligosaccharide that sequesters cholesterol, changed the morphology of the viruses and reduced their infectivity (4). Furthermore, several recent studies have demonstrated that depletion of lipids from target cells inhibits virus fusion and infection (4, 6, 16). In addition, Hug et al found that blocking the sphingolipid (SL) biosynthesis in cells reduced their susceptibility to retrovirus infection, which suggests that the sphingolipids of retroviruses play a critical role in virus fusion (6). Altogether, virus infection requires the interaction between viral envelope proteins and receptors on

the target cell. This interaction has been extensively studied, yet the role that specific lipids play in virus fusion remains poorly understood. We wondered if retroviruses require that their lipid bilayers contain specific types or amounts of lipids in order for fusion to occur efficiently.

Myriocin (ISP-1) is a potent inhibitor of serine palmitoyltransferase (SPT), an enzyme that is involved in the first step of the biosynthesis pathway of sphingolipid (17, 22). Myriocin has previously been shown to block HIV infection and replication in T-cell leukemia CEM cell line (17). In this study, we determine the effect of blocking *de novo* sphingolipid biosynthesis on virus function by treating stably transfected virus producer cells with myriocin. We investigated the mechanism and extent to which altering the lipid composition of retroviruses affects transduction.

3.3 Material and Methods

Chemicals and Antibodies. Myriocin was obtained from Biomol (Philadelphia, PA). Gluteraldehyde, and 1,5-dimethyl-1,5-diazaundecamethylene polymethobromide (Polybrene, PB) were from Sigma Chemical Co. (St. Louis, MO). Hydrogen peroxide 30%, and polyoxyethylene 20-sorbitan monolaurate (Tween 20) were from Fisher Scientific (Fair Lawn, NJ). Centrifugation filters to concentrate and purify virus stock were obtained from Millipore Corporation (Billerica, MA). Non-fat dry milk (blotting grade) was from Bio-Rad Laboratories (Hercules, CA). o-phenylenediamine dihydrochloride (OPD) was from Pierce (Rockford, IL). 5-bromo-4-chloro-3-indolyl- β -D-galactopyranoside (X-Gal) was from Denville Scientific, Inc. (Metuchen, NJ). Mouse anti-p30 and mouse anti-gp70 antibodies were purified from the supernatant of the CRL-1219 (ATCC, Rockville, MD) and the 83A25 [NL 37] hybridoma cell lines respectively, following standard procedures [NL 38]. The goat polyclonal anti-p30 antibody (78S221) and the goat polyclonal anti-gp70 (79S834) were from Quality Biotech (Camden, NJ).

The horseradish peroxidase conjugated rabbit anti-goat immunoglobulin G polyclonal antibody was from Zymed Laboratories (South San Francisco, CA).

Cell Culture. NIH 3T3 mouse fibroblast were cultured in Dulbecco's modified Eagle's medium (DMEM; Hyclone Labs Inc., Logan, UT) with 10% bovine calf serum (Hyclone Labs Inc.), 100 U/mL of penicillin, and 100 μ g/mL of streptomycin (Hyclone Labs Inc.) (DMEM/BCS). HeLa cells (human cervical kidney, ATCC) and 293T/17 cells (human embryonic kidney epithelial) were cultured in Dulbecco's modified Eagle's medium (Hyclone Labs Inc., Logan, UT) with 10% fetal bovine serum (Hyclone Labs Inc.), 100 U/mL of penicillin and 100 μ g/mL of streptomycin (DMEM/FBS). TELCeB6-A (TE671 (human rhabdomyosarcoma) cells stably transfected to express lacZ, Mo-MLVgagpol (13) and the amphotropic envelope glycoprotein (10)) were cultured in DMEM, 10% fetal bovine serum (Hyclone Labs, Inc.), 100 U/mL of penicillin, and 100 mg/mL of streptomycin (DMEM/FBS).

Virus Production. To generate retrovirus particles, TELCeB6-A cells were grown to confluence in T175 tissue culture flasks, and then incubated for 24 h with 20 mL of DMEM/FBS. The virus-laden tissue culture medium was harvested, filter-sterilized (0.45 μ m), then frozen (-80 °C) for later use.

Diluted Titer Assay. Ten-fold serial dilutions of *lacZ* virus stock were made in DMEM/BCS for NIH 3T3 transduction or in DMEM/FBS for HeLa transduction and were supplemented with Polybrene (8 μ g/mL). A 1-mL amount per well was used to transduce NIH 3T3 cells or HeLa cells that had been seeded (5×10^4 per well or 8×10^4 per well, respectively) the previous day in a 12-well plate. Two days after the start of the transduction, the cells were fixed and stained for β -galactosidase activity with X-Gal. Colonies of *lacZ*⁺ cells (typically in clusters of 2, 4, or 8 blue cells) were counted with the aid of a dissecting microscope. At appropriate dilutions of the virus stock, the clusters of

blue cells were sufficiently spread over the dish such that each cluster arose from a single transduction event.

Myriocin treatment. For all experiments using myriocin, Telceb6-A cells were incubated with the indicated concentration of myriocin for 24 h at 37 °C in DMEM/FBS or DMEM/BCS, depending on the cell type to be transduced.

Lipid analysis of virus particles and cells. Stably transfected virus producing cells, Telceb6-2A, and their parent cell line, Te671 which does not produce viruses, were used for lipid analysis. Cells were grown to confluence in T175 flasks in DMEM/FBS. Telceb6-2A cells were then either treated with 0 µM or 10 µM myriocin. Te671 cells were not treated with myriocin. For three days at every 24 hrs, cell supernatant was collected, filter sterilized (0.45 µm), then frozen (-80 °C). Harvested media was replaced with media either containing 0 µM or 10 µM myriocin. As a control for lipids present in conditioned culture medium from cells not producing virus particles, the supernatant of untreated Te671 cells was similarly harvested each day for 3 days. On the third day after harvest, the cells were put on ice and washed twice with cold phosphate buffered saline (PBS). The cells were then lifted from the flask using a cell scraper, resuspended in PBS, counted using trypan blue and aliquoted in 13 x 100mm screw-capped, borosilicate glass test tubes at 10^7 cells per tube. The cells were then centrifuged at 800 x g at 4 °C and the pellet was stored at -20 °C.

The filtered supernatant samples were concentrated using centrifugation filters from Millipore Corporation (Billerica, MA). A concentrated volume of 1.5 mL to 2 mL was obtained. The total volume was brought to 7 mL in DMEM/FBS for each sample and applied on top of a 2 mL 20% sucrose solution. The virus particles were then pelleted by centrifugation at 30,000 rpm in a Beckman SW41 rotor for 2 h at 4 °C. The supernatant was gently aspirated, the pellet was resuspended in 400 µL PBS and the protein content quantified using the Coomassie Plus-200 protein assay reagent. The

samples were stored in 13 x 100mm screw-capped, borosilicate glass test tubes with teflon caps and used for sphingolipid analysis.

The sphingolipid analyses were conducted by liquid chromatography (LC) and electrospray tandem mass spectrometry using a PE Sciex API 3000 triple quadrupole mass spectrometer equipped with a turbo ion-spray source, as described previously (AM methods). Internal standards for the mass spectrometric analyses were obtained from Avanti Polar Lipids (Alabaster, AL); these were C12-ceramide (*N*-dodecanoyl-sphingosine, d18:1/12:0), C12-glucosylceramide, and C12-sphingomyelin. Protocol adapted from Merrill et al. *Methods*. 36: 207-224 (2005).

Cells and virus samples in the borosilicate glass test tubes were mixed with 0.5ml of methanol then 0.25ml of chloroform and the internal standards. The internal standards were prepared as a working stock in methanol and chloroform (2:1 v/v) such that small volumes can be added to each test tube. In general, the internal standard mixture is prepared to deliver 0.5 nmol of each of the following (per sample): ceramide (d18:1/12:0-Cer), sphingomyelin (d18:1/12:0-SM), glucosylceramide (d18:1/12:0-GlcCer), and lactosylceramide (d18:1/12:0-LacCer) (note that all have a 12-carbon fatty acid side chain), and C17-sphingosine, C17-sphinganine, C17-sphingosine 1-phosphate, and C17-sphinganine 1-phosphate (the C17-chain length was not found in most samples, and was verified for each new type of sample that was analyzed). All of these are available from Avanti Polar Lipids (Alabaster, AL). The test tubes were then sonicated until they appeared evenly dispersed, then incubated overnight at 48 °C in a heating block. The samples were then cooled to room temperature, 75 µL 1M KOH in methanol was added, sonicated, and incubated for 2 h at 37 °C. These steps remove most of the interfering glycerolipids, in particular phosphatidylcholines that can mask sphingomyelins in a simple mass spectroscopy scan.

The samples were cooled to room temperature and half of the volume was transferred to a new test tube. This portion (named Extract A) was used for separation of the more polar sphingolipids by reverse-phase LC. The solvent was removed from the samples using a Speed Vac-type concentrator (ThermoSavant), and re-dissolved in the reverse-phase LC solvent. To the half of the extract that remained in the original test tube, 3 μ L of glacial acetic acid was added to bring the pH near neutral, then 1 mL of chloroform and 2 mL of water was added, sample was vortexed, and centrifuged to separate the phases. The upper layer was carefully removed using a Pasteur pipette (discard), leaving the interface (with water). The solvent was then evaporated from the lower layer (named Extract B) using a Speed Vac-type concentrator (ThermoSavant), and re-dissolved in the normal-phase LC solvent.

Protein assay. To quantify the amount of protein in purified virus stocks after filtration, concentration and sucrose-cushion ultracentrifugation, samples were analyzed with the Coomassie Plus-200 Protein Assay as per the manufacturer's protocol. Optical density was measured using an absorbance plate reader (Pierce, Rockford, IL) and bovine serum albumin was used to create standards.

Cell viability assay. Ten microliters per well of MTT solution (100 mg of MTT in 1 mL of PBS) were added per well to cells in a 96-well plate. The plate was incubated for 4 hours at 37°C, then 150 μ L of 10% sodium dodecylsulfate (SDS) was added per well and the plate incubated overnight at 37°C. The optical density at 570 nm was measured using an absorbance plate reader and the non-specific background at 650nm subtracted. Values for replicate wells without cells were subtracted as background. Values for each point are the average of triplicate wells.

Envelope function assay. To determine whether the structure of virus envelope protein (gp70) had been altered, amphotropic retroviruses produced with or without the treatment of myriocin were mixed with various concentration of gp70-specific monoclonal

antibody (83A25), and used to transduce NIH 3T3 cells. An ONPG assay was then conducted to quantify the inhibition of virus infection due to 83A25 binding to gp70, the virus envelope protein.

Virus stability. To determine virus particle stability, retrovirus (100 μ L) produced from myriocin treated or untreated cells were incubated at 37 °C for 0 hr to 24 hrs. At indicated time points, a small aliquot was collected and stored (-80 °C) for later use. These aliquots were then later used to transduce NIH 3T3 to determine virus activity.

ELISA for p30 and gp70. The concentration of virus capsid protein and envelope protein, p30 and gp70 respectively, were quantified using a previously described enzyme-linked immunosorbent assay (ELISA) (10). Briefly, ELISA plates (Nunc immuno Maxisorp 96-well plates, Nalgen Nunc International, Rochester, NY) were coated overnight at 4 °C with 10 μ g/mL of mouse anti-p30 antibody or mouse anti-gp70 antibody (100 μ L/well) in PBS. The next day, the antibody solution was removed and blocking buffer (PBS, 0.05% Tween-20, 5% non-fat milk) was added (200 μ L/well) for 2 h at 37°C to block non-specific binding sites. Virus particles were lysed using 0.5% Triton-X to expose the p30 antigen, then added to the ELISA plate (100 μ L/well) and incubated for 1 h at 37 °C. Bound p30 and gp70 were sandwiched by either the addition of the goat polyclonal anti-p30 antibody diluted 1:1000 or goat polyclonal anti-gp70 antibody diluted 1:300 in blocking buffer for 1 h at 37 °C (10), respectively. The horseradish peroxidase conjugated polyclonal rabbit anti-goat immunoglobulin G was diluted 1:5000 in blocking buffer and added to the ELISA plate (100 μ L/well) for 1 h at 37 °C to enable detection and quantitation of the p30 or gp70 antigen. The plates were developed for 5 min using hydrogen peroxide (H₂O₂) and OPD (100 μ g/well) from a solution of 3 mg of OPD and 3 μ L H₂O₂ in 7.5 mL of substrate buffer (24 mM citric acid-monohydrate, 51 mM Na₂HPO₄-7H₂O, pH 5.0). Sulfuric acid (8 N, 50 μ L/well) was used to stop the reaction, the optical density at 490 nm was measured using an absorbance plate reader, and the non-

specific background at 650 nm was subtracted. Values for replicate wells without virus were subtracted as background.

Beta-galactosidase (β -gal) transduction assay. Five thousand NIH 3T3 murine fibroblasts or eight thousand HeLa cells suspended in 100 μ L of medium were plated in each well of a 96-well flat-bottomed tissue culture dish with a low-evaporation lid (Costar Corp., Cambridge, MA) (20). The next day, the medium was removed and 100 μ L of the virus-containing solution was added to each well. Two days after transduction, the medium was removed and the cells washed once with 100 μ L of PBS containing 1mM MgCl₂. After removal of the wash solution, 50 μ L of lysis buffer (PBS with 1mM MgCl₂ and 0.5% Igepal) were added to each well, and the plate incubated at 37 °C. After 30 min, 50 μ L of lysis buffer with 6 mM ONPG was warmed to 37 °C, added to each well, and the plate incubated at 37°C for 5 to 60 min until a visible yellow color was obtained. The reactions were halted by the addition of 20 μ L per well of stop buffer (1M Na₂CO₃). The optical density at 420 nm (OD₄₂₀) was measured using an absorbance plate reader (Molecular Devices, Menlo Park, CA) and the non-specific background at 650 nm subtracted. Values for replicate wells without virus were subtracted as background. Values for each point are the averages of at least triplicate wells.

Virus binding assay. To determine if myriocin treatment altered virus binding, we incubated virus produced from varying doses of myriocin with NIH 3T3 cells and HeLa cells. NIH 3T3 or HeLa cells were plated to confluence in 6 well plates. The next day virus supernatant was applied to cells and incubated at 4 °C for 2 hrs. The cells were washed twice with cold PBS, lifted from the wells using a cell scraper, centrifuged (800 x g for 5 min) and the pellet resuspended in lysis buffer. Cell lysis samples were then used to quantify virus protein using the p30 ELISA.

Production of nef-luc laz retrovirus. Telceb6-A cells were plated at approximately 80% confluency in 10-cm tissue culture dishes. The cells were

transfected with 8 µg of pcDNA3-Nef-luc (kind gift of Robert Davey), diluted in 1.5 mL of DMEM, mixed with a solution of 1.5 mL of DMEM and 40 µL of Lipofectamine 2000 reagent (Invitrogen Life Technologies, Carlsbad, CA) and then added to the cells. The medium was replaced 6 hours later and 18 hours later with 10 mL of DMEM/FBS. Twenty four hours later the supernatant was removed from the cells and replaced with media containing varying concentrations of myriocin. After 24 hrs of treatment, the virus-laden cell culture supernatant was harvested, filter sterilized (0.45-µm) and frozen (-80°C) for later use. Virus capsid protein was quantified using p30 ELISA.

Virus Fusion assay. NIH 3T3 and HeLa cells were trypsinized, counted and pelleted in 1.5 mL tubes such that each pellet contained 1×10^5 cells. This protocol is adapted from Saeed et al (19). The cells were resuspended in 100 µL containing equal amount of virus protein (p30). Virus and cells were incubated at 37 °C for 2 hrs on a rotating platform. To remove virus particles that had not fused with the cell membrane, the cells were pelleted by centrifugation at 800 x g for 5 min, supernatant discarded, and the cell pellet washed twice in DMEM. The final cell pellet was resuspended in 0.1 mL of Luciferase Assay Buffer (Promega) and the luciferase activity was measured using a Turner Biosystems Modulus Microplate reader and expressed as relative luciferase units.

Statistical Analysis. Data are summarized as the mean \pm one standard deviation for triplicate samples. Statistical analysis was performed using one-way analysis of variance for repeated measurements of the same variable. The Tukey multiple comparison test was used to conduct pairwise comparisons between means. Differences at $p < 0.05$ were considered statistically significant.

3.4 Results

During virus budding, viruses acquire a lipid bilayer composed of signaling proteins and host lipids, both of which play a significant role in virus attachment, fusion and entry (14, 23). Although envelope proteins have been extensively studied and manipulated, little is known about the role lipids play in mediating virus binding and infection. Here we studied the effect of blocking *de novo* sphingolipid biosynthesis on virus function by treating virus producing cells with myriocin (ISP-1), a potent inhibitor of serine palmitoyl-CoA transferase (SPT), which is a rate limiting enzyme in the biosynthesis of sphingolipids (Figure 3.1) (Hojjati et al 2005).

As a first step toward investigating the effects of altering sphingolipid synthesis we wanted to determine the effect of treating the virus producer cells with ISP-1 on the lipid composition of the viruses that they produce, and on the composition of the cellular membrane. We treated TelCeB6 cells with 10 μ M ISP-1 for 24 hours, or left them untreated, harvested the virus supernatant and analyzed the lipid composition of the cells and virus particles using mass spectrometry (Figure 3.2 A-F). After virus producer cells were treated with ISP-1, they were washed with cold PBS three times, counted, pelleted and stored at -20°C . We also analyzed the lipid content of Te671 cells, the parent cell line of TelCeB6 cells, as a control to quantify the amount and type of lipids that are not virus-associated that are present in the conditioned medium. Conditioned medium, which was collected from cultures of Te671, TelCeB6, and TelCeB6 cells that had been treated with 10 μ M ISP-1, was thawed, concentrated, pelleted and purified two times with a 20 % sucrose cushion. Equal amount of virus protein was then used for lipid analysis using mass spectroscopy. Lipids were extracted from pellets of cells and supernatant and analyzed for three downstream products in the lipid synthesis pathway affected by ISP-1: ceramide, glycosylceramide and sphingomyelin. Cells treated with ISP-1 and their resulting virus supernatant contained significantly lower levels of all three

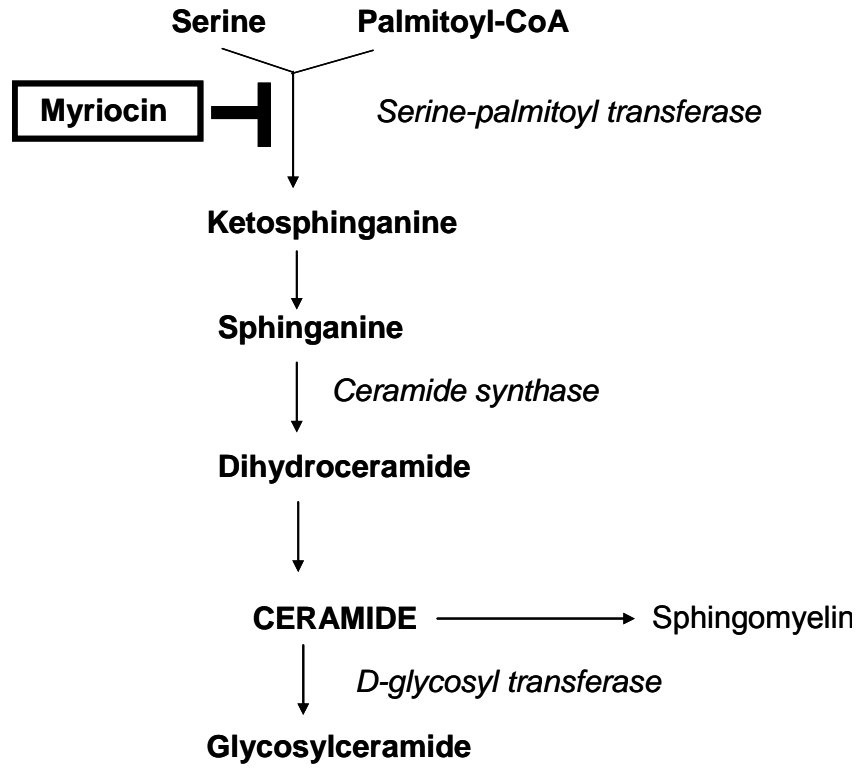


Figure 3.1: The pathway of *de novo* sphingolipid biosynthesis and sites of action of myriocin, a serine-palmitoyl transferase inhibitor.

A.

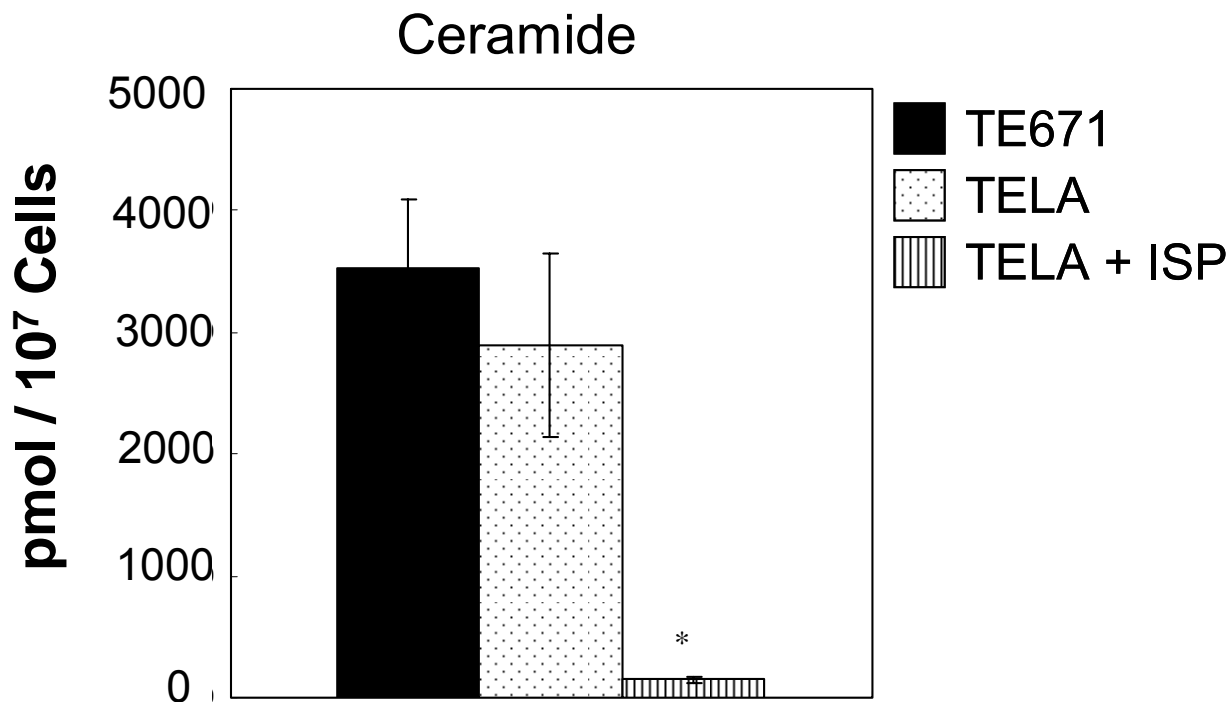


Figure 3.2 (A) Mass spectrometry analysis of ceramide present in virus producer cells. Stably transfected virus producing cells, Telceb6-2A, and their parent cell line, Te671 which does not produce viruses, were used for lipid analysis. Cells were grown to confluence in T175 flasks in DMEM/FBS. Telceb6-2A cells were then either treated with 0 μ M or 10 μ M myriocin. Te671 cells were not treated with myriocin. Every 24 hrs, for 72 hours, cell supernatant was collected, filter sterilized (0.45 μ m), then frozen (-80 $^{\circ}$ C). Harvested media was replaced with media either containing 0 μ M or 10 μ M myriocin. As a control for lipids present in conditioned culture medium from cells not producing virus particles, the supernatant of untreated Te671 cells was similarly harvested each day for 3 days. On the third day after harvest, the cells were put on ice and washed twice with cold phosphate buffered saline (PBS). Cells were then lifted from the flask using a cell scraper, resuspended in PBS, counted and aliquoted in borosilicate glass test tubes at 10^7 cells per tube and pelleted centrifuged at 800 x g at 4 $^{\circ}$ C. (*) denotes statistically significant differences between treated and untreated cells ($p < 0.05$).

B.

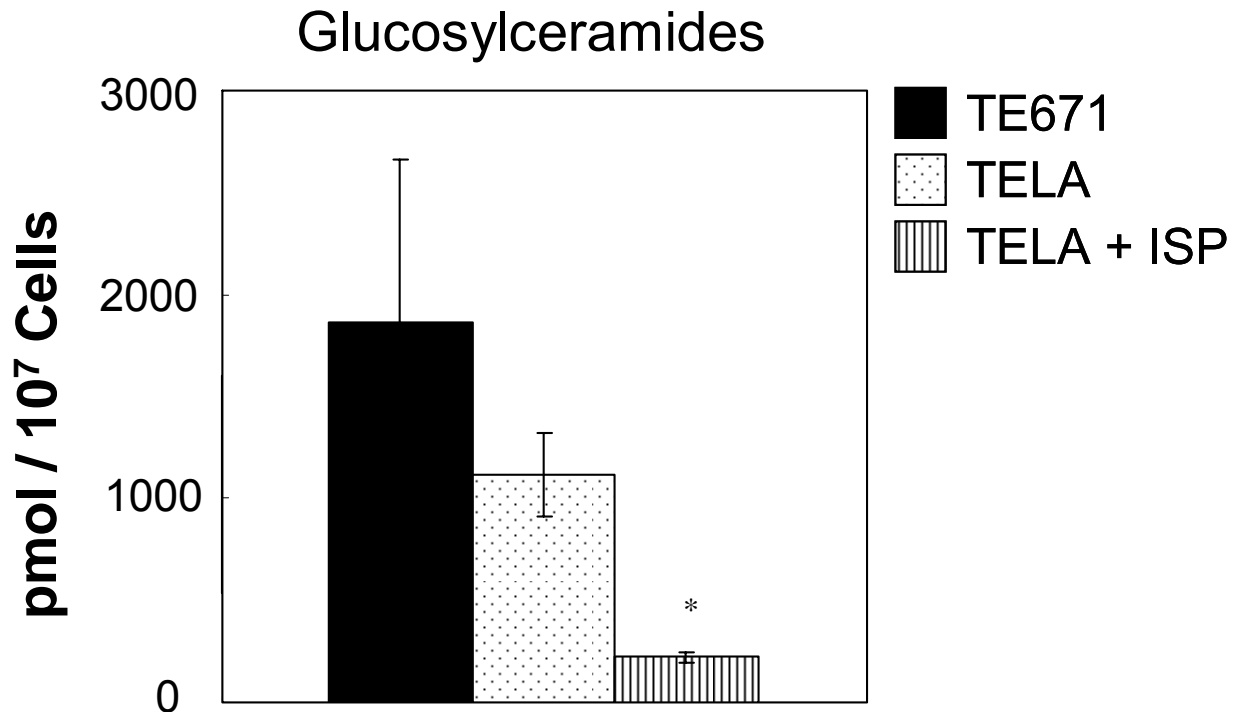


Figure 3.2 (B) Mass spectrometry analysis of glucosylceramides present in virus producer cells. Stably transfected virus producing cells, Telceb6-2A, and their parent cell line, Te671 which does not produce viruses, were used for lipid analysis. Cells were grown to confluence in T175 flasks in DMEM/FBS. Telceb6-2A cells were then either treated with 0 μ M or 10 μ M myriocin. Te671 cells were not treated with myriocin. Every 24 hrs, for 72 hours, cell supernatant was collected, filter sterilized (0.45 μ m), then frozen (-80 $^{\circ}$ C). Harvested media was replaced with media either containing 0 μ M or 10 μ M myriocin. As a control for lipids present in conditioned culture medium from cells not producing virus particles, the supernatant of untreated Te671 cells was similarly harvested each day for 3 days. On the third day after harvest, the cells were put on ice and washed twice with cold phosphate buffered saline (PBS). Cells were then lifted from the flask using a cell scraper, resuspended in PBS, counted and aliquoted in borosilicate glass test tubes at 10⁷ cells per tube and pelleted centrifuged at 800 x g at 4 $^{\circ}$ C. (*) denotes statistically significant differences between treated and untreated cells ($p < 0.05$).

c.

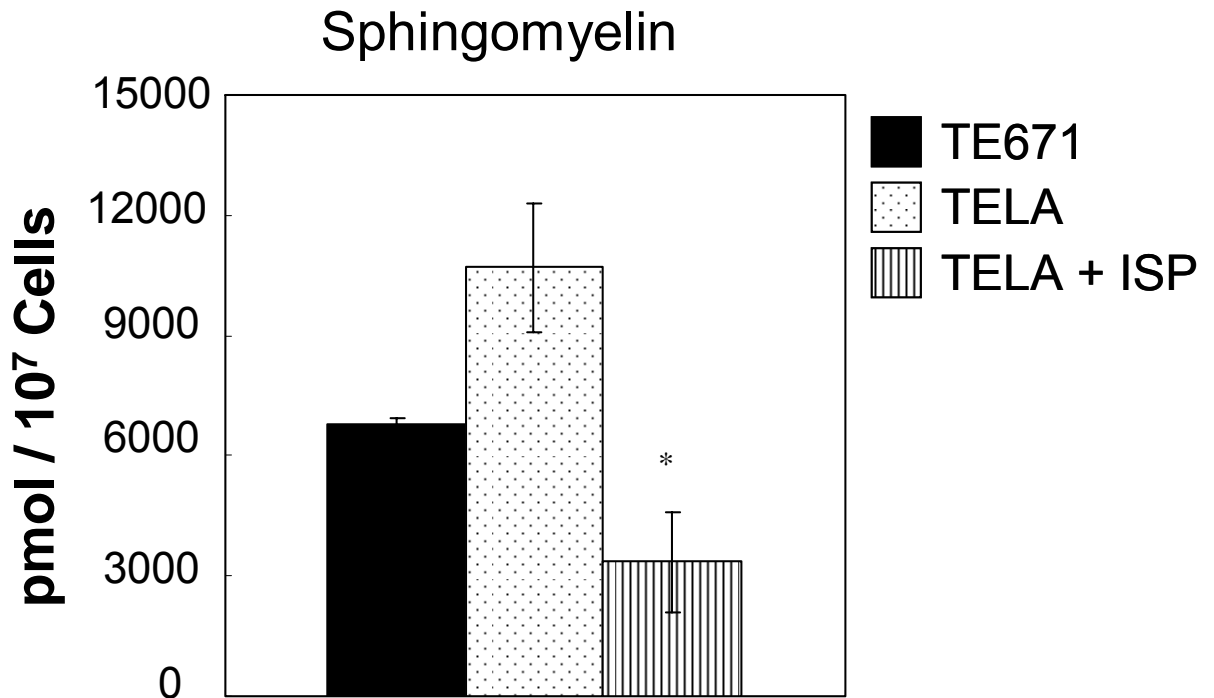


Figure 3.2 (C) Mass spectrometry analysis of sphingomyelin present in virus producer cells. Stably transfected virus producing cells, Telceb6-2A, and their parent cell line, Te671 which does not produce viruses, were used for lipid analysis. Cells were grown to confluence in T175 flasks in DMEM/FBS. Telceb6-2A cells were then either treated with 0 μ M or 10 μ M myriocin. Te671 cells were not treated with myriocin. Every 24 hrs, for 72 hours, cell supernatant was collected, filter sterilized (0.45 μ m), then frozen (-80 $^{\circ}$ C). Harvested media was replaced with media either containing 0 μ M or 10 μ M myriocin. As a control for lipids present in conditioned culture medium from cells not producing virus particles, the supernatant of untreated Te671 cells was similarly harvested each day for 3 days. On the third day after harvest, the cells were put on ice and washed twice with cold phosphate buffered saline (PBS). Cells were then lifted from the flask using a cell scraper, resuspended in PBS, counted and aliquoted in borosilicate glass test tubes at 10^7 cells per tube and pelleted centrifuged at 800 x g at 4 $^{\circ}$ C. (*) denotes statistically significant differences between treated and untreated cells ($p < 0.05$).

D.

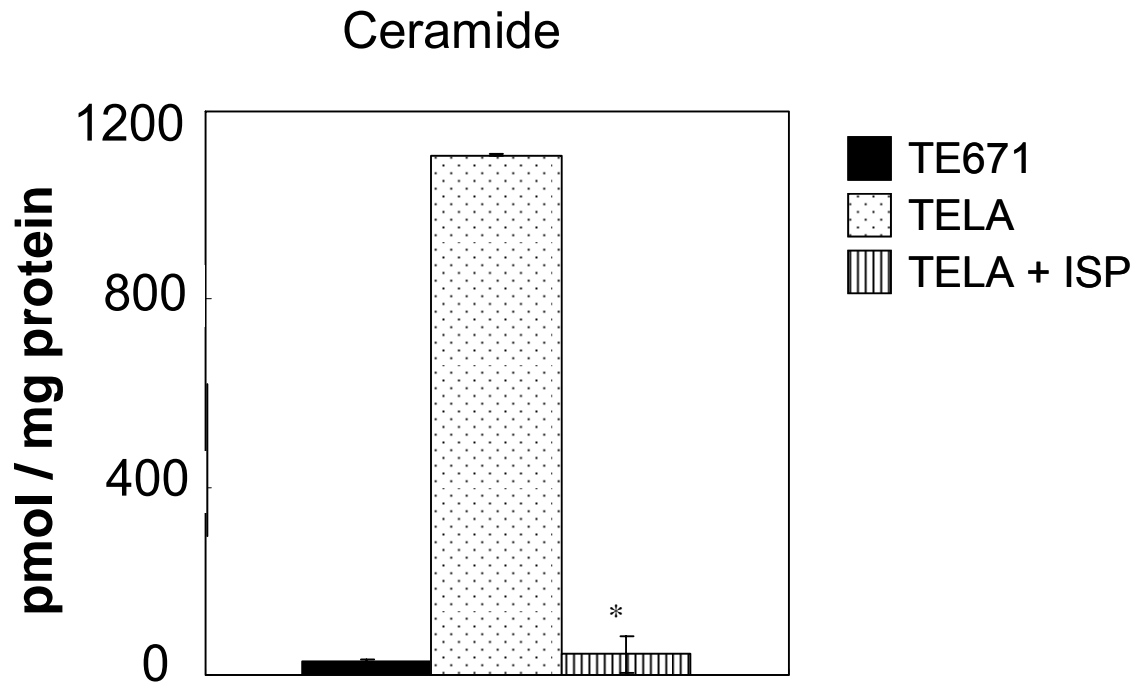


Figure 3.2 (D) Mass spectrometry analysis of ceramide in virus particles. Virus producer cells were treated as indicated in Figure 4.2 (A-C). The filtered supernatant samples were concentrated using centrifugation filters from Millipore Corporation (Billerica, MA). A concentrated volume of 1.5 mL to 2 mL was obtained. The total volume was brought to 7 mL in DMEM/FBS for each sample and applied on top of a 2 mL 20% sucrose solution. The virus particles were then pelleted by centrifugation at 30,000 rpm in a Beckman SW41 rotor for 2 h at 4 °C. The supernatant was gently aspirated, the pellet was resuspended in 400 μ L PBS and the protein content quantified using the Coomassie Plus-200 protein assay reagent. The samples were stored in 13 x 100mm screw-capped, borosilicate glass test tubes with teflon caps and used for sphingolipid analysis. (*) denotes statistically significant differences between treated and untreated cells ($p < 0.05$).

E.

Glucosylceramides

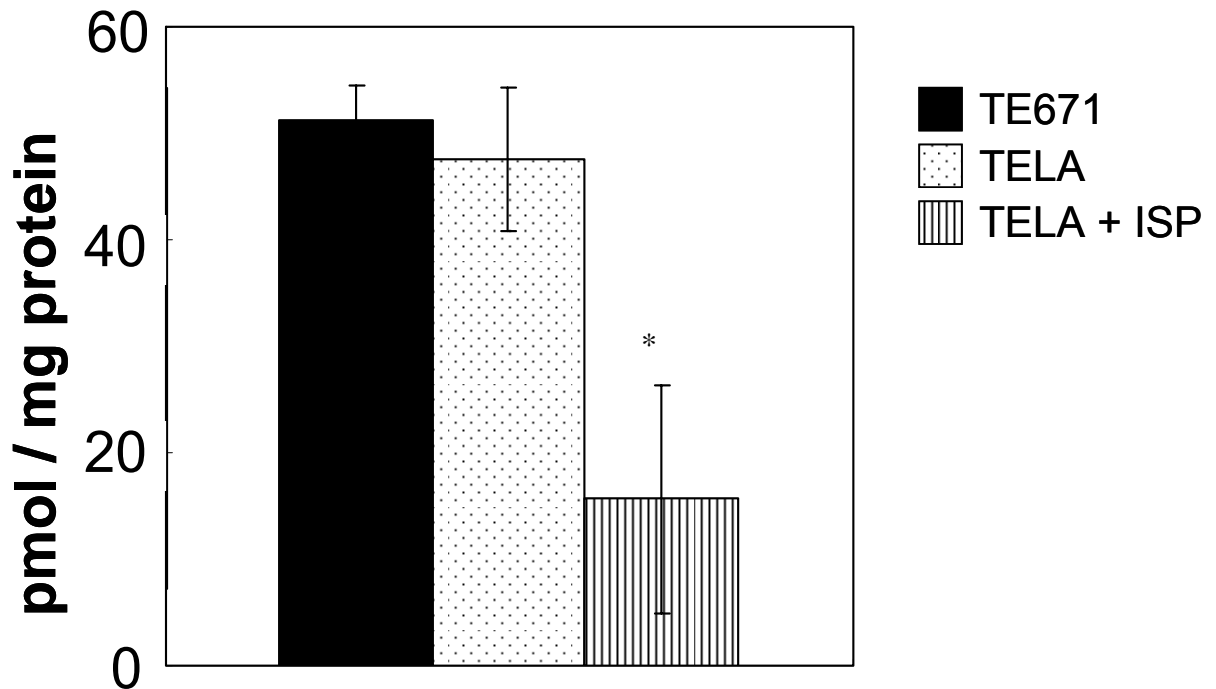


Figure 3.2 (E) Mass spectrometry analysis glucosylceramides in virus particles. Virus producer cells were treated as indicated in Figure 4.2 (A-C). The filtered supernatant samples were concentrated using centrifugation filters from Millipore Corporation (Billerica, MA). A concentrated volume of 1.5 mL to 2 mL was obtained. The total volume was brought to 7 mL in DMEM/FBS for each sample and applied on top of a 2 mL 20% sucrose solution. The virus particles were then pelleted by centrifugation at 30,000 rpm in a Beckman SW41 rotor for 2 h at 4 °C. The supernatant was gently aspirated, the pellet was resuspended in 400 μ L PBS and the protein content quantified using the Coomassie Plus-200 protein assay reagent. The samples were stored in 13 x 100mm screw-capped, borosilicate glass test tubes with teflon caps and used for sphingolipid analysis. (*) denotes statistically significant differences between treated and untreated cells ($p < 0.05$).

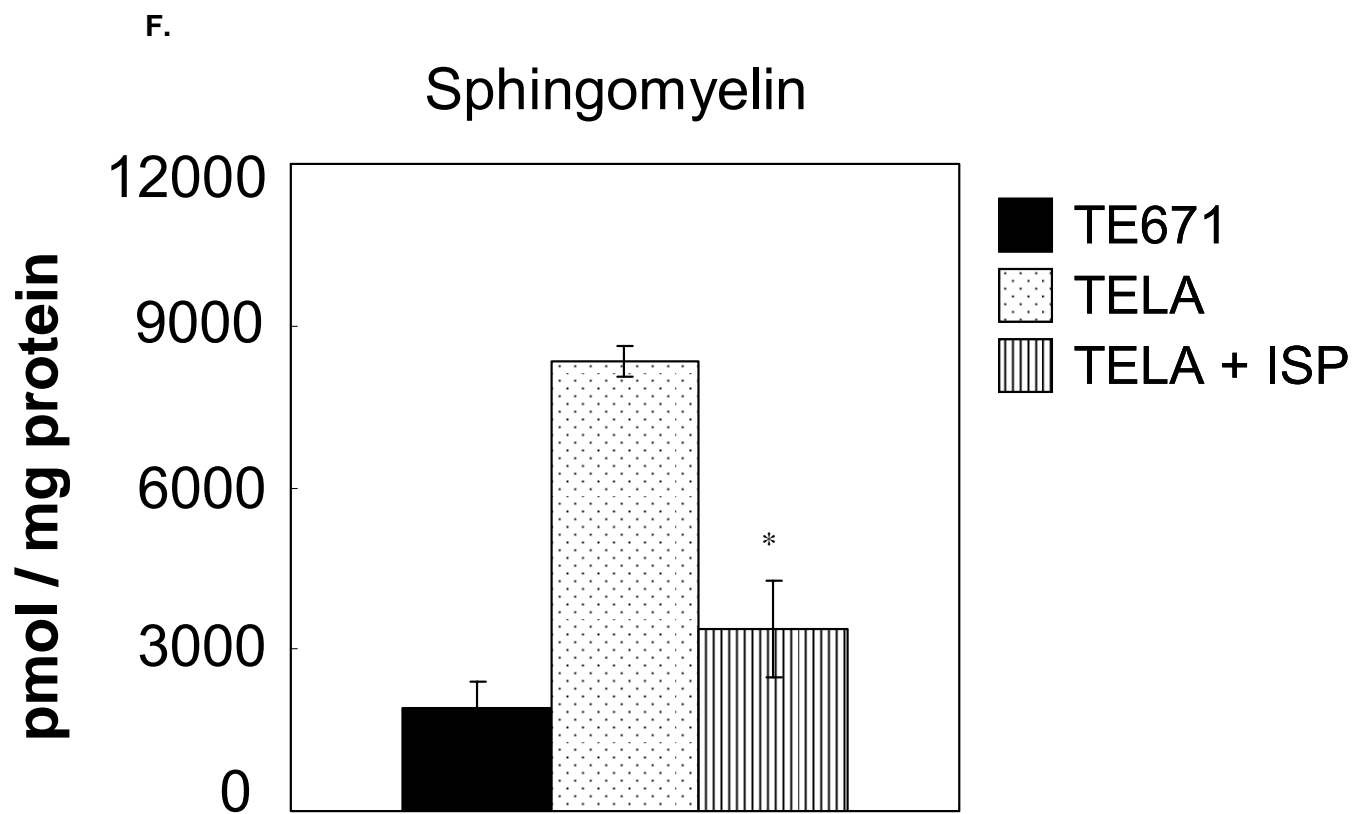


Figure 3.2 (F) Mass spectrometry analysis of sphingomyelin in virus particles. Virus producer cells were treated as indicated in Figure 3.2 (A-C). The filtered supernatant samples were concentrated using centrifugation filters from Millipore Corporation (Billerica, MA). A concentrated volume of 1.5 mL to 2 mL was obtained. The total volume was brought to 7 mL in DMEM/FBS for each sample and applied on top of a 2 mL 20% sucrose solution. The virus particles were then pelleted by centrifugation at 30,000 rpm in a Beckman SW41 rotor for 2 h at 4 °C. The supernatant was gently aspirated, the pellet was resuspended in 400 μ L PBS and the protein content quantified using the Coomassie Plus-200 protein assay reagent. The samples were stored in 13 x 100mm screw-capped, borosilicate glass test tubes with teflon caps and used for sphingolipid analysis. (*) denotes statistically significant differences between treated and untreated cells ($p < 0.05$).

sphingolipids as compared to untreated TelCeB6 cells. Since Te671 cells do not produce virus particles, the concentration of sphingolipids in Te671 supernatant was much lower than untreated TelCeB6 cells, as expected.

To determine the effect of ISP-1 treatment on virus production and infection, we treated a virus producing cell line (TelCeB6) with ISP-1 (0 to 30 μ M) and harvested the virus supernatant after 24 hours. We quantified the amount of virus produced by the treated cells using an ELISA for the viral capsid protein, p30 (Figure 3.3 A). Furthermore, the virus infectivity was measured by incubating particles with NIH 3T3 cells and HeLa cells for 48 hours and conducting an ONPG assay (Figure 3.3 B). Our data shows treating virus producer cells with 30 μ M ISP-1 did not affect virus production but it reduced the ability of the resulting virus particles to infect NIH 3T3 cells to 70%, and the infectivity to HeLa cells was reduced to 15%. To determine whether the decrease in infectivity was due to cell death after ISP-1 treatment, we measured the viability of the virus producing cells and the cells that were being transduced (Figure 3.4). Our results show that ISP-1 did not alter the viability of the cells, which indicates that the decreases in virus titer that were observed were not due to cytotoxic effects of the drug.

In order to determine the mechanism by which changes in the lipid content lead to changes in retrovirus transduction, we investigated different factors that may affect the fusion pathway. First, we determined whether changing the lipid content of virus producer cells had altered the number of envelope proteins incorporated into virus particles. We measured the extent of fusion protein (gp70) incorporation into virus particles produced from ISP-1 treated cells by ELISA (Figure 3.5 A). Furthermore, we hypothesized that changing the lipid environment in the virus bilayer may also affect the structure of the transmembrane envelope proteins which interact with the lipids in the

A.

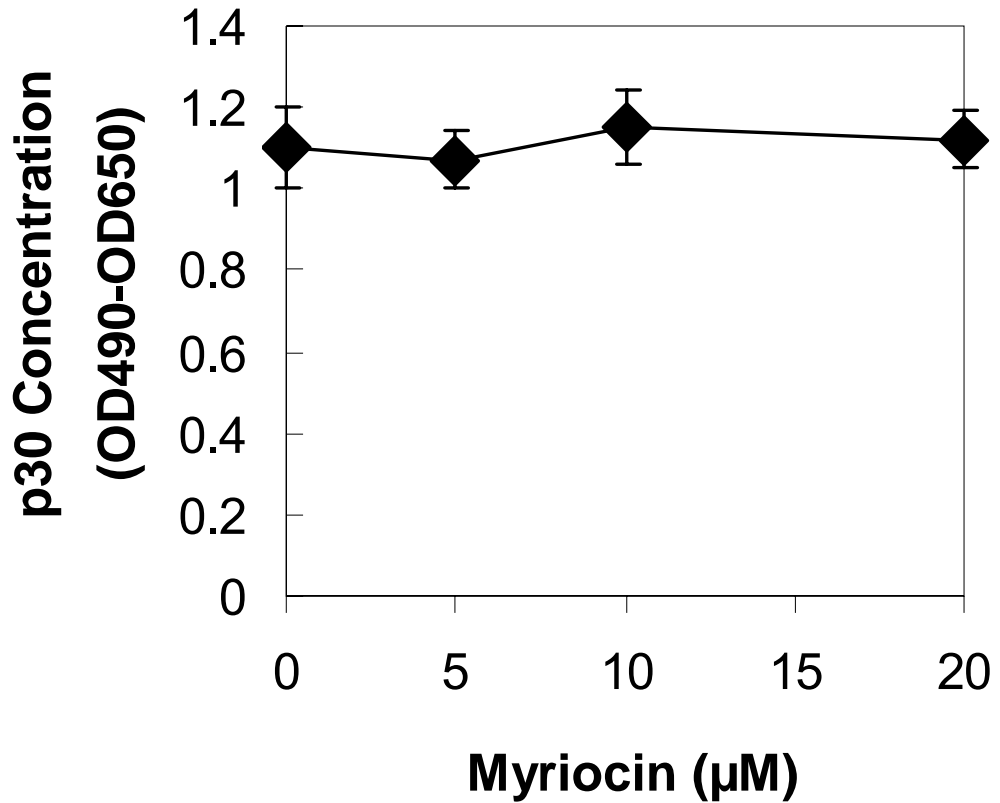


Figure 3.3 (A) Myriocin treatment does not affect virus production. Virus producer cells, TeiCeB6, were plated at 240, 000 cells per well of a 6-well plate and grown to confluency. The next day, cell culture media was removed and replaced with media containing varying doses of ISP-1 as indicated. After 24 hours, the conditioned cell media was collected and filter sterilized (0.45 µm). The concentration of virus in the supernatant after treating virus producing cells with different doses of ISP-1 was determined using the p30 ELISA. Each point shows the mean ± standard deviation of three replicates.

B.

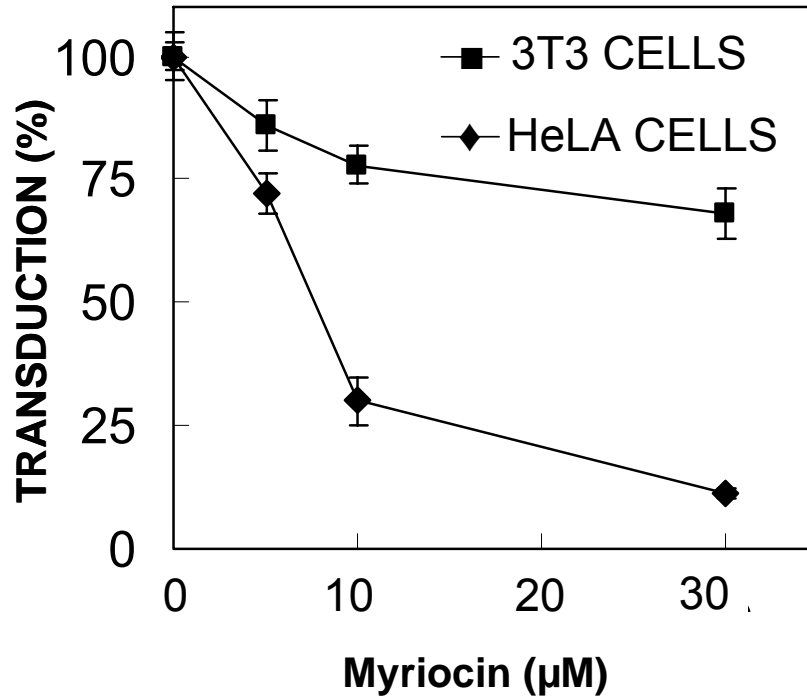


Figure 3.3 (B) Treatment of virus producer cells with ISP-1 decreases the titer of the virus produced from those cells. Virus stock was produced after various doses of ISP-1 treatment of TeLceB6 cells. NIH 3T3 cells were plated at 60 000 cells per well and HeLa cells were plated at 80 000 cells per well of 96 well plates. The next day, the ten-fold serial dilutions of virus stock were made in DMEM/BCS for NIH 3T3 transduction or in DMEM/FBS for HeLa transduction, supplemented with Polybrene (8 µg/mL) and incubated with cells. Two days after the start of the transduction, the cells were fixed and stained for β -galactosidase activity with X-Gal. Colonies were counted with the aid of a dissecting microscope. At appropriate dilutions of the virus stock, the clusters of blue cells were sufficiently spread over the dish such that each cluster arose from a single transduction event. Each point shows the mean \pm standard deviation of three replicates.

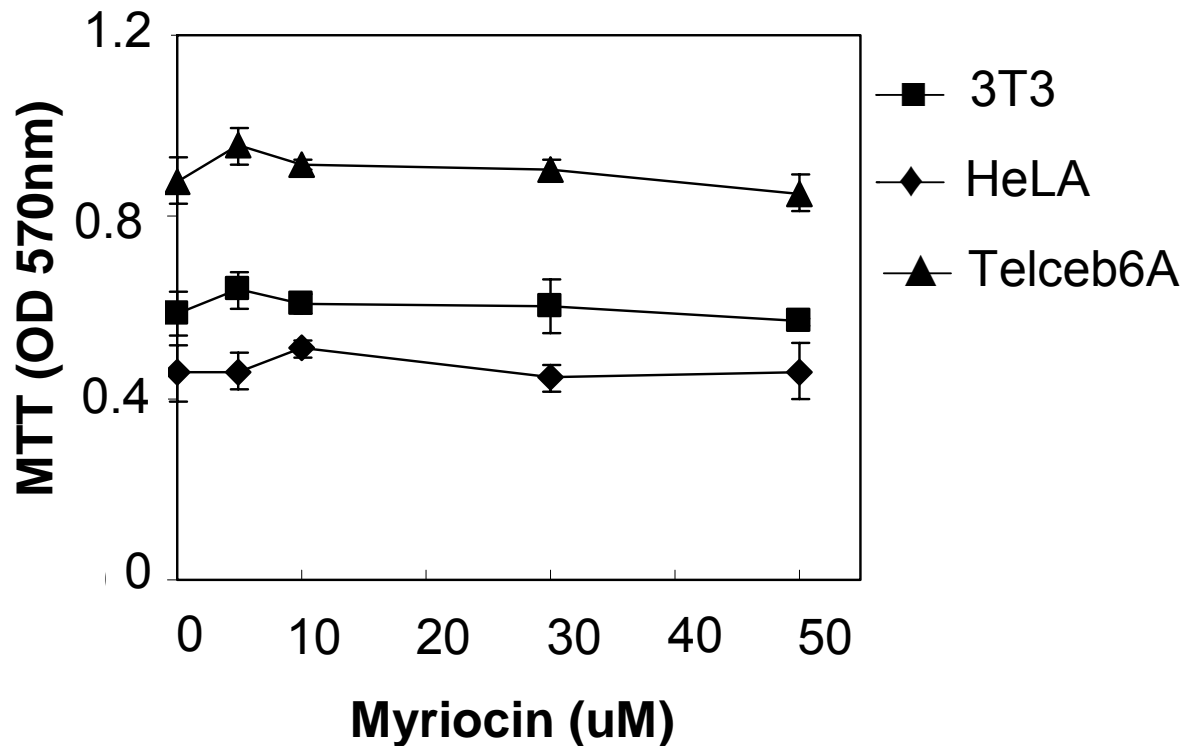


Figure 3.4 Effect of ISP-1 treatment on cell viability. Virus producer cell line (TelCeb6) and target cells (NIH 3T3 and HeLa cells) were plated at a density of 10,000 cells per well and 5,000 cells per well in 96-well plates. The next day, the cells were treated with varying doses of ISP-1 as indicated. TelCeb6 were assayed for cell viability after 24 hours of ISP-1 treatment and NIH 3T3 and HeLa cells were assayed after 48 hours of treatment. After 24 or 48 hours, 10 μ L per well of MTT solution (100 mg of MTT in 1 mL of PBS) were added per well to cells in a 96-well plate. The plate was incubated for 4 hours at 37°C, then 150 μ L of 10% SDS were added per well and the plate incubated overnight. The optical density at 570 nm was measured using an absorbance plate reader and the non-specific background at 650nm subtracted. Values for replicate wells without cells were subtracted as background. Values for each point are the average of triplicate wells.

virus bilayer. Therefore, to determine whether the structure and function of the envelope protein, gp70, was affected, we measured virus transduction in the presence of an envelope-specific monoclonal antibody, 83A25 (Figure 3.5 B). This antibody detects a specific structural motif on the ectodomain of the gp70 protein, and hence, would not bind to the gp70 protein with the same affinity if the protein significantly changed in structure. Therefore, we would observe a lower IC_{50} for virus particles produced from ISP-1 treated virus producer cells than untreated cells. Our results show that there was no statistical difference between the IC_{50} of virus particles produced after ISP-1 treatment as compared to untreated cells. We obtained IC_{50} values of 4.5 $\mu\text{g/mL}$ for 30 μM and 4.7 $\mu\text{g/mL}$ for control virus. To further determine if altering the lipid composition of virus particles affected gp70-dependant fusion of virus particles, we mixed virus produced from cells treated with various concentration of ISP-1 concentrations in media containing free gp70 and incubated with 3T3 cells to measure the effect on transduction (Figure 3.6 A-B). We found an approximately 50% reduction in infection occurred for all samples of virus when they were incubated in the presence of 25% (by volume) of free gp70. In addition, we observed a decrease in infection with increasing amount of free gp70 and found that the inhibitory concentration of gp70 for all virus samples was similar. These results indicate that ISP-1 treatment does not reduce envelope incorporation into virus particles. Altogether, this data suggests that the structure of the envelope proteins is not significantly different in the control viruses as compared to viruses produced from the ISP-1 treatment.

Changing the lipid content of virus producing cells may also affect the stability of the virus that is produced from those cells, as has been shown to be the case with cholesterol depletion. To determine the stability of ISP-1 treated virus particles, we incubated virus at 37°C for up to 24 hours, after which we used samples from different time points to transduce NIH 3T3 cells (Figure 3.7). Infectivity of ISP-1 treated virus was

A.

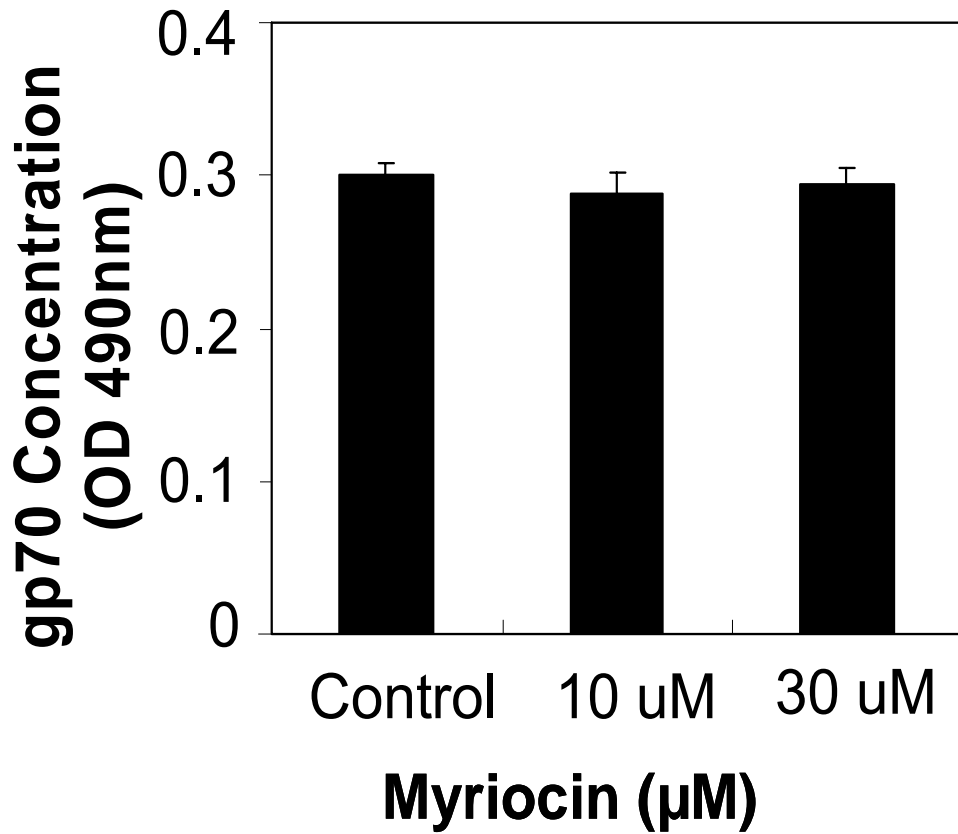


Figure 3.5 (A) Myriocin treatment does not affect amount of gp70 incorporation into virus particles. Virus producer cells, TelCeB6, were plated at 240, 000 cells per well of a 6-well plate and grown to confluency. The next day, cell culture media was removed and replaced with media containing varying doses of ISP-1 as indicated. After 24 hours, the conditioned cell media was collected and filter sterilized (0.45 μm). The concentration of virus in the supernatant after treating virus producer cells with different doses of ISP-1 was determined using the gp70 ELISA. Each point shows the mean \pm standard deviation of three replicates.

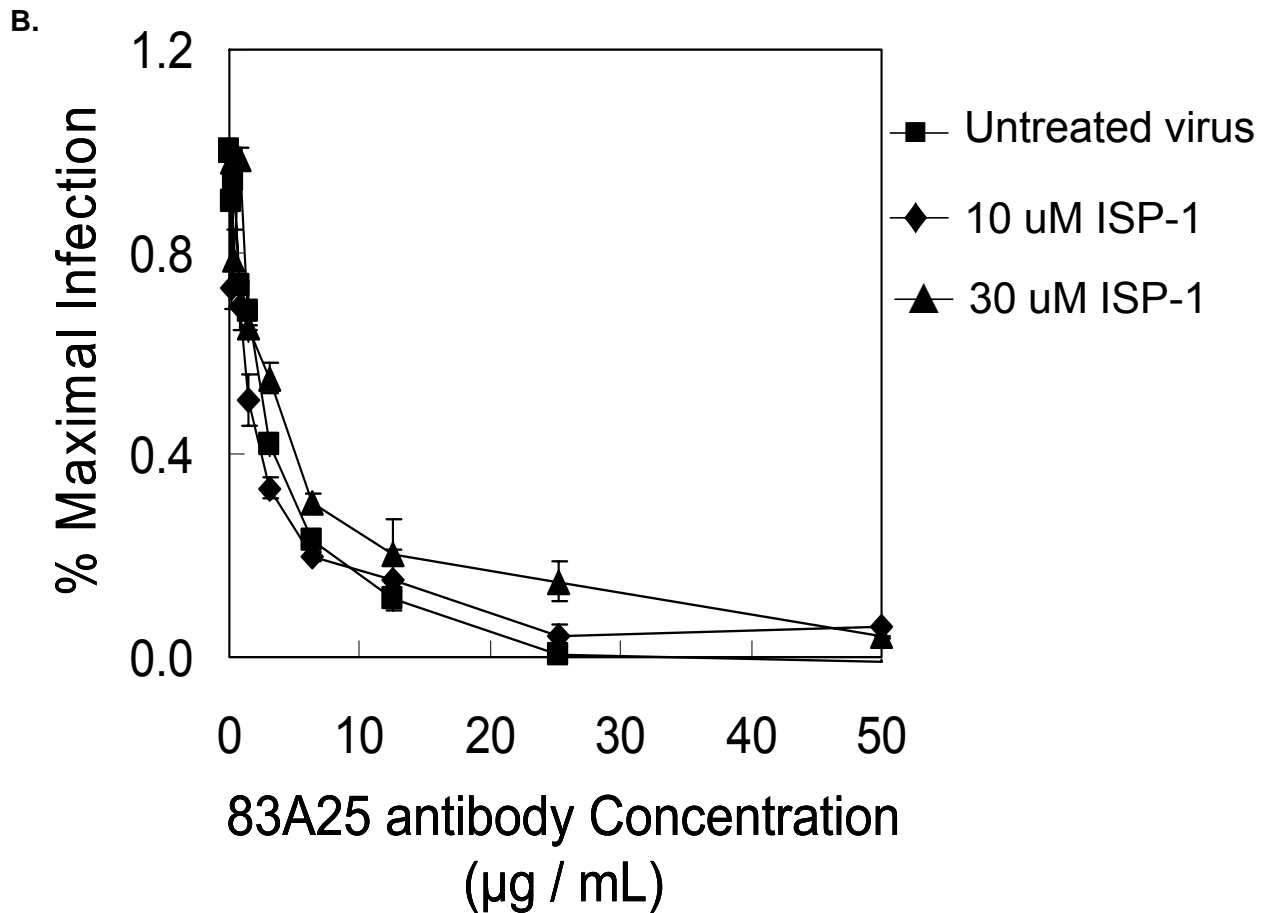


Figure 3.5 (B). Myriocin treatment of virus producer cells does not affect structure of the gp70 incorporated into the virus particles. Virus stock was produced by treating virus producing cells with 0, 10 or 30 µM ISP-1. Virus samples were mixed with various concentrations with gp70-specific monoclonal antibody (83A25) as indicated, and the mixture was used to transduce NIH 3T3 cells which has been plated at a 5 000 cells per well of a 96 well one day earlier. Two days later, the ONPG assay was conducted to quantify the virus infection.

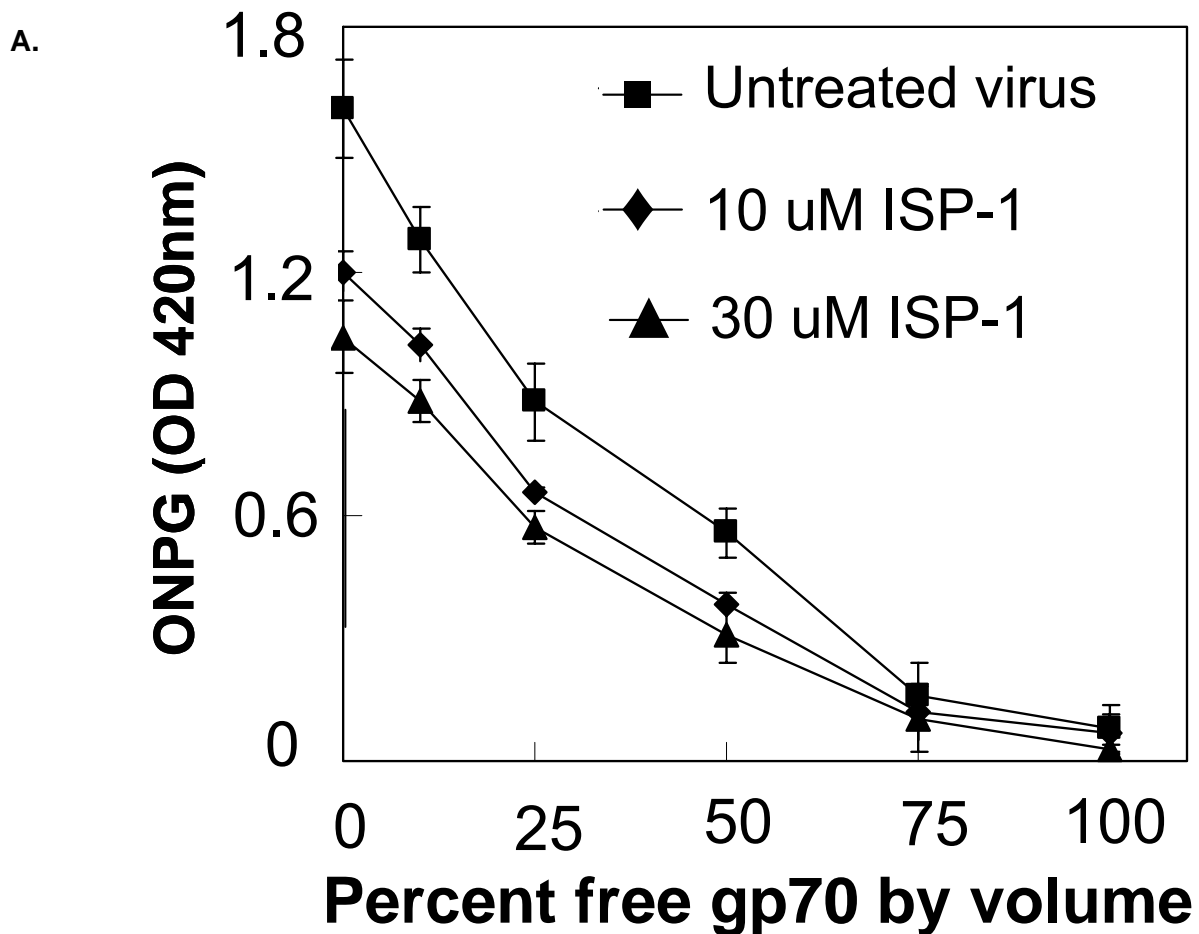


Figure 3.6(A). Treating virus producer cells with ISP-1 does not decrease the amount of gp70 incorporated into the virus particles. Virus particles were produced from the treatment of Telceb6 cells with 0, 10 or 30 μ M ISP-1. Virus particles were diluted in various concentrations of free gp70 as indicated, and the mixture was to transduce NIH 3T3 cells which has been plated at a 5 000 cells per well of a 96 well one day earlier. Two days later, the ONPG assay was conducted to quantify the virus infection.

B.

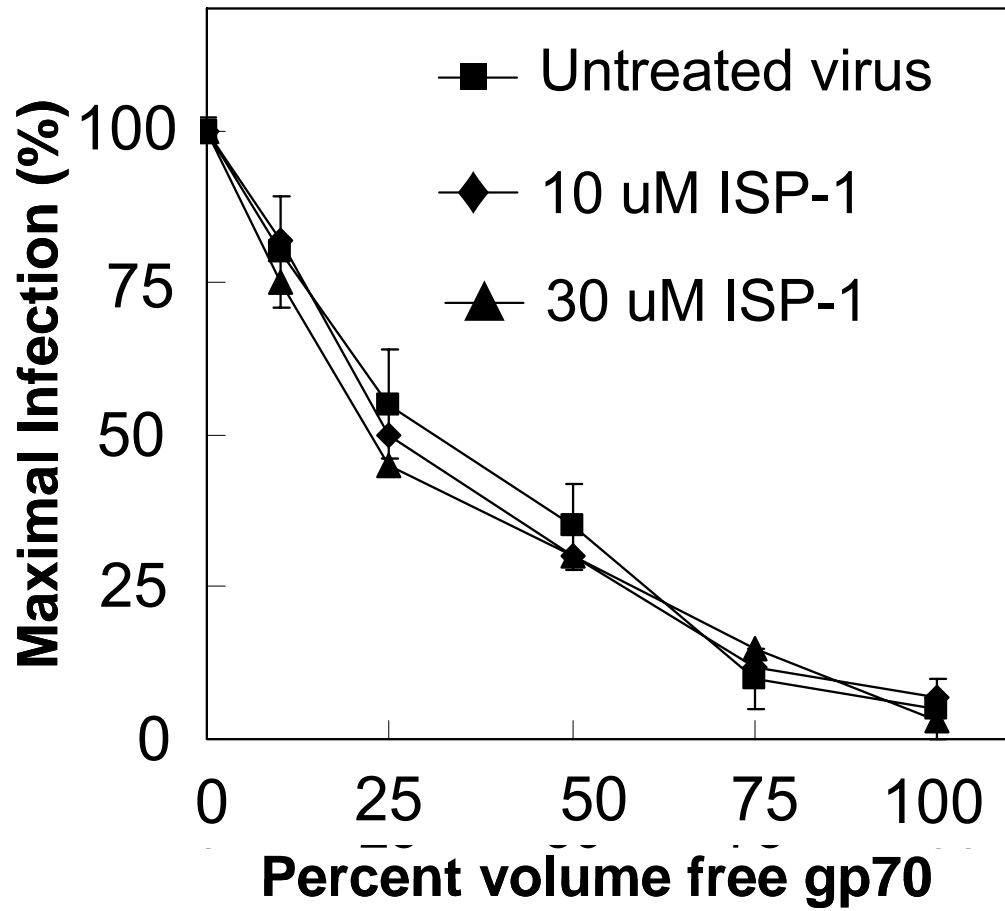


Figure 3.6(B). Treating virus producer cells with ISP-1 does not decrease the amount of gp70 incorporated into the virus particles. Data from part (A) is normalized to the level of infection obtained in the absence of gp70 (maximal infection).

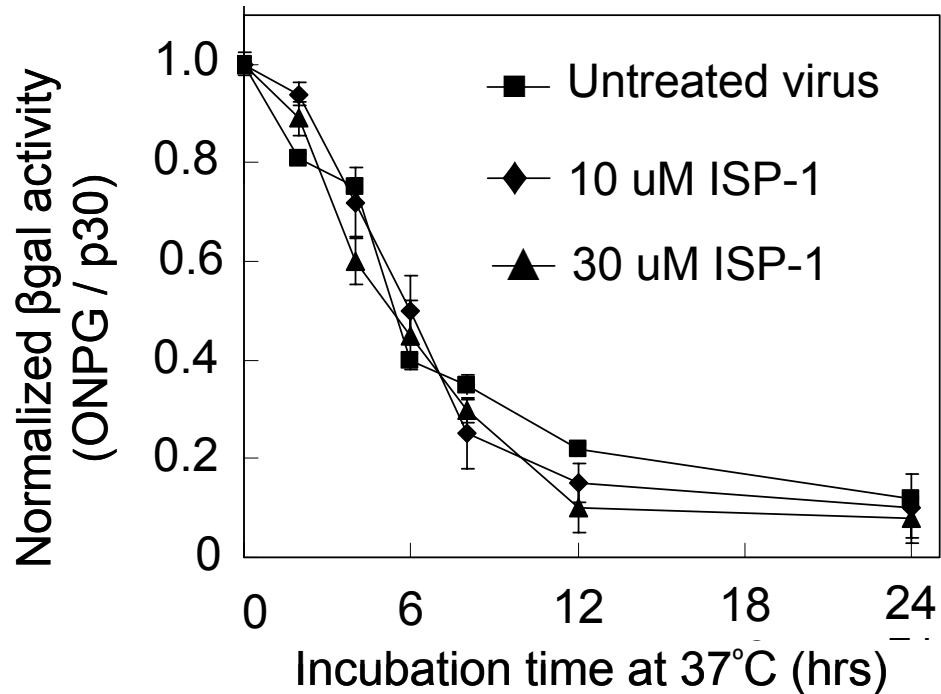


Figure 3.7. Stability of virus particles is not affected by myriocin treatment. TelCeb6 cells were plated at 240 000 cells per well in 6-well plates. The next day, the cell culture media was supplemented with 0, 10 or 30 μ M ISP-1. After 24 hours, the virus supernatant was harvested and filter sterilized. Retrovirus (100 μ L) produced from ISP-1 treated or untreated virus producing cells were incubated at 37 °C for 0 hr to 24 hrs. At indicated time points, a small aliquot was collected and stored (-80 °C) for later use. These aliquots were then later used to transduce NIH 3T3 to determine virus activity.

similar to untreated virus at all time points measured, indicating that altering lipid content in the virus lipid bilayer did not affect the stability of the virus particles. To determine if ISP-1 treatment altered virus binding properties, we harvested virus from Telceb6 cells after ISP-1 treatment as before, mixed in a 100,000 3T3 cells or HeLa cells at 4 °C for 2 hours, washed twice with cold PBS, lysed the cells and quantified p30, the virus capsid protein (Figure 3.8). We found that untreated virus bound to both cell types to the same extent as ISP-1 treated virus, suggesting that ISP-1 does not adversely affect the virus binding the cell surface.

Next we tested the fusogenicity of ISP-1 treated virus particles by using the nef-luciferase assay (9). In this experiment, virus producer cells were plated to confluency, transfected with 8 µg of pcDNA3-Nef-luc using Lipofectamine. This plasmid contained the *nef* gene tagged with a gene for luciferase, allowing for the measurement of luciferase activity after virus particles fused with the target membrane and released the substrate into the cytoplasm of the cells. Interestingly, we found that levels of luciferase activity decreased by about 25% in NIH 3T3 at dose of 30 µM ISP-1 and a decrease of nearly 80% treated in HeLa cells at similar concentrations of ISP-1 (Figure 3.9). Also, the extent of reduction in luciferase activity corresponded to the extent of reduction in virus infection after ISP-1 treatment. Therefore, our data suggests that depleting lipids from virus particles reduces their infectivity by altering their ability to fuse with the target cell membrane.

The presence of specific lipids in the virus lipid bilayer has been shown to be important for successful virus infection to occur, however, it is also known that the lipids in the target cell plasma membrane also contribute to efficient virus infection. Therefore, we wanted to determine whether the difference in infection of ISP-1 treated virus in NIH 3T3 and HeLa cells (Figure 3.10) was due to the lipid composition of the cells and whether the treatment of these target cells with ISP-1 affected virus infection

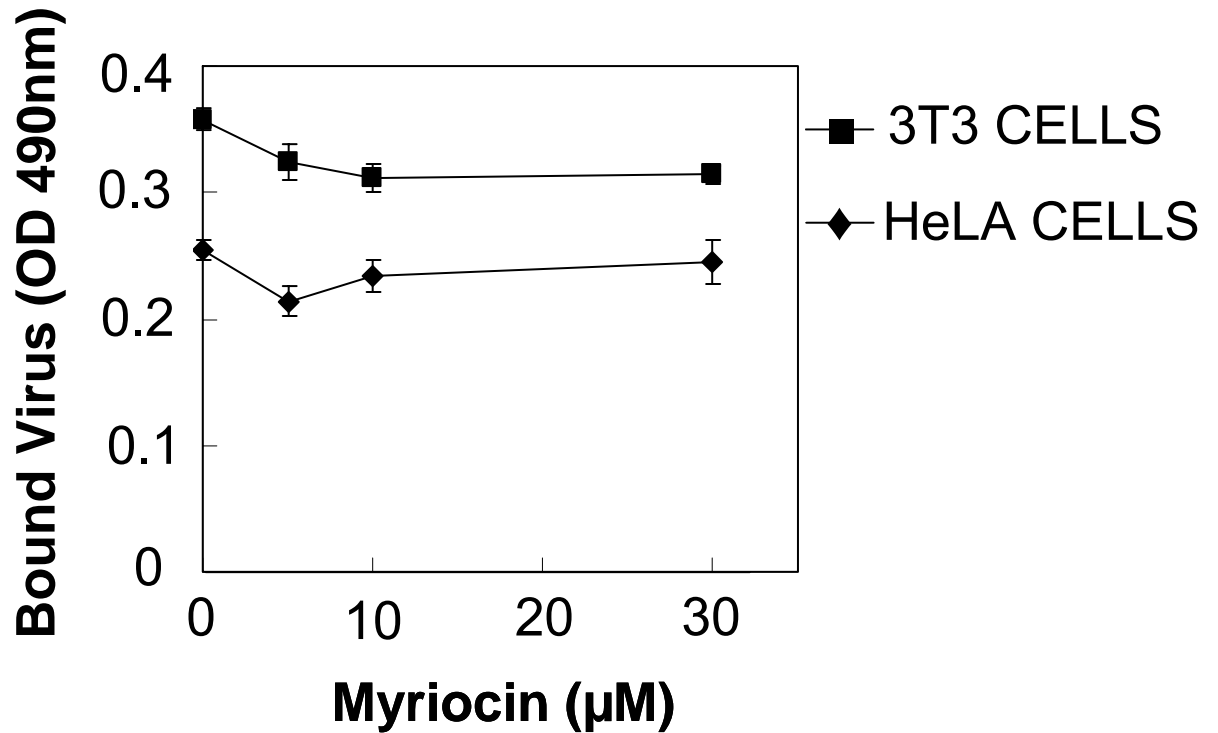


Figure 3.8 Binding of virus particles produced from myriocin treated virus producer cells is not adversely affected. NIH 3T3 or HeLa cells were plated to confluence in 6 well plates. The next day virus produced after various concentrations of ISP-1 treatment of virus producing cells, was applied to cells and incubated at 4 °C for 2 hrs. The cells were washed twice with cold PBS, lifted from the wells using a cell scraper, centrifuged (800 x g for 5 min) and the pellet resuspended in lysis buffer. Cell lysis samples were then used to quantify virus protein using the p30 ELISA.

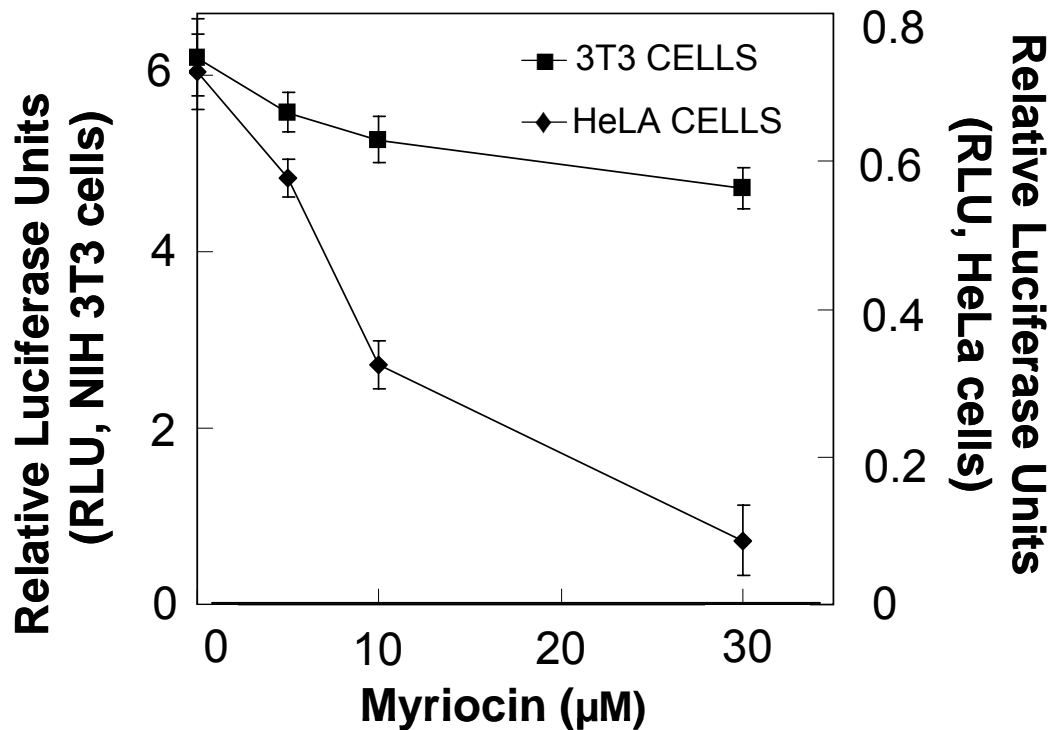


Figure 3.9 Virus particles produced by ISP-1 treated cells fuses less efficiently with target cells membrane. Telceb6-A cells were plated at approximately 80% confluency in 10-cm tissue culture dishes. The cells were transfected with 8 μg of pcDNA3-Nef-luc using Lipofectamine and added to the cells. The medium was replaced 6 hours later and replaced with DMEM/FBS. After 24 hours the supernatant was removed from the cells and replaced with media containing varying concentrations of ISP-1. After 24 hrs of treatment, the virus-laden cell culture supernatant was harvested, filter sterilized (0.45- μm) and used to infect NIH 3T3 and HeLa cells. NIH 3T3 and HeLa cells were incubated with virus at 37 $^{\circ}\text{C}$ for 2 hrs on a rotating platform. After this, the cells were pelleted by centrifugation at 800 x g for 5 min, supernatant discarded, and the cell pellet washed twice in DMEM. The final cell pellet was resuspended in 0.1 mL of Luciferase Assay Buffer (Promega) and the luciferase activity was measured using a Turner Biosystems Modulus Microplate reader and expressed as relative luciferase units. This protocol is adapted from Saeed et al (19).

A.

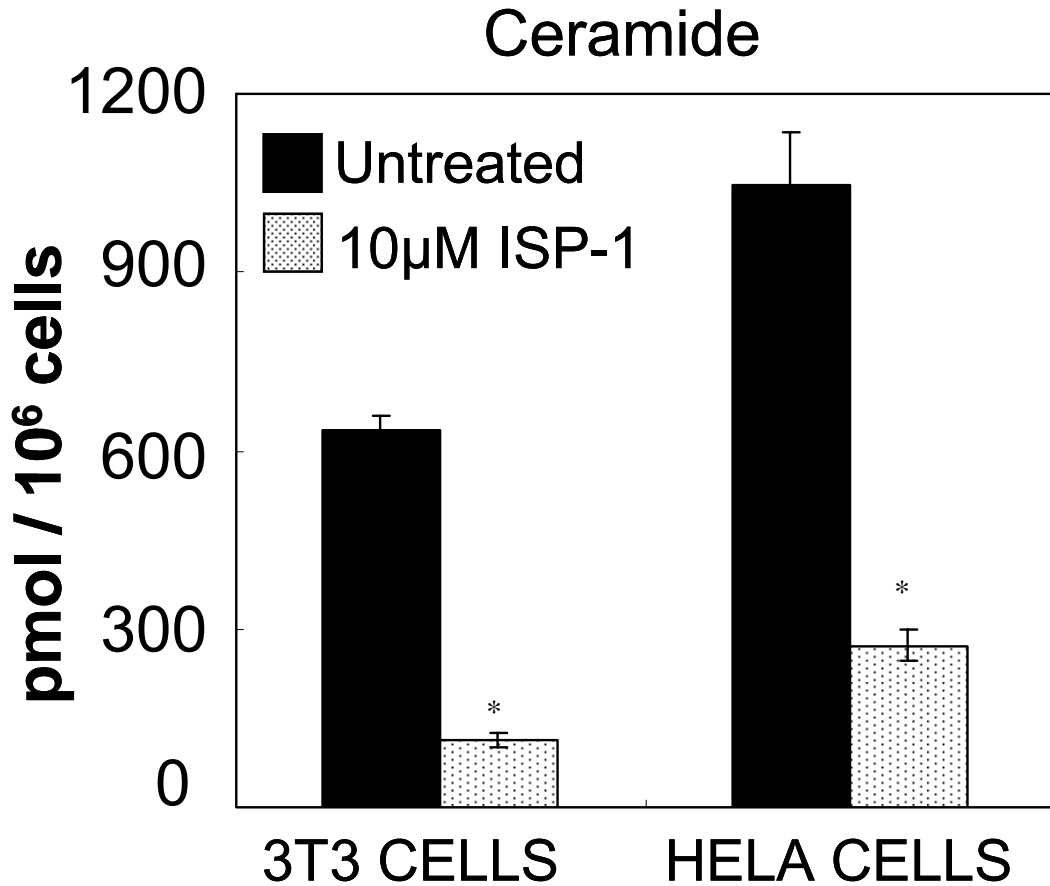


Figure 3.10 (A). Mass spectrometry analysis of ceramide present in the target cell membranes before and after myriocin treatment. Target cells, 3T3 cell and HeLa cells were grown to confluence in T175 flasks in DMEM/BCS and DMEM/FBS, respectively. Cells were then either treated with 0 μM or 10 μM ISP-1 for 72 hours and every 24 hrs, cell supernatant was changed with fresh media. After 3 days of ISP-1 treatment, the cells were put on ice and washed twice with cold phosphate buffered saline (PBS). Cells were then lifted from the flask using a cell scraper, resuspended in PBS, counted and aliquoted in borosilicate glass test tubes at 10⁷ cells per tube and pelleted centrifuged at 800 x g at 4 °C. (*) denotes statistical significant differences between treated and untreated cells (p<0.05).

B.

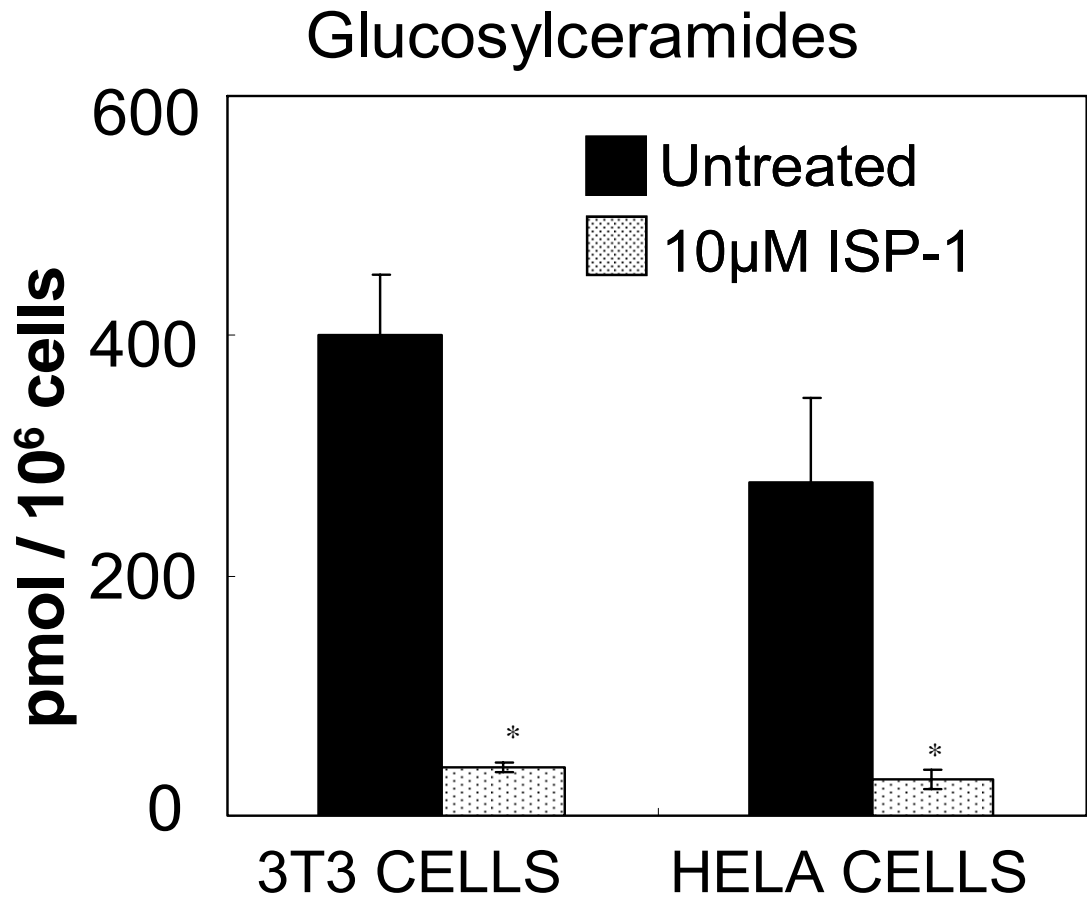


Figure 3.10 (B). Mass spectrometry analysis of glucosylceramide present in the target cell membranes before and after myriocin treatment. Target cells, 3T3 cell and HeLa cells were grown to confluence in T175 flasks in DMEM/BCS and DMEM/FBS, respectively. Cells were then either treated with 0 µM or 10 µM ISP-1 for 72 hours and every 24 hrs, cell supernatant was changed with fresh media. After 3 days of ISP-1 treatment, the cells were put on ice and washed twice with cold phosphate buffered saline (PBS). Cells were then lifted from the flask using a cell scraper, resuspended in PBS, counted and aliquoted in borosilicate glass test tubes at 10⁷ cells per tube and pelleted centrifuged at 800 x g at 4 °C. (*) denotes statistically significant differences between treated and untreated cells (p<0.05).

c.

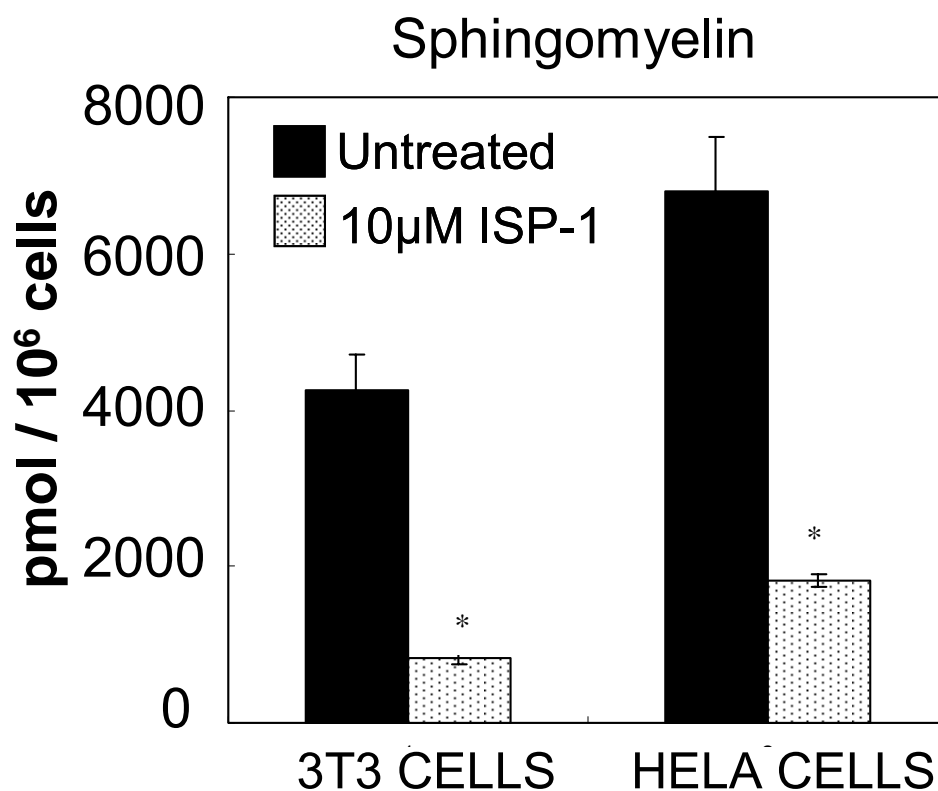


Figure 3.10 (C). Mass spectrometry analysis of sphingomyelin present in the target cell membranes before and after myriocin treatment. Target cells, 3T3 cell and HeLa cells were grown to confluence in T175 flasks in DMEM/BCS and DMEM/FBS, respectively. Cells were then either treated with 0 µM or 10 µM ISP-1 for 72 hours and every 24 hrs, cell supernatant was changed with fresh media. After 3 days of ISP-1 treatment, the cells were put on ice and washed twice with cold phosphate buffered saline (PBS). Cells were then lifted from the flask using a cell scraper, resuspended in PBS, counted and aliquoted in borosilicate glass test tubes at 10⁷ cells per tube and pelleted centrifuged at 800 x g at 4 °C. (*) denotes statistically significant differences between treated and untreated cells (p<0.05).

(Figure 3.10 A-C). We measured the levels of sphingolipids (specifically ceramide, glucosylceramide and sphingomyelin) in the two target cell types before and after 10 μ M ISP-1 treatment. We found that HeLa cells contained slightly more ceramide and sphingomyelin as compared to NIH 3T3 cells. The levels of glucosylceramide were similar for both cell types. As expected, after ISP-1 treatment the level of all three sphingolipids significantly decreased. The level of decrease between the two cell types was similar for all sphingolipids. Our results also suggest that the lipid composition of the two cell types is similar.

Lastly, since the virus lipid bilayer must work cooperatively with the cell membrane lipids for efficient fusion to occur, we measured the infectivity of ISP-1 treated or untreated virus particles on the two target cell types after the cells had been ISP-1 treated (Figure 3.11 A-B). The target cells were plated and the cell culture medium was supplemented with various concentrations of ISP-1. After 12 hours of treatment, the cells were incubated with virus particles, either produced from untreated or ISP-1 treated virus producer cells. Our data indicates that treating target cells with even low doses of ISP-1 causes a significant decrease in infection for all virus samples. Furthermore, the extent to which infection was inhibited was higher for HeLa cells after ISP-1 treatment than for NIH 3T3 cells, indicating that sphingolipids in HeLa cell membranes is critical for virus fusion. Therefore, the significant decrease in infection after ISP-1 treatment of target cells implies that the presence of sphingolipids is not only important in the virus lipid membrane but it is also critical in target cell membranes.

A.

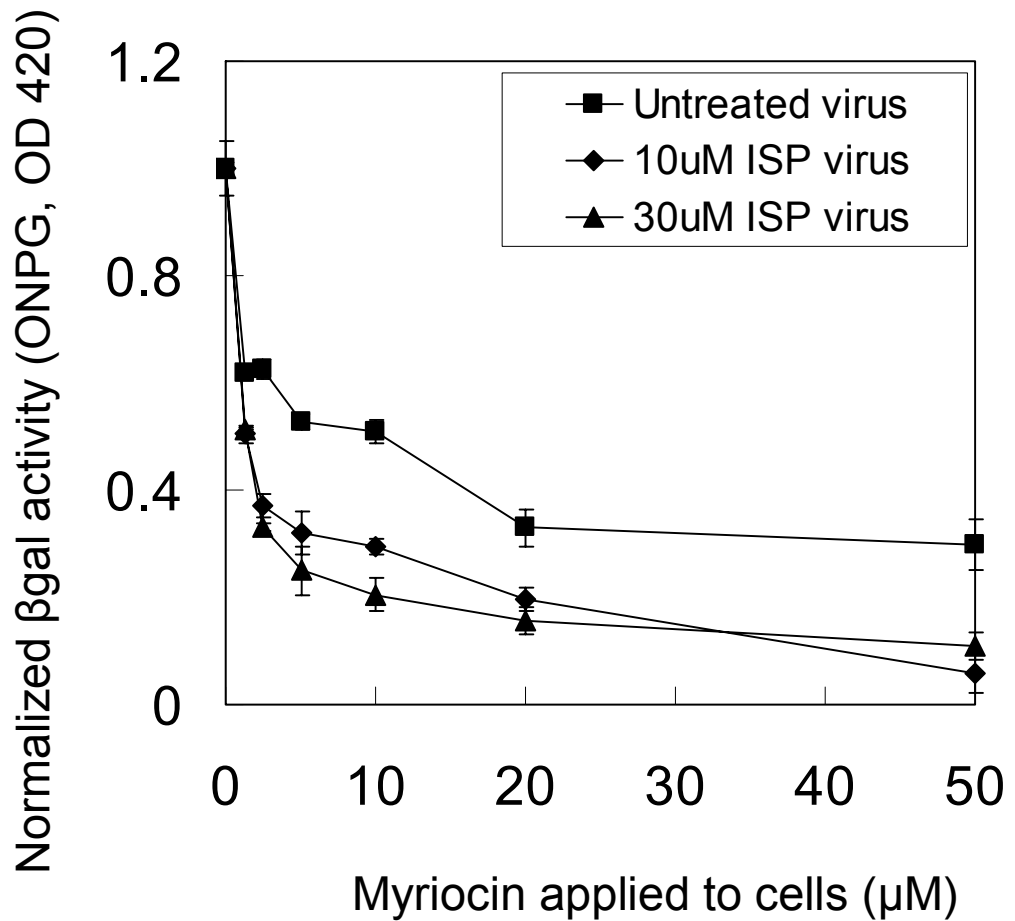


Figure 3.11. (A) Treatment of NIH 3T3 cells with ISP-1 decreases virus infection. Virus was produced from the treatment of Telceb6 cells with ISP-1 with concentrations of 0 μM, 10 μM and 30μM. After 24 hours the virus was harvested and diluted in a range of concentrations of ISP-1, as indicated, and this mixture was used to transduce NIH 3T3 cells. NIH 3T3 cells had been plated at 5 000 cells per well of a 96 well one day earlier. Two days later, the ONPG assay was conducted to quantify the virus infection.

B.

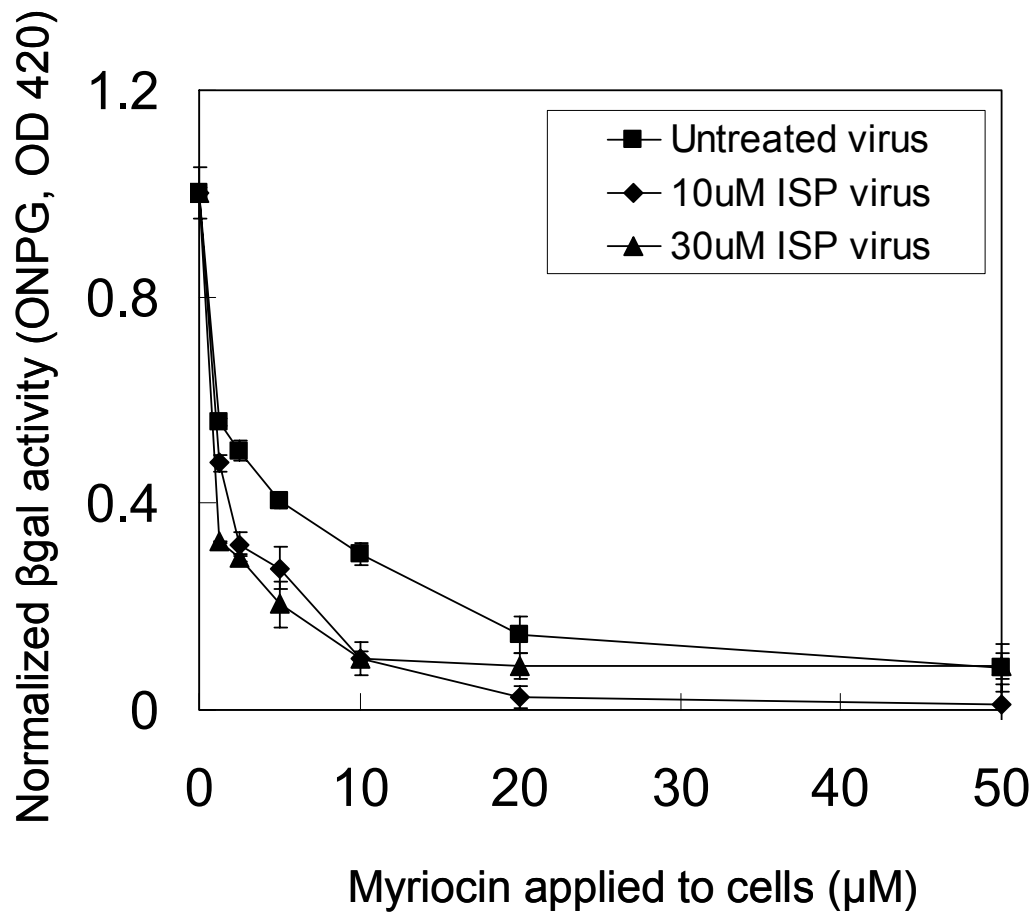


Figure 3.11 (B). Treatment of HeLa cells with ISP-1 decreases virus infection. Virus was produced from the treatment of Telceb6 cells with ISP-1 with concentrations of 0 μM, 10 μM and 30μM. After 24 hours the virus was harvested and diluted in a range of concentrations of ISP-1, as indicated, and this mixture was used to transduce HeLa cells. HeLa cells had been plated at 8 000 cells per well of a 96 well one day earlier. Two days later, the ONPG assay was conducted to quantify the virus infection.

3.5 Discussion

Fusion between the virus lipid bilayer and the host membrane is absolutely required for retrovirus infection to occur. Once virus envelope proteins interact with their cognate cellular receptors, several envelope glycoproteins oligomerize and assemble into a viral fusion machine which facilitates the movement of the two membranes into close apposition to allow fusion events to occur (1, 3, 23). Both viral and cellular lipids and proteins mediate the formation and expansion of the fusion pore (5, 21). Retroviral lipid bilayers are enriched in cholesterol and sphingolipids, and many studies have found that changes in the concentration of these components in the virus membrane can modulate viral fusion and entry (6, 16, 17).

In recent years, several groups have investigated the contribution of the cholesterol and sphingolipids to retrovirus entry and fusion (17). For example, Liao et al have shown that when cholesterol synthesis is inhibited in retrovirus producer cells or when cholesterol is extracted from target cells, virus production and infection is significantly reduced (11). Similarly, sphingolipid synthesis has been blocked in target cells to study the effects of complex sphingolipids (glycosphingolipids) in virus fusion and infection. The inhibition of human immunodeficiency virus (HIV-1) fusion in CD-positive cell lines has been shown to occur after glycosphingolipids depletion.

To test whether altering the levels of sphingolipids is important for MLV production and infection, we treated virus producer cells with myriocin (ISP-1). ISP-1 blocks the first step of the sphingolipid biosynthesis pathway, which causes significant changes in the cellular concentrations of many downstream bioactive intermediates, including ceramides, sphingomyelin and glucosylceramide. We analyzed the effect of myriocin treatment on the lipid composition of the cells and found that there was significant reduction in the amount of sphingolipids in the myriocin treated cells as compared to untreated cells. Specifically, ceramide levels were reduced by 94%

ceramide, glucosylceramide levels were reduced by 80%, and sphingomyelin were reduced by 70%. Furthermore, we purified and analyzed the virus particles that were produced by cells that had been treated with ISP-1. The virus particles contained significantly lower concentrations of sphingolipids as compared to virus particles that were produced from untreated cells. Reductions of approximately 90% in ceramides, 60% glucosylceramides, and 60% sphingomyelin were observed for the different species of sphingolipids.

Next we analyzed the effect of virus production and infection after ISP-1 treatment. Results from measuring virus capsid protein in stocks 24 hrs after ISP-1 treatment indicate that the treatment had no significant effect on virus production or release. Interestingly, we observed a reproducible decrease in virus infectivity. Virus particles released from ISP-1 treated cells (30 μ M) were 10-fold less infectious to HeLa cells than virus produced from untreated cells. Our results suggest that the changes in virus infectivity after ISP-1 treatment were cell-type dependant. When ISP-1 treated virus were incubated with NIH 3T3, the virus particles retained 70% of their infectivity versus an almost 10% infectivity in HeLa cells. These results suggest that the concentration of sphingolipids in the lipid bilayers of retroviruses appears to be important for maintaining virus infectivity but are not required for virus budding. Since ISP-1 can have cytotoxic effects, we wondered if the decrease in virus infectivity was due a decrease in cell number after ISP-1 treatment. Our cell viability assays indicate that there was no significance difference in viability of the target cells or virus producing cells after ISP-1 treatment.

Changing the lipid content of virus producing cells has been shown to cause severe changes in virus stability (6, 11). For instance, depletion of cholesterol from virus particles or virus producing cells has been shown to inactivate virus particles (11). Our results indicate that the stability of virus particles produced from ISP-1 treated cells was

similar to that of virus particles produced from untreated cells. Lastly, we investigated the ability of the virus particles to fuse with the target cell membrane. Interestingly, we observed similar trends in fusigenicity of the virus particles as we had with virus infection. Depleting lipids from virus particles reduced their infectivity by altering their ability to fuse with the target cell membrane.

The presence of specific lipids in the virus lipid bilayer have been shown to be important for successful virus infection to occur, however, it is also known that the lipids in the target cell plasma membrane also contribute to efficient virus infection. Treatment of target cells with 10 μ M ISP-1 resulted in significant decreases in the cell membrane. We observed 6 to 10 fold decreases in sphingolipids in both cell types for all three species of sphingolipids. Furthermore, since the virus lipid bilayer must work cooperatively with the cell membrane lipids for efficient fusion to occur, we measured the infectivity of ISP-1 treated or untreated virus particles on the two target cell types after the cells had been ISP-1 treated. Our data indicates that treating target cells with even low doses of ISP-1 causes a significant decrease in infection for all virus samples. Furthermore, the extent of inhibition of infection was higher for HeLa cells after ISP-1 treatment than for NIH 3T3 cells, indicating that sphingolipids in HeLa cell membranes is critical for virus fusion.

Previous studies that have investigated the role of glycosphingolipids in virus fusion and entry have concentrated their efforts on altering the composition of the target cell membrane. For example, Rawat et al showed that depletion of glycosphingolipids using PPMP (inhibitor of UDP: glycosyl transferase) from Sup-T1 cells (a suspension T cell line expressing low levels of CD4 and CXCR4) blocked HIV-1 envelope mediated fusion (17). Interestingly, similar studies using the GM95 cell line, which expresses high levels of the HIV -1 receptors, showed no significant effect in the absence of glycosphingolipids (6).

These observations have led to the hypothesis that glycosphingolipids may facilitate the recruitment of receptors on the target membrane to the fusion site. Therefore, in cells with high levels of receptor expression, fusion is not likely to be limited by the need to recruit receptors to the site of virus entry, and fusion is likely to occur even if there is a local depletion in the number of glycosphingolipids present in the membrane of the cell. Interestingly, NIH 3T3 cells express high levels of the Pit-2 receptor proteins versus the expression in HeLa cells (7, 12). These studies have investigated the importance of glycosphingolipids in the target membrane for virus fusion, however, our study we observe that for adequate fusion to occur, sphingolipids must also be present in the virus particle lipid bilayer, possibly facilitating the movement of virus envelope proteins such that the multivalent binding that is required for virus fusion can occur. Altogether, our data suggests that depleting glycosphingolipids from virus particles reduces their infectivity by altering their ability to fuse with the target cell membrane.

3.6 References

1. **Albanes, J. P., and V. S. Markin.** 2002. Membrane Fusion: Stalk Model Revisited. *Biophysical Journal* **82**:693.
2. **Goff, S. P.** 2007. Host factors exploited by retroviruses. *Nat Rev Microbiol* **5**:253-63.
3. **Harrison, S. C.** 2008. Viral membrane fusion. *Nat Struct Mol Biol* **15**:690-8.
4. **Hildreth, J. E., and Z. Liao.** 2001. Lipid rafts and HIV pathogenesis: Host membrane cholesterol is required for infection by HIV type-1. *AIDS Res Hum Retroviruses* **17**:1009.
5. **Hoekstra, D., and N. Duzgunes.** 1993. Lipid mixing assays to determine fusion in liposome systems. *Methods Enzymol* **220**:15-32.
6. **Hug, P., H. M. Lin, and J. M. Wang.** 2000. Glycosphingolipids promote entry of a broad range of human immunodeficiency virus type 1 isolates into cell lines expressing CD4, CXCR4, and/or CCR5. *Journal of virology* **74**:6377.
7. **Jobbagy, Z., S. Garfield, L. Baptiste, M. V. Eiden, and W. B. Anderson.** 2000. Subcellular redistribution of Pit-2 P(i) transporter/amphotropic leukemia virus (A-MuLV) receptor in A-MuLV-infected NIH 3T3 fibroblasts: involvement in superinfection interference. *J Virol* **74**:2847-54.
8. **Kavanaugh, M. P., D. G. Miller, W. Zhang, W. Law, S. L. Kozak, D. Kabat, and A. D. Miller.** 1994. Cell-surface receptors for gibbon ape leukemia virus and amphotropic murine retrovirus are inducible sodium-dependent phosphate symporters. *Proc Natl Acad Sci U S A* **91**:7071-7075.
9. **Kolokoltssov, A. A., and R. A. Davey.** 2004. Rapid and sensitive detection of retrovirus entry by using a novel luciferase-based content-mixing assay. *J Virol* **78**.
10. **Landazuri, N., and J. M. Le Doux.** 2004. Complexation of retroviruses with charged polymers enhances gene transfer by increasing the rate that viruses are delivered to cells. *J Gene Med* **6**:1304-19.
11. **Liao, Z., J. W. Roos, and J. E. Hildreth.** 2000. Increased infectivity of HIV type 1 particles bound to cell surface and solid-phase ICAM-1 and VCAM-1 through acquired adhesion molecules LFA-1 and VLA-4. *AIDS Res Hum Retroviruses* **16**:355-366.
12. **Logan, A. C., S. J. Nightingale, D. L. Haas, G. J. Cho, K. A. Pepper, and D. B. Kohn.** 2004. Factors influencing the titer and infectivity of lentiviral vectors. *Hum Gene Ther* **15**:976-88.
13. **Marandin, A., A. Dubart, F. Pflumio, F. L. Cosset, V. Cordette, S. Chapel-Fernandes, L. Coulombel, W. Vainchenker, and F. Louache.** 1998. Retrovirus-mediated gene transfer into human CD34⁺38^{low} primitive cells

capable of reconstituting long-term cultures in vitro and nonobese diabetic-severe combined immunodeficiency mice in vivo. *Hum Gene Ther* **9**:1497-511.

14. **Nayak, S., and L. A. Lyon.** 2004. Ligand-functionalized core/shell microgels with permselective shells. *Angew Chem Int Ed Eng* **43**:6706-6709.
15. **Ono, A., and E. O. Freed.** 2005. Role of lipid rafts in virus replication. *Adv Virus Res* **64**:311-58.
16. **Puri, A., R. Blumenthal, and A. Rein.** 2003. Modulation of entry of enveloped viruses by cholesterol and sphingolipids (review). *Molecular membrane Biology* **20**:243-254.
17. **Rawat, S. S., B. T. Johnson, and A. Puri.** 2005. Sphingolipids: modulators of HIV-1 infection and pathogenesis. *Biosci Rep* **25**:329-43.
18. **Sabatino, D. E., B. Q. Do, L. C. Pyle, N. E. Seidel, L. J. Girard, S. K. Spratt, D. Orlic, and D. M. Bodine.** 1997. Amphotropic or gibbon ape leukemia virus retrovirus binding and transduction correlates with the level of receptor mRNA in human hematopoietic cell lines. *Blood Cells Mol Dis* **23**:422-33.
19. **Saeed, M. F., A. A. Kolokoltsov, and R. A. Davey.** 2006. Novel, rapid assay for measuring entry of diverse enveloped viruses, including HIV and rabies. *J Virol Methods*.
20. **Smith, R. F.** 1994. *Microscopy and Photomicrography*, Boca Raton.
21. **Teissier, E., and E. I. Pecheur.** 2007. Lipids as modulators of membrane fusion mediated by viral fusion proteins. *Eur Biophys J* **36**:887-99.
22. **Wang, E., and A. Merrill.** 2005. Sphingolipidomics: high-throughput, structure-specific, and quantitative analysis of sphingolipids by lipid chromatography tandem mass spectrometry. *Methods* **36**:207.
23. **Wickner, W., and R. Schekman.** 2008. Membrane fusion. *Nat Struct Mol Biol* **15**:658-64.

CHAPTER 4

ALTERATION OF VIRAL LIPID COMPOSITION BY FUMONISIN INCREASES RETROVIRAL INFECTIVITY AND REDUCES VIRUS BUDDING

4.1 Abstract

The lipids of enveloped viruses play an important role in viral morphogenesis and infectivity. These lipids are derived from host cell membranes during virus budding, which has been shown to occur in regions of the host cell enriched in cholesterol and sphingomyelin. In this study, we use the fungal endotoxin, fumonisin B-1 (FB-1), to inhibit sphingolipid synthesis in virus producer cells. We examine the effect on the lipid composition of virus producing cells and the virus particles produced from them. Our results suggest that the virus lipid composition can be significantly altered by FB-1 treatment and that this treatment increases the specific infectivity of virus particles by affecting their ability to fuse with the target cell membrane.

4.2 Introduction

Retrovirus particles are composed of nucleic acids surrounded by a protein shell that is further protected by a lipid membrane bilayer. It is suggested that viruses acquire signaling proteins and lipids during the budding process and that these proteins and lipids play a significant role in virus attachment, fusion, and entry (7, 16). Retroviral infection is a multistep process that begins with adsorption of the virus particle to the cell surface (6). Amphotropic Moloney leukemia virus particles are known to initiate infection after engagement between the viral envelope protein and the receptors at the cell membrane. This interaction induces conformational changes in the envelope receptor proteins and ultimately results in the mixing of the viral lipids with the host cell membrane lipids.

The first point of contact that a virus makes with the host is with its lipid envelope, which consists of viral envelope lipids and proteins. Accumulating evidence suggests that lipids within the viral membrane are not incorporated randomly, and are heavily enriched in cholesterol and sphingomyelin (SM), possibly because retroviruses bud from specialized sites within the plasma membrane, called lipid rafts (15). The budding and assembly of several enveloped viruses has been shown to occur selectively from lipid rafts on the surface of infected cells (7, 13, 16, 23). For instance, it has been reported that the lipid bilayer of the human immunodeficiency virus (HIV-1) contains a high concentration of cholesterol, sphingomyelin and proteins that are known to be associated with lipid raft domains (2, 4, 18).

Many groups have also shown that sphingolipids in the target cell membrane are important for virus fusion and entry. An inhibitor in the synthesis of glycosphingolipids, UDP: glucosyl transferase (PPMP) has been widely used to study the role of plasma membrane sphingolipids (18). Studies conducted by Hug et al have found that treating target cells with PPMP down regulated the production of glycosphingolipids in the target cells and blocked HIV-1 entry and receptor mediated fusion in various cell lines expressing the HIV-1 receptors (8). Furthermore, Chieco-Bianchi et al have shown that blocking the synthesis of glycosphingolipids in target cells using L-cycloserine, an inhibitor of serine palmitoyltransferase, interferes with HIV-1 infection and replication in CEM cells, a CD4+ T-lymphocyte cell line (5).

Based on these findings, we hypothesized that altering the concentration of glycosphingolipids in virus producer cells will affect the lipid composition of viruses they produce, and by studying the function of these viruses, insights will be gained into the role sphingolipids play in the virus lifecycle. To test this hypothesis, we treated the stably transfected cell line, TelceB6 cells, with fumonisin B-1 (FB-1). FB-1 is a potent inhibitor of *de novo* sphingolipid biosynthesis that interferes with the formation of lipid

rafts (2). In this study, we investigated the effect of altering the lipid content of virus producing cells on virus production and budding, and the effect of altering the lipid composition of virus particles on their ability to bind, fuse, and infect target cells.

4.3 Material and Methods

Chemicals and Antibodies. Fumonisin B-1 was obtained from Biomol (Philadelphia, PA). Glutaraldehyde, and 1,5-dimethyl-1,5-diazaundecamethylene polymethobromide (Polybrene, PB) were from Sigma Chemical Co. (St. Louis, MO). Hydrogen peroxide 30%, and polyoxyethylene 20-sorbitan monolaurate (Tween 20) were from Fisher Scientific (Fair Lawn, NJ). Centrifugation filters to concentrate and purify virus stock were obtained from Millipore Corporation (Billerica, MA). Non-fat dry milk (blotting grade) was from Bio-Rad Laboratories (Hercules, CA). o-phenylenediamine dihydrochloride (OPD) was from Pierce (Rockford, IL). 5-bromo-4-chloro-3-indolyl- β -D-galactopyranoside (X-Gal) was from Denville Scientific, Inc. (Metuchen, NJ). Mouse anti-p30 and mouse anti-gp70 antibodies were purified from the supernatant of the CRL-1219 (ATCC, Rockville, MD) and the 83A25 [NL 37] hybridoma cell lines respectively, following standard procedures [NL 38]. The goat polyclonal anti-p30 antibody (78S221) and the goat polyclonal anti-gp70 (79S834) were from Quality Biotech (Camden, NJ). The horseradish peroxidase conjugated rabbit anti-goat immunoglobulin G polyclonal antibody was from Zymed Laboratories (South San Francisco, CA).

Cell Culture. NIH 3T3 mouse fibroblast were cultured in Dulbecco's modified Eagle's medium (DMEM; Hyclone Labs Inc., Logan, UT) with 10% bovine calf serum (Hyclone Labs Inc.), 100 U/mL of penicillin, and 100 μ g/mL of streptomycin (Hyclone Labs Inc.) (DMEM/BCS). HeLa cells (human cervical kidney, ATCC) and 293T/17 cells (human embryonic kidney epithelial) were cultured in Dulbecco's modified Eagle's medium (Hyclone Labs Inc., Logan, UT) with 10% fetal bovine serum (Hyclone Labs

Inc.), 100 U/mL of penicillin and 100 μ g/mL of streptomycin (DMEM/FBS). TELCeB6-A (TE671 (human rhabdomyosarcoma) cells stably transfected to express lacZ, Mo-MLVgagpol (12) and the amphotropic envelope glycoprotein (9) were cultured in DMEM, 10% fetal bovine serum (Hyclone Labs, Inc.), 100 U/mL of penicillin, and 100 mg/mL of streptomycin (DMEM/FBS).

Fumonisin B-1 treatment. For all experiments using fumonisin B-1, Telceb6-A cells were incubated with the indicated concentration of fumonisin B-1 for 24 h at 37 °C in DMEM/FBS or DMEM/BCS, depending on the cell type to be transduced.

Lipid analysis of virus particles and cells. Stably transfected virus producing cells, Telceb6-2A, and their parent cell line, Te671 which does not produce viruses, were used for lipid analysis. Cells were grown to confluence in T175 flasks in DMEM/FBS. Telceb6-2A cells were then either treated with 0 μ M or 50 μ M fumonisin B-1. Te671 cells were not treated with fumonisin B-1. For three days at every 24 hrs, cell supernatant was collected, filter sterilized (0.45 μ m), and then frozen (-80 °C) for later use. Harvested media was replaced with media either containing 0 μ M or 50 μ M fumonisin B-1. As a control for lipids present in conditioned culture medium from cells not producing virus particles, the supernatant of untreated Te671 cells was similarly harvested each day for 3 days. On the third day after harvest, the cells were put on ice and washed twice with cold phosphate buffered saline (PBS). The cells were then lifted from the flask using a cell scraper, resuspended in PBS, counted using trypan blue and aliquoted in 13 x 100mm screw-capped, borosilicate glass test tubes at 10^7 cells per tube. The cells were then centrifuged at 800 x g at 4 °C and the pellet was stored at -20 °C.

The filtered supernatant samples were concentrated using centrifugation filters from Millipore Corporation (Billerica, MA). A concentrated volume of 1.5 mL to 2 mL

was obtained. The total volume was brought to 7 mL in DMEM/FBS for each sample and applied on top of a 2 mL 20% sucrose solution. The virus particles were then pelleted by centrifugation at 30,000 rpm in a Beckman SW41 rotor for 2 h at 4 °C. The supernatant was gently aspirated, the pellet was resuspended in 400 µL PBS and the protein content quantified using the Coomassie Plus-200 protein assay reagent. The samples were stored in 13 x 100mm screw-capped, borosilicate glass test tubes with TeXon caps and used for sphingolipid analysis.

The sphingolipid analyses were conducted by liquid chromatography (LC) and electrospray tandem mass spectrometry using a PE Sciex API 3000 triple quadrupole mass spectrometer equipped with a turbo ion-spray source, as described previously (AM methods). Internal standards for the mass spectrometric analyses were obtained from Avanti Polar Lipids (Alabaster, AL); these were C12-ceramide (*N*-dodecanoyl-sphingosine, d18:1/12:0), C12-glucosylceramide, and C12-sphingomyelin. Protocol adapted from Merrill et al. *Methods*. 36: 207-224 (2005).

Cells and virus samples in the borosilicate glass test tubes were mixed with 0.5ml of methanol then 0.25ml of chloroform and the internal standards. The internal standards were prepared as a working stock in methanol and chloroform (2:1 v/v) such that small volumes can be added to each test tube. In general, the internal standard mixture is prepared to deliver 0.5 nmol of each of the following (per sample): ceramide (d18:1/12:0-Cer), sphingomyelin (d18:1/12:0-SM), glucosylceramide (d18:1/12:0-GlcCer), and lactosylceramide (d18:1/12:0-LacCer) (note that all have a 12-carbon fatty acid side chain), and C17-sphingosine, C17-sphinganine, C17-sphingosine 1-phosphate, and C17-sphinganine 1-phosphate (the C17-chain length was not found in most samples, and was verified for each new type of sample that was analyzed). All of these are available from Avanti Polar Lipids (Alabaster, AL). The test tubes were then sonicated until they appeared evenly dispersed, then incubated overnight at 48 °C in a

heating block. The samples were then cooled to room temperature, 75 μ L 1M KOH in methanol was added, sonicated, and incubated for 2 h at 37 °C. These steps remove most of the interfering glycerolipids, in particular phosphatidylcholines that can mask sphingomyelins in a simple MS scan.

The samples were cooled to room temperature and half of the volume was transferred to a new test tube. This portion (named Extract A) was used for separation of the more polar sphingolipids by reverse-phase LC. The solvent was removed from the samples using a Speed Vac-type concentrator (ThermoSavant), and re-dissolved in the reverse-phase LC solvent. To the half of the extract that remained in the original test tube, 3 μ L of glacial acetic acid was added to bring the pH near neutral, then 1 mL of chloroform and 2 mL of water was added, sample was vortexed, and centrifuged to separate the phases. The upper layer was carefully removed using a Pasteur pipette (discard), leaving the interface (with water). The solvent was then evaporated from the lower layer (named Extract B) using a Speed Vac-type concentrator (ThermoSavant), and re-dissolved in the normal-phase LC solvent.

Protein assay. To quantify the amount of protein in purified virus stocks after filtration, concentration and sucrose-cushion ultracentrifugation, samples were analyzed with the Coomassie Plus-200 Protein Assay as per the manufacturer's protocol. Optical density was measured using an absorbance plate reader (Pierce, Rockford, IL) and bovine serum albumin was used to create standards.

Cell viability assay. Ten microliters per well of MTT solution (100 mg of MTT in 1 mL of PBS) were added per well to cells in a 96-well plate. The plate was incubated for 4 hours at 37°C, then 150 μ L of 10% sodium dodecyl sulfate (SDS) was added per well and the plate incubated overnight at 37°C. The optical density at 570 nm was measured using an absorbance plate reader and the non-specific background at 650nm

subtracted. Values for replicate wells without cells were subtracted as background. Values for each point are the average of triplicate wells.

Virus Production. To generate retrovirus particles, TELCeB6-A cells were grown to confluence in T175 tissue culture flasks, and then incubated for 24 h with 20 mL of DMEM/FBS. The virus-laden tissue culture medium was harvested, filter-sterilized (0.45 μ m), then frozen (-80 °C) for later use.

Diluted Titer Assay. Ten-fold serial dilutions of *lacZ* virus stock were made in DMEM/BCS for NIH 3T3 transduction or in DMEM/FBS for HeLa transduction and were supplemented with Polybrene (8 μ g/mL). A 1-mL amount per well was used to transduce NIH 3T3 cells or HeLa cells that had been seeded (5 x 10⁴ per well or 8 x 10⁴ per well, respectively) the previous day in a 12-well plate. Two days after the start of the transduction, the cells were fixed and stained for β -galactosidase activity with X-Gal. Colonies of *lacZ*⁺ cells (typically in clusters of 2, 4, or 8 blue cells) were counted with the aid of a dissecting microscope. At appropriate dilutions of the virus stock, the clusters of blue cells were sufficiently spread over the dish such that each cluster arose from a single transduction event.

Virus stability. To determine virus particle stability, retrovirus (100 μ L) produced from fumonisin B-1 treated or untreated cells were incubated at 37 °C for 0 hr to 24 hrs. At indicated time points, a small aliquot was collected and stored (-80 °C) for later use. These aliquots were then later used to transduce NIH 3T3 to determine virus activity.

Virus binding assay. To determine if fumonisin B-1 treatment altered virus binding, we incubated virus produced from varying doses of fumonisin B-1 with NIH 3T3 cells and HeLa cells. NIH 3T3 or HeLa cells were plated to confluence in 6 well plates. The next day virus supernatant was applied to cells and incubated at 4 °C for 2 hrs. The cells were washed twice with cold PBS, lifted from the wells using a cell scraper,

centrifuged (800 x g for 5 min) and the pellet resuspended in lysis buffer. Cell lysis samples were then used to quantify virus protein using the p30 ELISA.

Production of nef-luc laz retrovirus. Telceb6-A cells were plated at approximately 80% confluency in 10-cm tissue culture dishes. The cells were transfected with 8 µg of pcDNA3-Nef-luc (kind gift of Robert Davey), diluted in 1.5 mL of DMEM, mixed with a solution of 1.5 mL of DMEM and 40 µL of Lipofectamine 2000 reagent (Invitrogen Life Technologies, Carlsbad, CA) and then added to the cells. The medium was replaced 6 hours later and 18 hours later with 10 mL of DMEM/FBS. Twenty four hours later the supernatant was removed from the cells and replaced with media containing varying concentrations of fumonisin B-1. After 24 hrs of treatment, the virus-laden cell culture supernatant was harvested, filter sterilized (0.45-µm) and frozen (-80°C) for later use. Virus capsid protein was quantified using p30 ELISA.

Virus Fusion assay. NIH 3T3 and HeLa cells were trypsinized, counted and pelleted in 1.5 mL tubes such that each pellet contained 1×10^5 cells. This protocol is adapted from Saeed et al (20). The cells were resuspended in 100 µL containing equal amount of virus protein (p30). Virus and cells were incubated at 37 °C for 2 hrs on a rotating platform. To remove virus particles that had not fused with the cell membrane, the cells were pelleted by centrifugation at 800 x g for 5 min, supernatant discarded, and the cell pellet washed twice in DMEM. The final cell pellet was resuspended in 0.1 mL of Luciferase Assay Buffer (Promega) and the luciferase activity was measured using a Turner Biosystems Modulus Microplate reader and expressed as relative luciferase units.

Beta-galactosidase (β-gal) transduction assay. Five thousand NIH 3T3 murine fibroblasts or eight thousand HeLa cells suspended in 100 µL of medium were plated in each well of a 96-well flat-bottomed tissue culture dish with a low-evaporation lid (Costar Corp., Cambridge, MA) (21). The next day, the medium was removed and 100 µL of the

virus-containing solution was added to each well. Two days after transduction, the medium was removed and the cells washed once with 100 μ L of PBS containing 1mM MgCl₂. After removal of the wash solution, 50 μ L of lysis buffer (PBS with 1mM MgCl₂ and 0.5% Igepal) were added to each well, and the plate incubated at 37 °C. After 30 min, 50 μ L of lysis buffer with 6 mM ONPG was warmed to 37 °C, added to each well, and the plate incubated at 37°C for 5 to 60 min until a visible yellow color was obtained. The reactions were halted by the addition of 20 μ L per well of stop buffer (1M Na₂CO₃). The optical density at 420 nm (OD₄₂₀) was measured using an absorbance plate reader (Molecular Devices, Menlo Park, CA) and the non-specific background at 650 nm subtracted. Values for replicate wells without virus were subtracted as background. Values for each point are the averages of at least triplicate wells.

ELISA for p30 and gp70. The concentration of virus capsid protein and envelope protein, p30 and gp70 respectively, were quantified using a previously described enzyme-linked immunosorbent assay (ELISA) (10). Briefly, ELISA plates (Nunc immuno Maxisorp 96-well plates, Nalgen Nunc International, Rochester, NY) were coated overnight at 4 °C with 10 μ g/mL of mouse anti-p30 antibody or mouse anti-gp70 antibody (100 μ L/well) in PBS. The next day, the antibody solution was removed and blocking buffer (PBS, 0.05% Tween-20, 5% non-fat milk) was added (200 μ L/well) for 2 h at 37°C to block non-specific binding sites. Virus particles were lysed using 0.5% Triton-X to expose the p30 antigen, then added to the ELISA plate (100 μ L/well) and incubated for 1 h at 37 °C. Bound p30 and gp70 were sandwiched by either the addition of the goat polyclonal anti-p30 antibody diluted 1:1000 or goat polyclonal anti-gp70 antibody diluted 1:300 in blocking buffer for 1 h at 37 °C (10), respectively. The horseradish peroxidase conjugated polyclonal rabbit anti-goat immunoglobulin G was diluted 1:5000 in blocking buffer and added to the ELISA plate (100 μ L/well) for 1 h at 37 °C to enable detection and quantitation of the p30 or gp70 antigen. The plates were developed for 5 min using

hydrogen peroxide (H₂O₂) and OPD (100 µg/well) from a solution of 3 mg of OPD and 3 µl H₂O₂ in 7.5 mL of substrate buffer (24 mM citric acid-monohydrate, 51 mM Na₂HPO₄·7H₂O, pH 5.0). Sulfuric acid (8 N, 50 µL/well) was used to stop the reaction, the optical density at 490 nm was measured using an absorbance plate reader, and the non-specific background at 650 nm was subtracted. Values for replicate wells without virus were subtracted as background.

Virus Budding Assay. Telceb6-A cells were plated to confluence in 6-well tissue culture plates and cultured in DMEM/FBS media. The next day, the cells were treated with 50 µM fumonisin B-1 or left untreated. The next day, the cell culture media was replaced with media containing 50 µM fumonisin B-1 or 0 µM fumonisin B-1. After 24 hours the supernatant was harvested, filter-sterilized (0.45 µm), then frozen (-80 °C) for later use. An aliquot of the supernatant (STOCK) was collected and stored separately. After harvesting the supernatant the cells were washed with cold PBS and removed from the tissue culture plates using a cell scraper. The cells were then pelleted at 800 x g for 5 min and resuspended in 0.5% Triton-X to lyse the cells and expose the p30 antigen inside the cells. These cell lyses samples were used to measure p30 inside the cells using the p30 ELISA. Also, to measure pelletable virus, the virus stored supernatant was mixed with 80 µg/mL of Polybrene and chondroitin sulfate-C, incubated for 20 min at 37 °C and centrifuged at 6000 x g for 20 min. The supernatant was collected and p30 in the samples was measured to determine the amount of p30 that could not be pelleted (SN, supernatant). The pellet was resuspended in PBS and p30 was measured to determine the amount of pelletable p30 (PELLET).

Statistical Analysis. Data are summarized as the mean ± one standard deviation for triplicate samples. Statistical analysis was performed using one-way analysis of variance for repeated measurements of the same variable. The Tukey

multiple comparison test was used to conduct pairwise comparisons between means. Differences at $p < 0.05$ were considered statistically significant.

4.4 Results

During virus budding, viruses acquire a lipid bilayer composed of signaling proteins and host lipids, both of which play a significant role in virus attachment, fusion and entry. The role of the envelope proteins in the retrovirus lifecycle has been extensively studied. Much less is known about the role of specific lipids in virus binding and infection. Here we studied the effect of blocking *de novo* sphingolipid biosynthesis on virus function by treatment of virus producing cells with fumonisin (FB-1), a potent inhibitor of serine palmitoyl-CoA transferase (SPT) which is a rate limiting enzyme in the biosynthesis of sphingolipids (Figure 4.1) (Hojjati et al 2005).

As a first step toward investigating the effects of altering sphingolipid synthesis in virus producer cells on the lipid composition of the virus lipid bilayer, we treated TelCeB6 cells with 50 μ M FB-1 (added from a 1 mM stock solution in phosphate-buffered saline) for 24 hours, or left them untreated, harvested the virus supernatant and analyzed the lipid composition of the cells and virus particles using mass spectrometry (Figure 4.2 A-C). After the virus producer cells were treated with FB-1, they were washed with cold PBS three times, counted, pelleted and stored at -20°C . The TelCeB6 parent cell line, Te671, the parent cell line of Telceb6, was used as a control for determining how many lipids that are not associated with viruses are present in medium conditioned by the cells. Conditioned medium that we had previously collected from Te671, TelCeB6 and TelCeB6 cells treated with 50 μ M FB-1 was thawed, concentrated, pelleted and purified two times with a 20% sucrose cushion. Protein concentration in the pelleted supernatant was quantified and aliquots of the sample, each of which contained equal amounts of protein, were analyzed for lipid content by mass spectrometry. Lipids were extracted from pellets of cells and supernatant and analyzed for three downstream

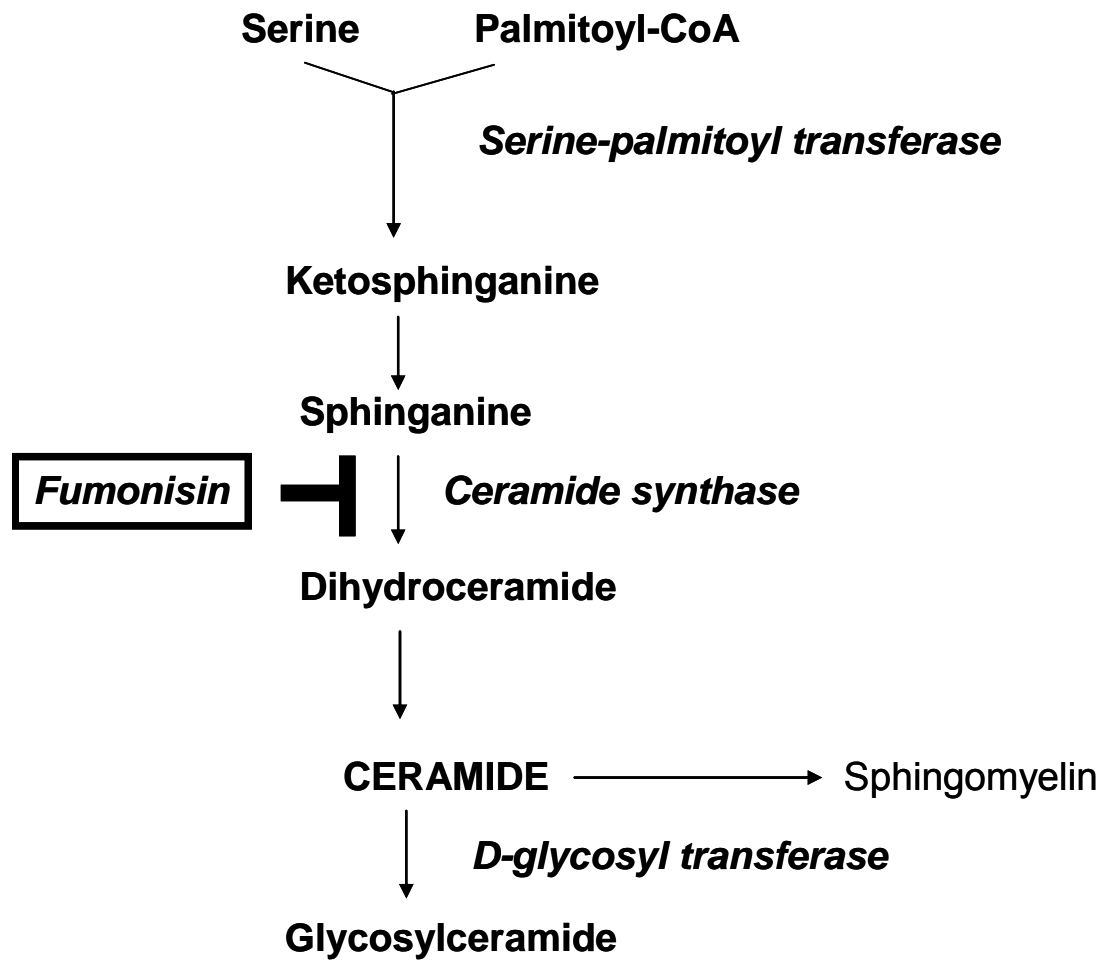


Figure 4.1. The pathway of *de novo* sphingolipid biosynthesis and sites of action of fumonisin B-1.

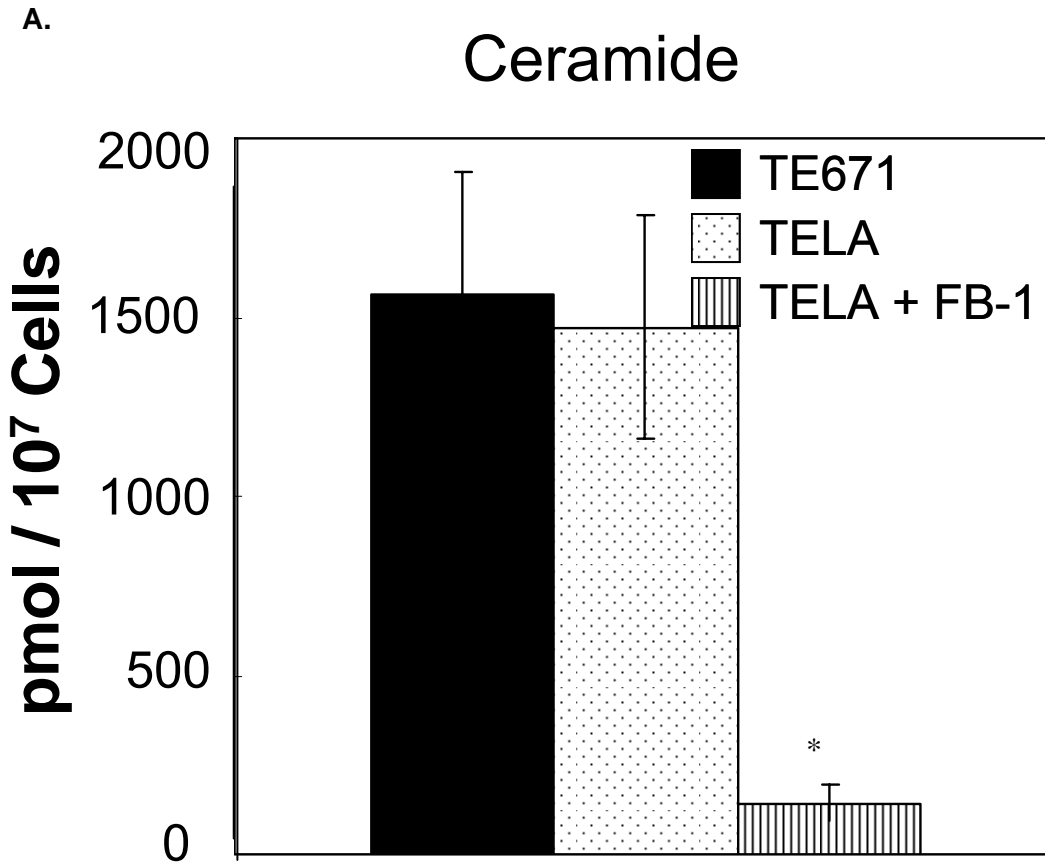


Figure 4.2 (A). Mass spectrometry analysis of ceramide present in virus producer cells. Stably transfected virus producing cells, Telceb6-2A, and their parent cell line, Te671 which does not produce viruses, were used for lipid analysis. Cells were grown to confluence in T175 flasks in DMEM/FBS. Telceb6-2A cells were then either treated with 0 μ M or 50 μ M FB-1. Te671 cells were not treated with FB-1. Every 24 hrs, for 72 hours, cell supernatant was collected, filter sterilized (0.45 μ m), then frozen (-80 $^{\circ}$ C). Harvested media was replaced with media either containing 0 μ M or 50 μ M FB-1. As a control for lipids present in conditioned culture medium from cells not producing virus particles, the supernatant of untreated Te671 cells was similarly harvested each day for 3 days. On the third day after harvest, the cells were put on ice and washed twice with cold phosphate buffered saline (PBS). Cells were then lifted from the flask using a cell scraper, resuspended in PBS, counted and aliquoted in borosilicate glass test tubes at 10^7 cells per tube and pelleted centrifuged at 800 x g at 4 $^{\circ}$ C. (*) denotes statistically significant differences between treated and untreated cells ($p < 0.05$).

B.

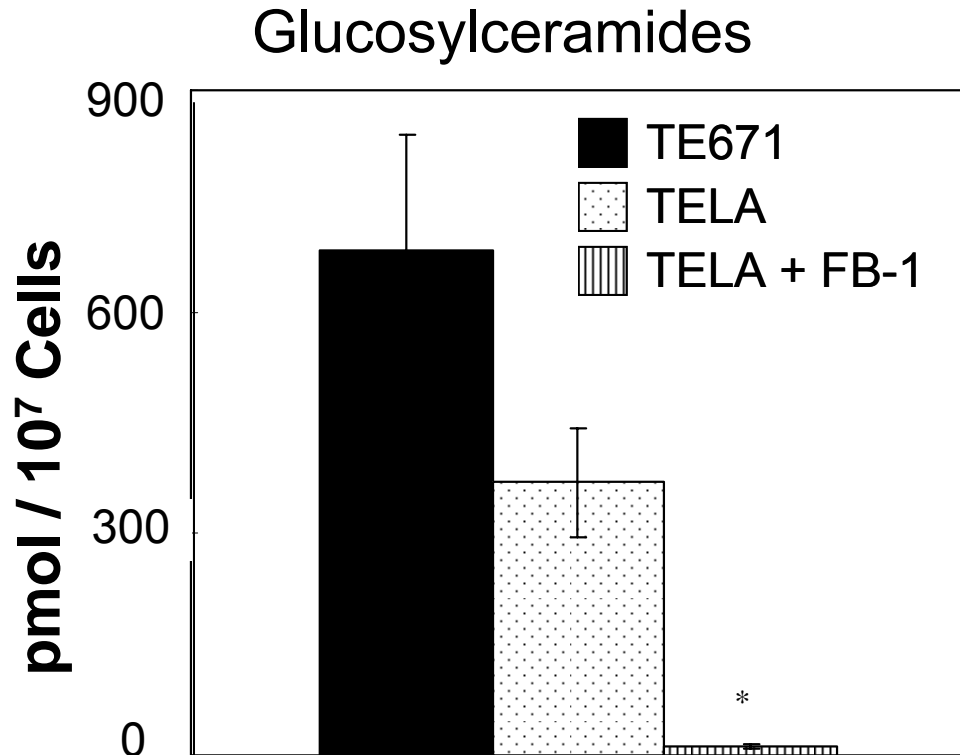


Figure 4.2 (B). Mass spectrometry analysis of glucosylceramide present in virus producer cells. Stably transfected virus producing cells, Telceb6-2A, and their parent cell line, Te671 which does not produce viruses, were used for lipid analysis. Cells were grown to confluence in T175 flasks in DMEM/FBS. Telceb6-2A cells were then either treated with 0 μ M or 50 μ M FB-1. Te671 cells were not treated with FB-1. Every 24 hrs, for 72 hours, cell supernatant was collected, filter sterilized (0.45 μ m), then frozen (-80 $^{\circ}$ C). Harvested media was replaced with media either containing 0 μ M or 50 μ M FB-1. As a control for lipids present in conditioned culture medium from cells not producing virus particles, the supernatant of untreated Te671 cells was similarly harvested each day for 3 days. On the third day after harvest, the cells were put on ice and washed twice with cold phosphate buffered saline (PBS). Cells were then lifted from the flask using a cell scraper, resuspended in PBS, counted and aliquoted in borosilicate glass test tubes at 10^7 cells per tube and pelleted centrifuged at 800 x g at 4 $^{\circ}$ C. (*) denotes statistically significant differences between treated and untreated cells ($p < 0.05$).

c.

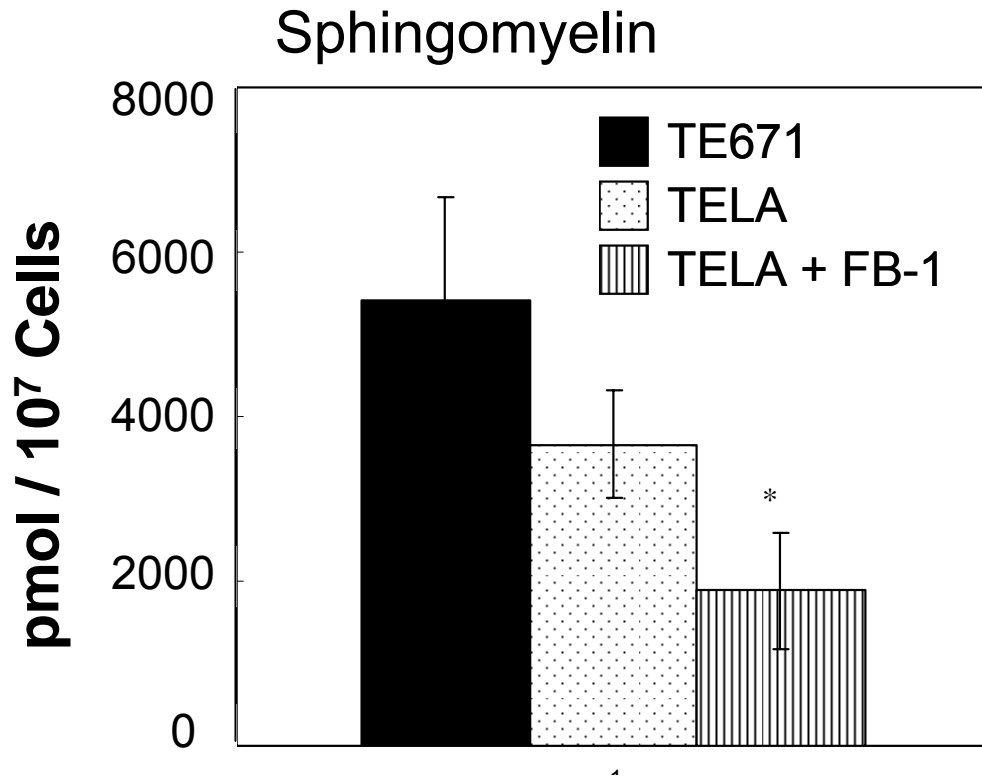


Figure 4.2 (C). Mass spectrometry analysis of sphingomyelin present in virus producer cells. Stably transfected virus producing cells, Telceb6-2A, and their parent cell line, Te671 which does not produce viruses, were used for lipid analysis. Cells were grown to confluence in T175 flasks in DMEM/FBS. Telceb6-2A cells were then either treated with 0 μ M or 50 μ M FB-1. Te671 cells were not treated with FB-1. Every 24 hrs, for 72 hours, cell supernatant was collected, filter sterilized (0.45 μ m), then frozen (-80 $^{\circ}$ C). Harvested media was replaced with media either containing 0 μ M or 50 μ M FB-1. As a control for lipids present in conditioned culture medium from cells not producing virus particles, the supernatant of untreated Te671 cells was similarly harvested each day for 3 days. On the third day after harvest, the cells were put on ice and washed twice with cold phosphate buffered saline (PBS). Cells were then lifted from the flask using a cell scraper, resuspended in PBS, counted and aliquoted in borosilicate glass test tubes at 10^7 cells per tube and pelleted centrifuged at 800 x g at 4 $^{\circ}$ C. (*) denotes statistically significant differences between treated and untreated cells ($p < 0.05$).

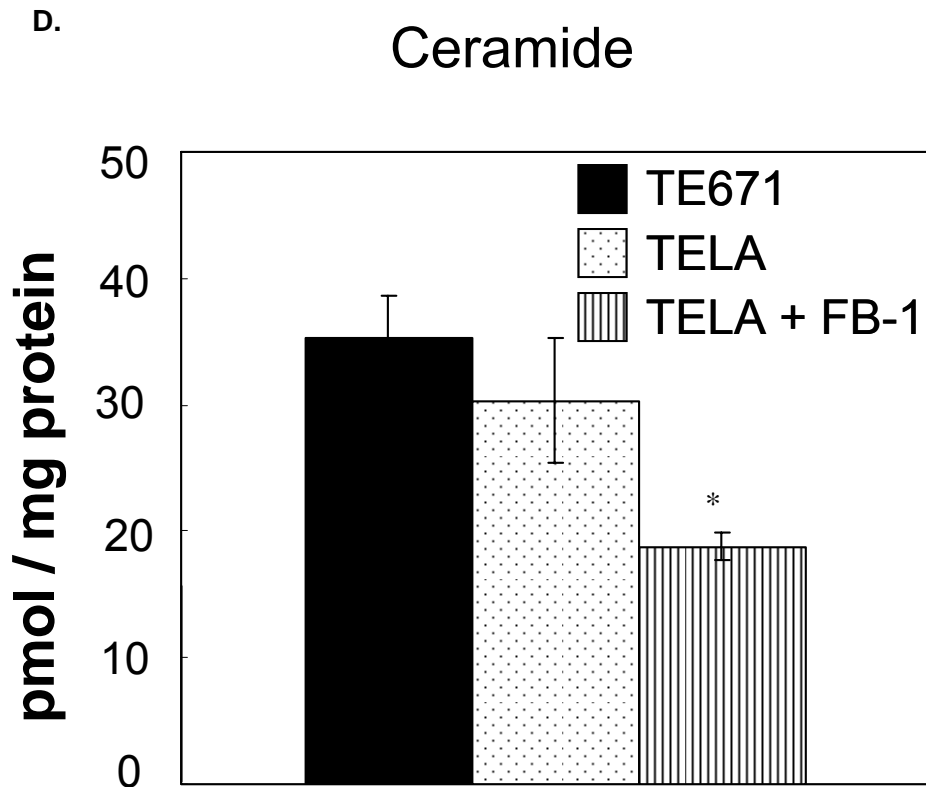


Figure 4.2 (D). Mass spectrometry analysis of ceramide in virus particles. Virus producer cells were treated as indicated in Figure 4.2 (A-C). The filtered supernatant samples collected from these cells were concentrated using centrifugation filters from Millipore Corporation (Billerica, MA). A concentrated volume of 1.5 mL to 2 mL was obtained. The total volume was brought to 7 mL in DMEM/FBS for each sample and applied on top of a 2 mL 20% sucrose solution. The virus particles were then pelleted by centrifugation at 30,000 rpm in a Beckman SW41 rotor for 2 h at 4 °C. The supernatant was gently aspirated, the pellet was resuspended in 400 μ L PBS and the protein content quantified using the Coomassie Plus-200 protein assay reagent. The samples were stored in 13 x 100mm screw-capped, borosilicate glass test tubes with teflon caps and used for sphingolipid analysis. (*) denotes statistically significant differences between treated and untreated cells ($p < 0.05$).

E.

Glucosylceramides

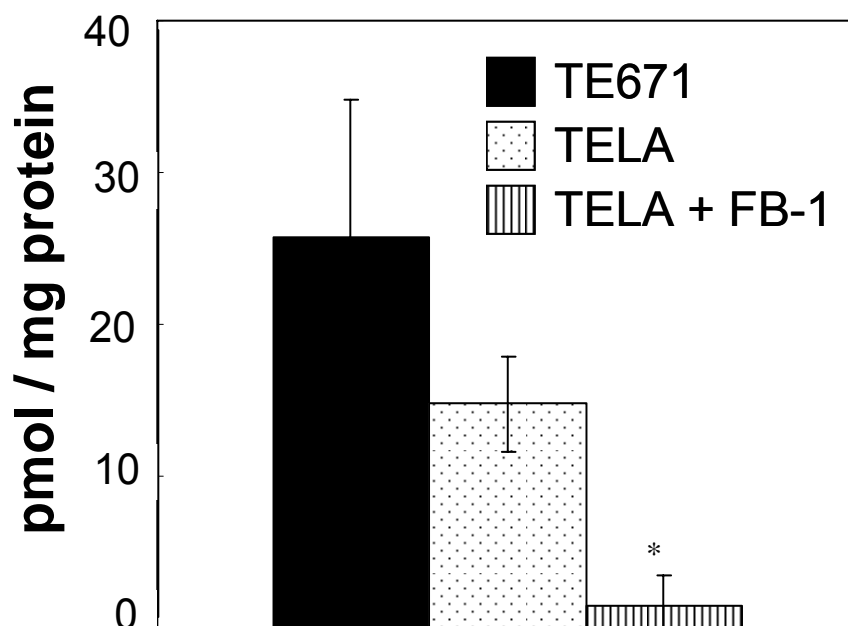


Figure 4.2 (E). Mass spectrometry analysis of glucosylceramide in virus particles. Virus producer cells were treated as indicated in Figure 4.2 (A-C). The filtered supernatant samples were concentrated using centrifugation filters from Millipore Corporation (Billerica, MA). A concentrated volume of 1.5 mL to 2 mL was obtained. The total volume was brought to 7 mL in DMEM/FBS for each sample and applied on top of a 2 mL 20% sucrose solution. The virus particles were then pelleted by centrifugation at 30,000 rpm in a Beckman SW41 rotor for 2 h at 4 °C. The supernatant was gently aspirated, the pellet was resuspended in 400 μ L PBS and the protein content quantified using the Coomassie Plus-200 protein assay reagent. The samples were stored in 13 x 100mm screw-capped, borosilicate glass test tubes with teflon caps and used for sphingolipid analysis. (*) denotes statistically significant differences between treated and untreated cells ($p < 0.05$).

F.

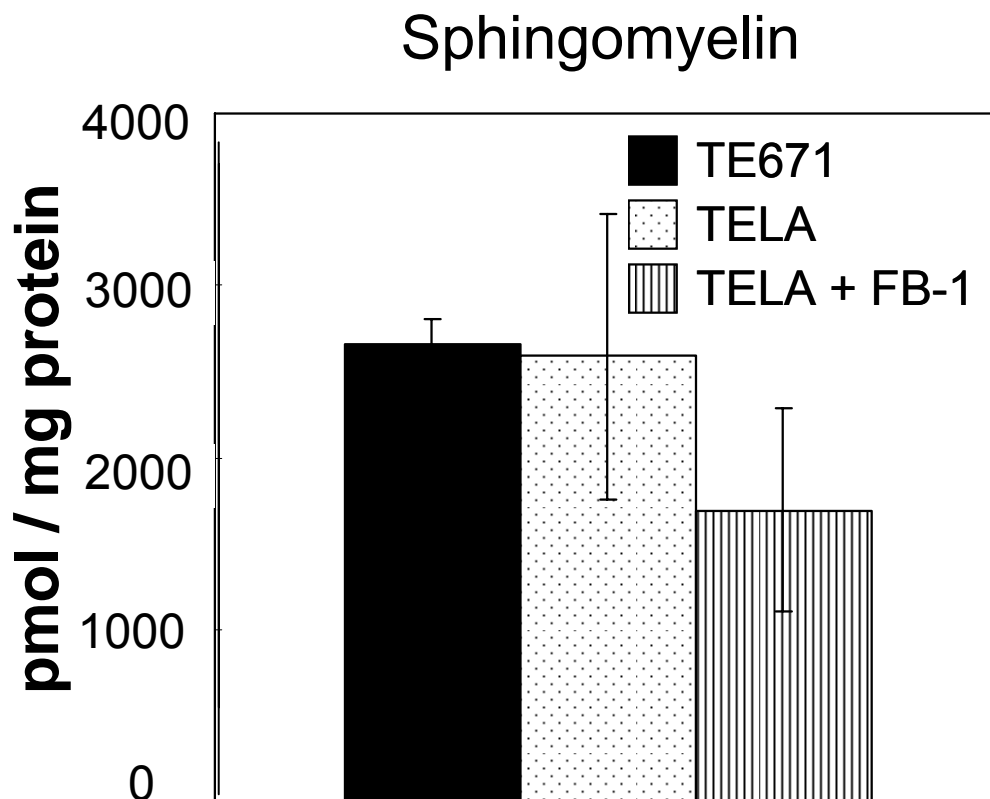


Figure 4.2 (F). Mass spectrometry analysis of sphingomyelin in virus particles. Virus producer cells were treated as indicated in Figure 4.2 (A-C). The filtered supernatant samples were concentrated using centrifugation filters from Millipore Corporation (Billerica, MA). A concentrated volume of 1.5 mL to 2 mL was obtained. The total volume was brought to 7 mL in DMEM/FBS for each sample and applied on top of a 2 mL 20% sucrose solution. The virus particles were then pelleted by centrifugation at 30,000 rpm in a Beckman SW41 rotor for 2 h at 4 °C. The supernatant was gently aspirated, the pellet was resuspended in 400 μ L PBS and the protein content quantified using the Coomassie Plus-200 protein assay reagent. The samples were stored in 13 x 100mm screw-capped, borosilicate glass test tubes with teflon caps and used for sphingolipid analysis.

products in the lipid synthesis pathway affected by FB-1: ceramide, glycosylceramide and sphingomyelin (Figure 4.2 D-F). Cells treated with FB-1 and their resulting conditioned medium showed a marked decrease in the concentration of all three sphingolipids species as compared to untreated TelCeB6 cells. Our results show that significant decreases in all three subspecies of lipids occurs after 24 hours of 50 μ M FB-1 treatment, suggesting that the toxin is active and elicits the expected effects. Also, since the accumulation of sphingolipid metabolites can affect cell function, we measured the cell viability of the virus producing cells as well as of the target cells (Figure 4.3). Our results suggest that FB-1 was not cytotoxic at the tested doses and that the decrease in virus titer was not due to decreased number of cells.

Next, to determine the effect of FB-1 treatment on virus production and infection, we treated Telceb6 cells with a range of concentrations, 0 to 100 μ M of FB-1 and harvested the virus supernatant after 24 hours. We quantified by ELISA the amount of virus that was produced by the treated cells (Figure 4.4 A). Interestingly, we found that FB-1 treatment decreased the amount of virus produced from the virus producer cells. To further investigate the increase in virus infectivity, we measured the extent of envelope incorporation into virus particles after FB-1 treatment (Figure 4.4 B-C). Interestingly, our results suggest that although there is a decrease in virus capsid protein (p30) production, the amount of virus envelope protein in each virus particle actually increases.

Although we observed a decrease in p30 concentration in the virus supernatant, it was unclear whether this was due to a decrease in p30 production by the cell, or if p30 production per cell remained constant and the decrease in p30 was due to less budding from the producer cells. Therefore, we measured the amount of p30 protein produced inside Telceb6-A cells after FB-1 treatment (Figure 4.5). Cells were plated to confluence

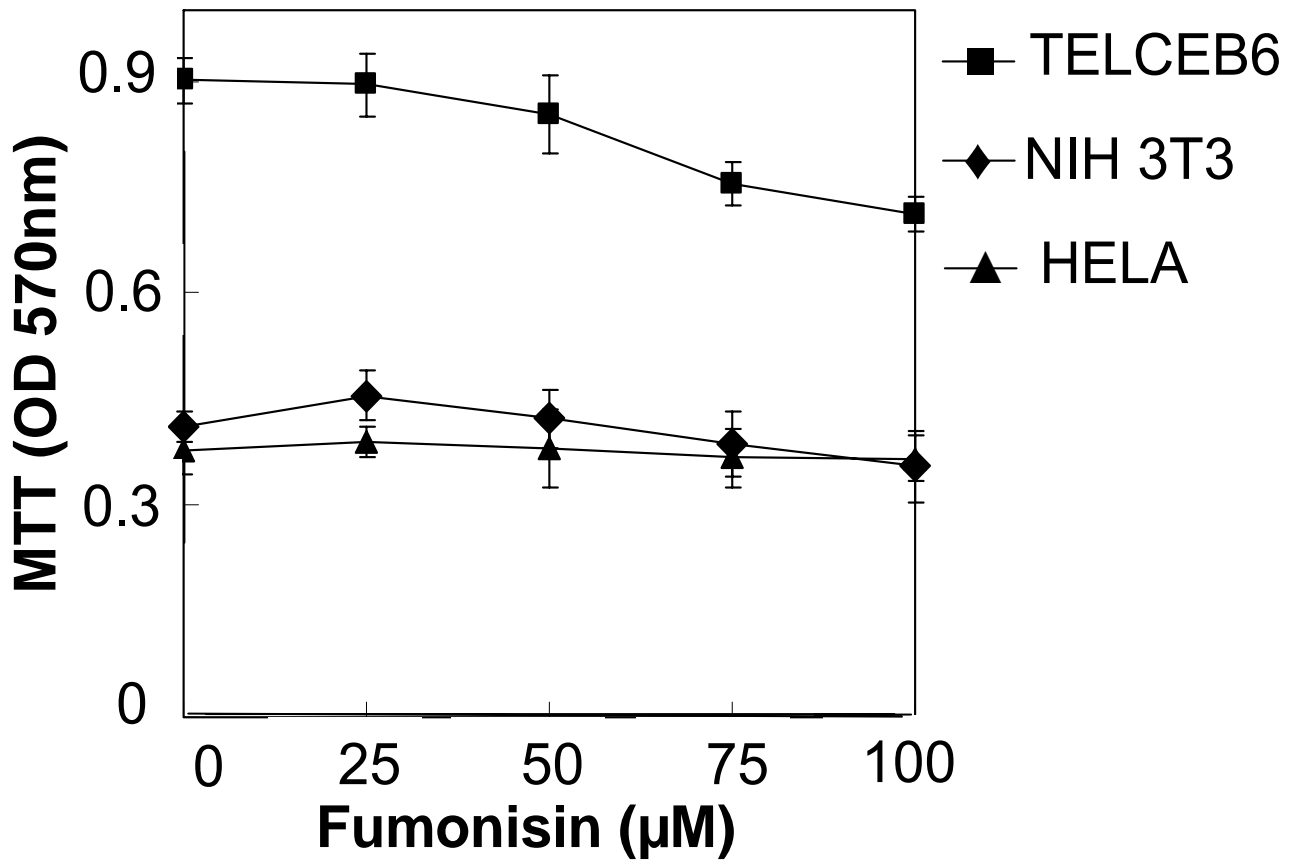


Figure 4.3 Effect of varying doses of FB-1 treatment on cell viability. Virus producer cell line (TelCeb6) and target cells (NIH 3T3 and HeLa cells) were plated at a density of 10,000 cells per well and 5,000 cells per well in 96-well plates. The next day, the cells were treated with varying doses of FB-1 as indicated. TelCeb6 were assayed for cell viability after 24 hours of FB-1 treatment and NIH 3T3 and HeLa cells were assayed after 48 hours of treatment. After 24 or 48 hours, 10 µL per well of MTT solution (100 mg of MTT in 1 mL of PBS) were added per well to cells in a 96-well plate. The plate was incubated for 4 hours at 37°C, then 150 µL of 10% SDS were added per well and the plate incubated overnight. The optical density at 570 nm was measured using an absorbance plate reader and the non-specific background at 650nm subtracted. Values for replicate wells without cells were subtracted as background. Values for each point are the average of triplicate wells.

A.

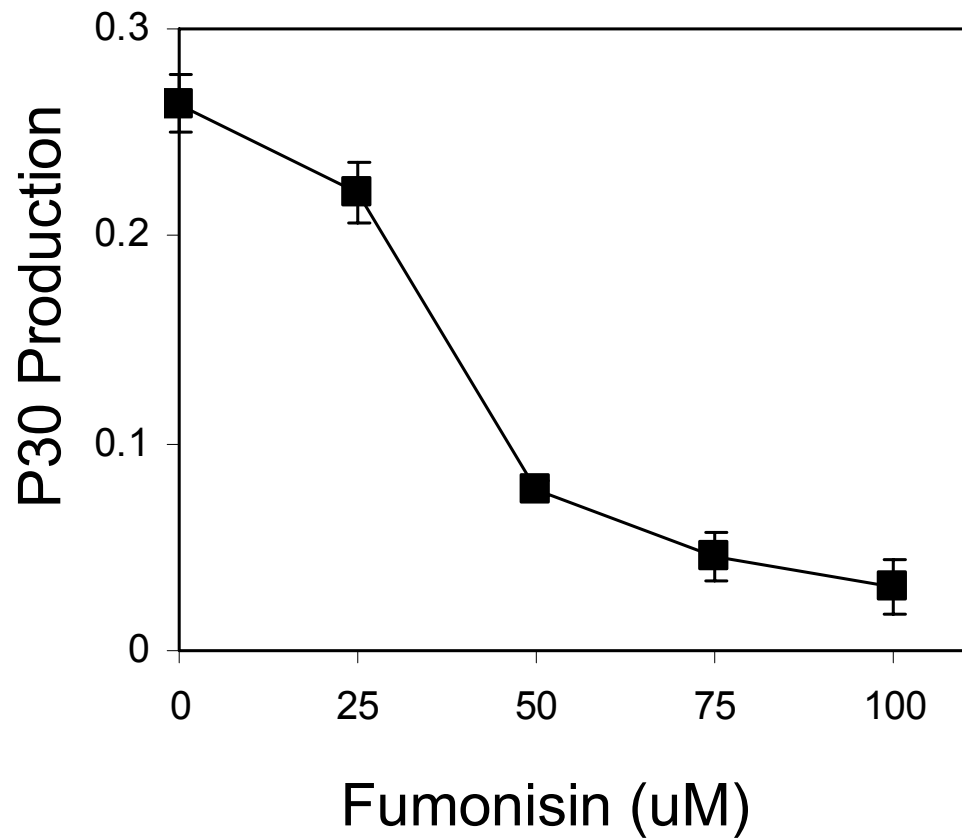


Figure 4.4 (A). Fumonisin treatment affects virus production. TelCeB6, were plated at 240, 000 cells per well of a 6-well plate and grown to confluency. The next day, cell culture media was removed and replaced with media containing varying doses of FB-1 as indicated. After 24 hours, the conditioned cell media was collected and filter sterilized (0.45 μ m). The concentration of virus in the supernatant after treating virus producer cells with different doses of FB-1 was determined using the p30 ELISA. Each point shows the mean \pm standard deviation of three replicates.

B.

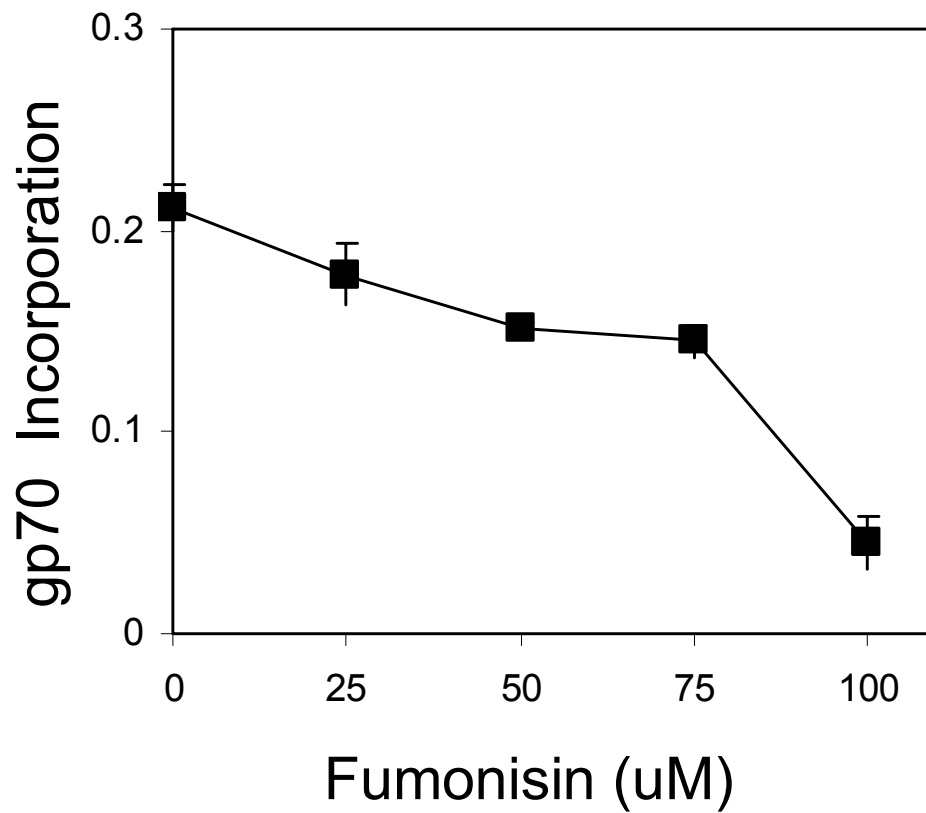


Figure 4.4 (B). Effect of fumonisin treatment on gp70 incorporation. Virus producer cells, TelCeB6, were plated at 240, 000 cells per well of a 6-well plate and grown to confluency. The next day, cell culture media was removed and replaced with media containing varying doses of FB-1 as indicated. After 24 hours, the conditioned cell media was collected and filter sterilized (0.45 μm). The concentration of virus in the supernatant after treating virus producer cells with different doses of FB-1 was determined using the gp70 ELISA. Each point shows the mean \pm standard deviation of three replicates.

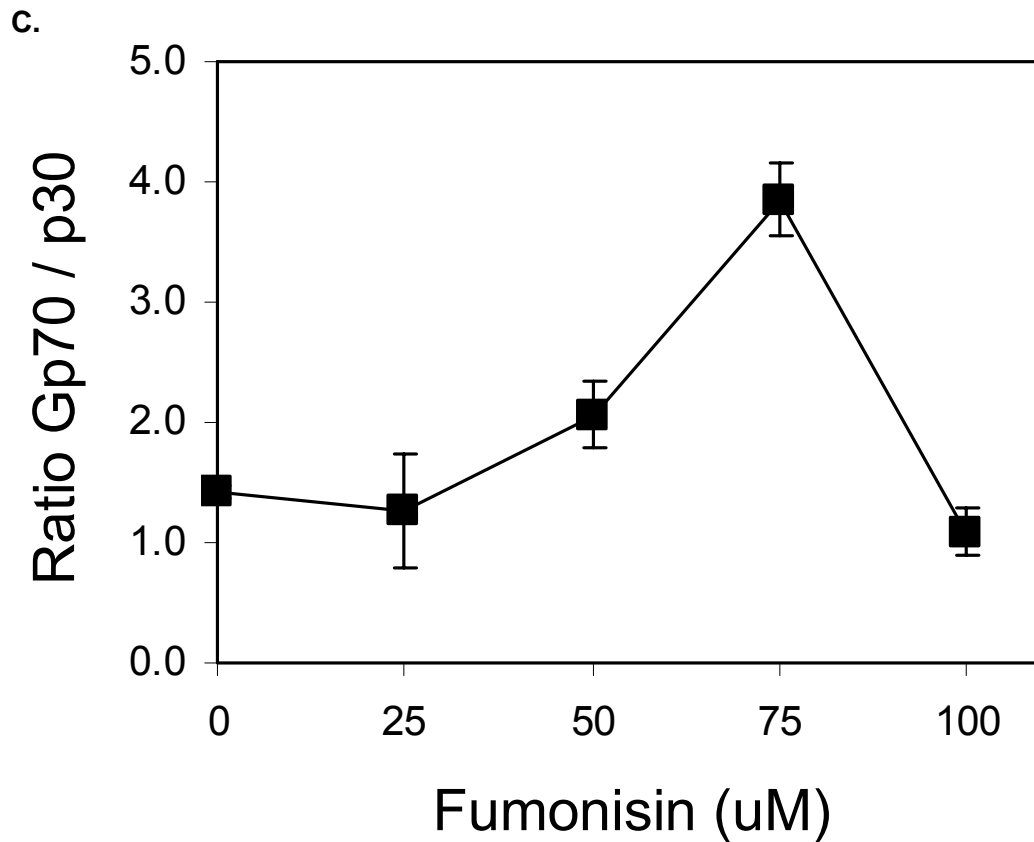


Figure 4.4 (C). Amount of gp70 proteins per p30 virus capsid protein. The gp70 virus fusion protein was normalized to the concentration of virus protein p30 (part A and B). TelCeB6, were plated at 240, 000 cells per well of a 6-well plate and grown to confluency. The next day, cell culture media was removed and replaced with media containing varying doses of FB-1 as indicated. After 24 hours, the conditioned cell media was collected and filter sterilized (0.45 μ m). The concentration of virus in the supernatant after treating virus producer cells with different doses of FB-1 was determined using the p30 ELISA and gp70.

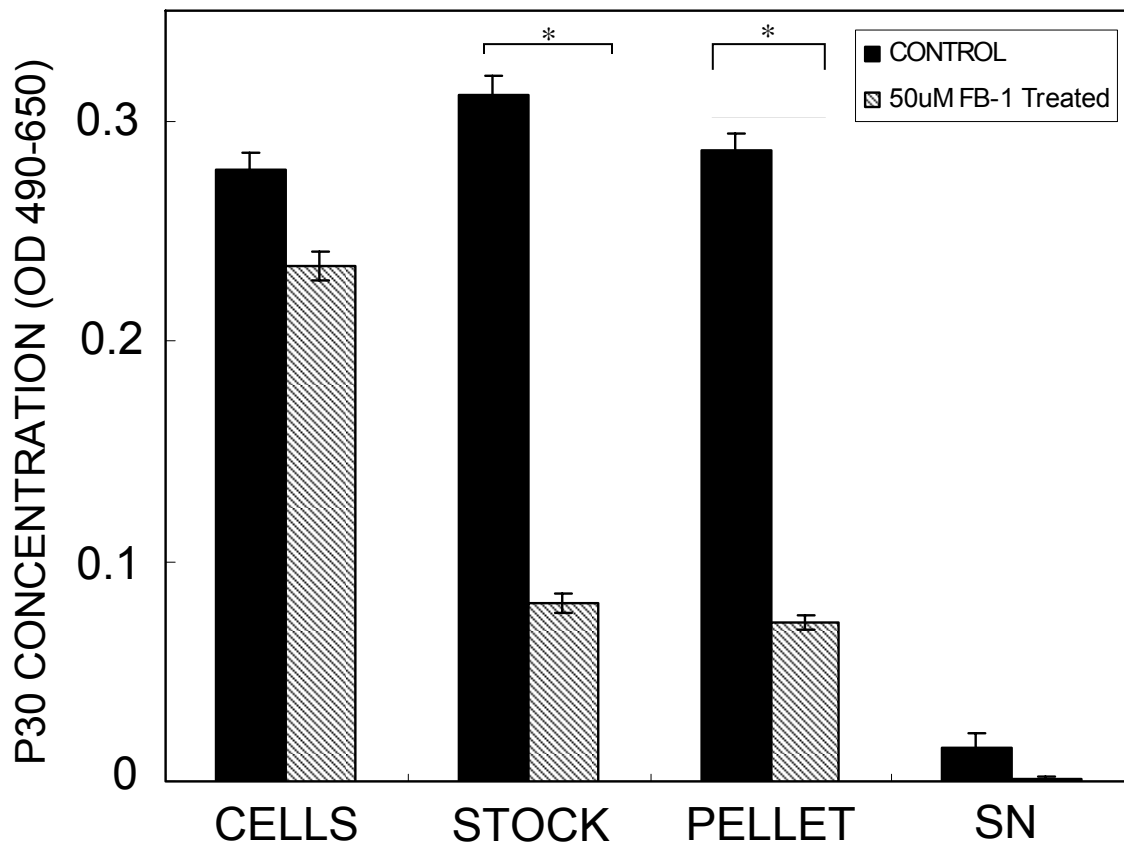


Figure 4.5. Fumonisin treatment affects the ability of virus to bud from target cell membranes. Telceb6-A cells were plated to confluence in 6-well tissue culture plates and cultured in DMEM/FBS media. The next day, the cells were treated with 50 μ M fumonisin B-1 or left untreated. The next day, the cell culture media was replaced with media containing 50 μ M fumonisin B-1 or 0 μ M fumonisin B-1. After 24 hours the supernatant was harvested, filter-sterilized (0.45 μ m), then frozen (-80 $^{\circ}$ C) for later use. An aliquot of the supernatant (STOCK) was collected and stored separately. After harvesting the supernatant the cells were washed with cold PBS and removed from the tissue culture plates using a cell scraper. The cells were then pelleted at 800 x g for 5 min and resuspended in 0.5% Triton-X to lyse the cells and expose the p30 antigen inside the cells. These cell lyses samples were used to measure p30 inside the cells using the p30 ELISA. Also, to measure pelletable virus, the virus stored supernatant was mixed with 80 μ g/mL of Polybrene and chondroitin sulfate-C, incubated for 20 min at 37 $^{\circ}$ C and centrifuged at 6000 x g for 20 min. The supernatant was collected and p30 in the samples was measured to determine the amount of unpelletable p30 (SN, supernatant). The pellet was resuspended in PBS and p30 was measured to determine the amount of pelletable p30 (PELLET). (*) denotes statistically significant differences between treated and untreated cells ($p < 0.05$).

and treated with FB-1 for 48 hours. Then virus supernatant was harvested (STOCK), centrifuged and pelleted using polybrene and chondroitin sulfate – C. The supernatant was collected (SN) and the pellet (PELLET) was resuspended in PBS and used in the p30 ELISA. The cells were washed with cold PBS, and removed from the tissue culture plates using a cell scraper. The cells were then centrifuged, counted and lysed to measure p30 protein. From these studies, we found that although virus producer cells contained similar amounts of p30 protein after FB-1 treatment, the viral supernatant had significant lower levels of p30. These results suggest that viral protein p30 is being produced inside the cells but lipid biosynthesis is interfering with its budding and release from the cell membrane.

To determine the effect of FB-1 treatment on virus infectivity, we treated a virus producing cell line (TelCeB6) with FB-1 (0 to 100 μ M) and harvested the virus supernatant after 24 hours. We measured virus titer on NIH 3T3 cells and HeLa cells using the β -gal assay (Figure 4.6 A-B). Our results suggest that the virus particles produced from the treatment were more fusogenic than particles produced from untreated cell. Specifically, we found that the virus titer increased by 2-6 fold depending on the dose of the treatment and the cell type. To determine whether the increase in virus infectivity was due to the production of more stable virus particles, we incubated virus at 37°C for up to 24 hours, after which we used samples from different time points to transduce NIH 3T3 cells (Figure 4.7). We found that there was no statistical difference between the half-life of FB-1 treated virus of 8.3 hours and that of the untreated virus 8.8 hours ($p < 0.05$) indicating that altering lipid content in the virus lipid bilayer does not affect the stability of the virus particles.

In order to determine the mechanism by which changes in the lipid content elicit a change in retrovirus transduction, we investigated retrovirus binding and fusion after FB-1 treatment. Initially, we incubated cells with increasing concentrations of virus

A.

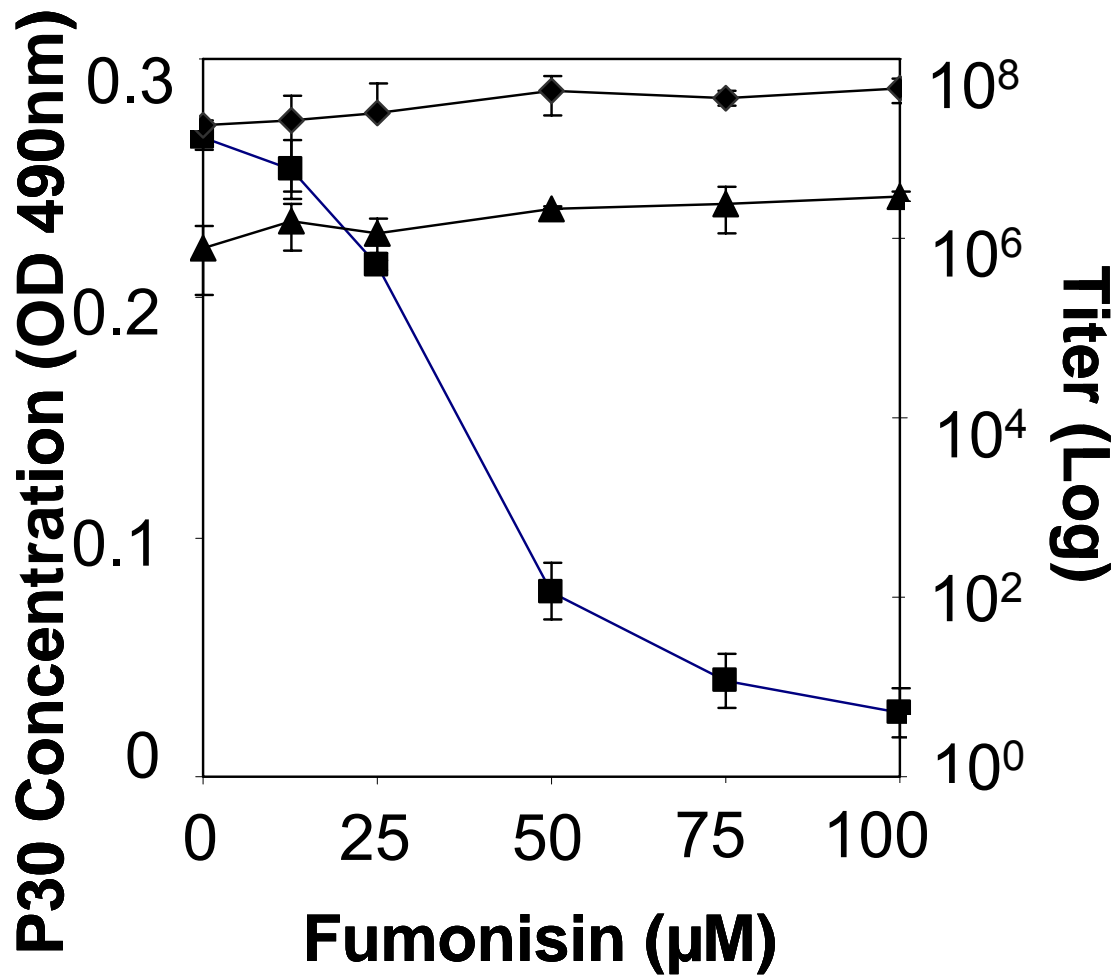


Figure 4.6 (A). Effect on virus production and infection after treating virus producer cells with FB-1. TelCeB6, were plated at 240, 000 cells per well of a 6-well plate and grown to confluency. The next day, cell culture media was removed and replaced with media containing varying doses of FB-1 as indicated. After 24 hours, the conditioned cell media was collected and concentration of p30 determined using the p30 ELISA. Same virus stock was used to measure titer. NIH 3T3 cells were plated at 60 000 cells per well and HeLa cells were plated at 80 000 cells per well of 12-well plates. The next day, the ten-fold serial dilutions of virus stock were made in DMEM/BCS for NIH 3T3 transduction or in DMEM/FBS for HeLa transduction, supplemented with Polybrene (8 µg/mL) and incubated with cells. Two days after the start of the transduction, the cells were fixed and stained for β-galactosidase activity with X-Gal. Colonies were counted with the aid of a dissecting microscope. At appropriate dilutions of the virus stock, the clusters of blue cells were sufficiently spread over the dish such that each cluster arose from a single transduction event. Each point shows the mean ± standard deviation of three replicates.

B.

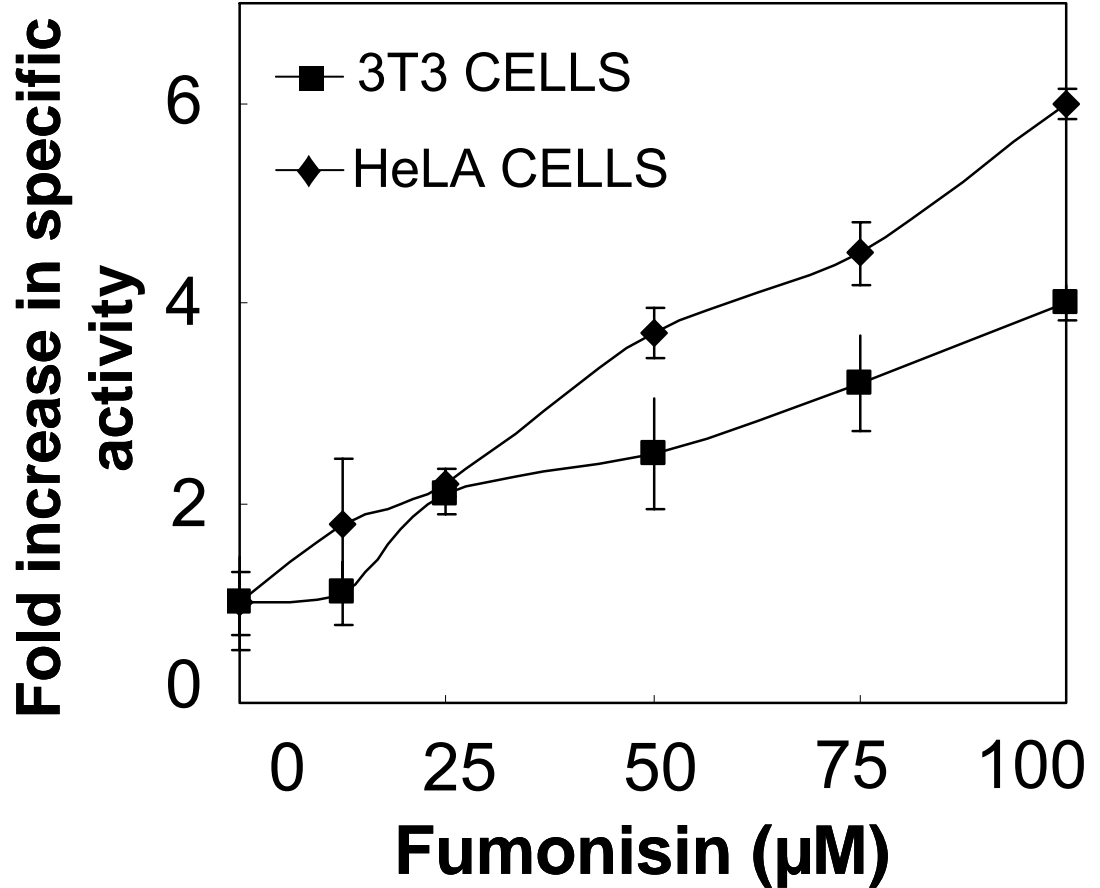


Figure 4.6 (B). Treatment of virus producer cells with FB-1 increases the titer of the virus produced from those cells. Titer data shown in Figure 4.6 was normalized to the respective p30 concentration and are reported here as fold-increase in specific activity. Virus stock was produced after various doses of FB-1 treatment of TeLceB6 cells. NIH 3T3 cells were plated at 60 000 cells per well and HeLa cells were plated at 80 000 cells per well of 12-well plates. The next day, the ten-fold serial dilutions of virus stock were made in DMEM/BCS for NIH 3T3 transduction or in DMEM/FBS for HeLa transduction, supplemented with Polybrene (8 µg/mL) and incubated with cells. Two days after the start of the transduction, the cells were fixed and stained for β-galactosidase activity with X-Gal. Colonies were counted with the aid of a dissecting microscope. At appropriate dilutions of the virus stock, the clusters of blue cells were sufficiently spread over the dish such that each cluster arose from a single transduction event. Each point shows the mean ± standard deviation of three replicates.

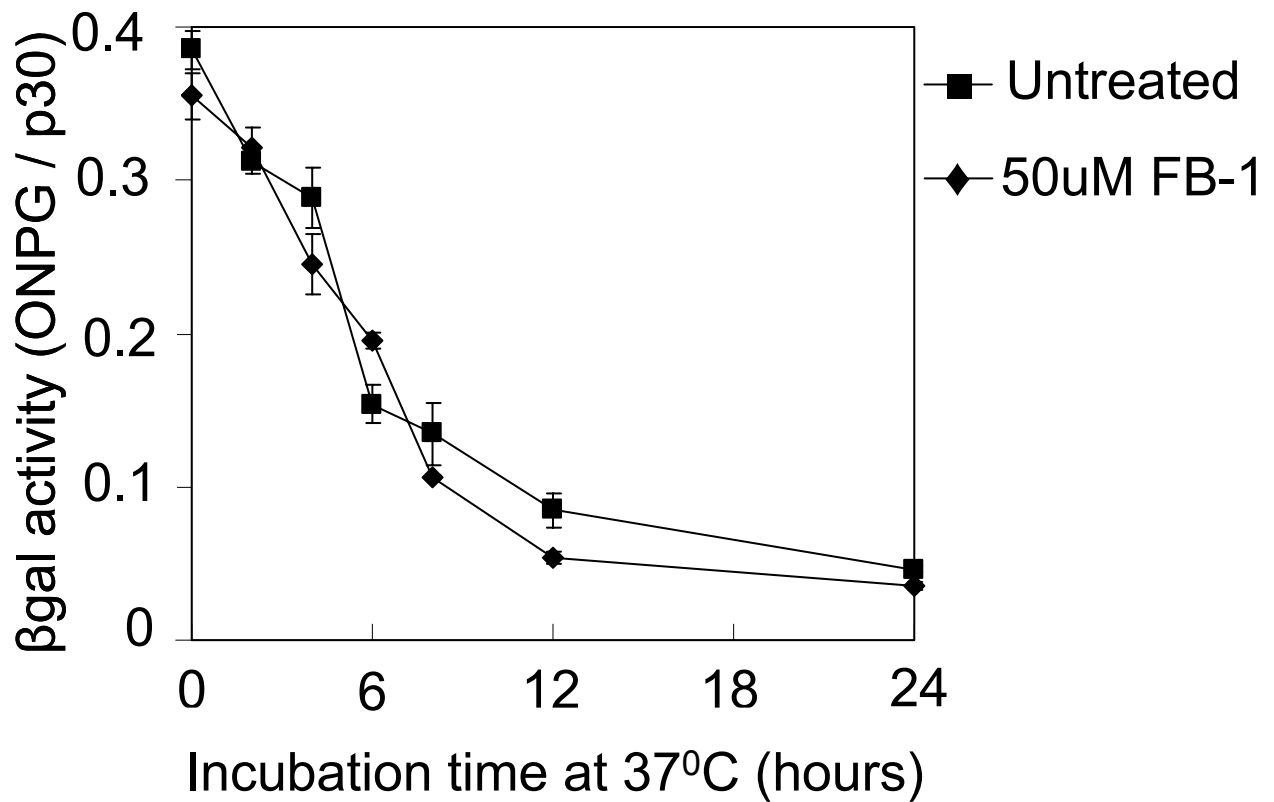


Figure 4.7. Stability of virus particles is not affected by fumonisin treatment. TelCeb6 cells were plated at 240 000 cells per well in 6-well plates. The next day, the cell culture media was supplemented with 0 or 50 μ M FB-1. After 24 hours, the virus supernatant was harvested and filter sterilized. Retrovirus (100 μ L) produced from FB-1 treated or untreated virus producing cells were incubated at 37 °C for 0 hr to 24 hrs. At indicated time points, a small aliquot was collected and stored (-80 °C) for later use. These aliquots were then later used to transduce NIH 3T3 to determine virus activity.

stock to determine the linear range of virus binding so as to avoid saturating virus particles on the cell surface (Figure 4.8 A). We incubated virus stock with NIH 3T3 cell or HeLa cells at 4 °C for 2 hours. The cells were then washed twice with cold PBS, lysed and p30 concentration was quantified. Our results revealed that even with 100% virus supernatant, we did not saturate the surface of target cells. Next, we conducted this assay to measure the extent of binding of virus particles that had been produced after FB-1 treatment (Figure 4.8 B). Our results indicated that untreated virus bound to both cell types to the same extent as FB-1 treated virus, suggesting that FB-1 treatment does not reduce binding of virus particles. Next, we used a nef-luciferase assay to measure the change in virus fusion (Figure 4.9). The pcDNA3-Nef-luc plasmid was transfected into virus producing cells, which were then treated with FB-1. Interestingly we found that the increase in virus titer occurred due to increased virus fusigenicity. In both cell types, we observed a 2 fold increase in infection at 25 µM FB-1 and a 4 to 6-fold increase at 100 µM for NIH 3T3 and HeLa cells, respectively. Altogether, this data suggests that depleting lipids by using FB-1 from virus particles significantly increased the infectivity.

The lipid composition of the target cell membrane is also known to be important for virus fusion and entry. To determine whether altering the lipid composition of target cells by FB-1 treatment could affect the infectivity of virus, we incubated target cells with virus, either produced from FB-1 treatment or not, in the presence of various concentrations of FB-1 (Figure 4.10 A-B). We then measured virus infectivity. We found that in the presence of FB-1 there was no significant difference in virus infection of NIH 3T3 cells. Interestingly, in similar experiments with HeLa cells we found that virus infectivity decreased by approximately 50% when cells were incubated with FB-1.

A.

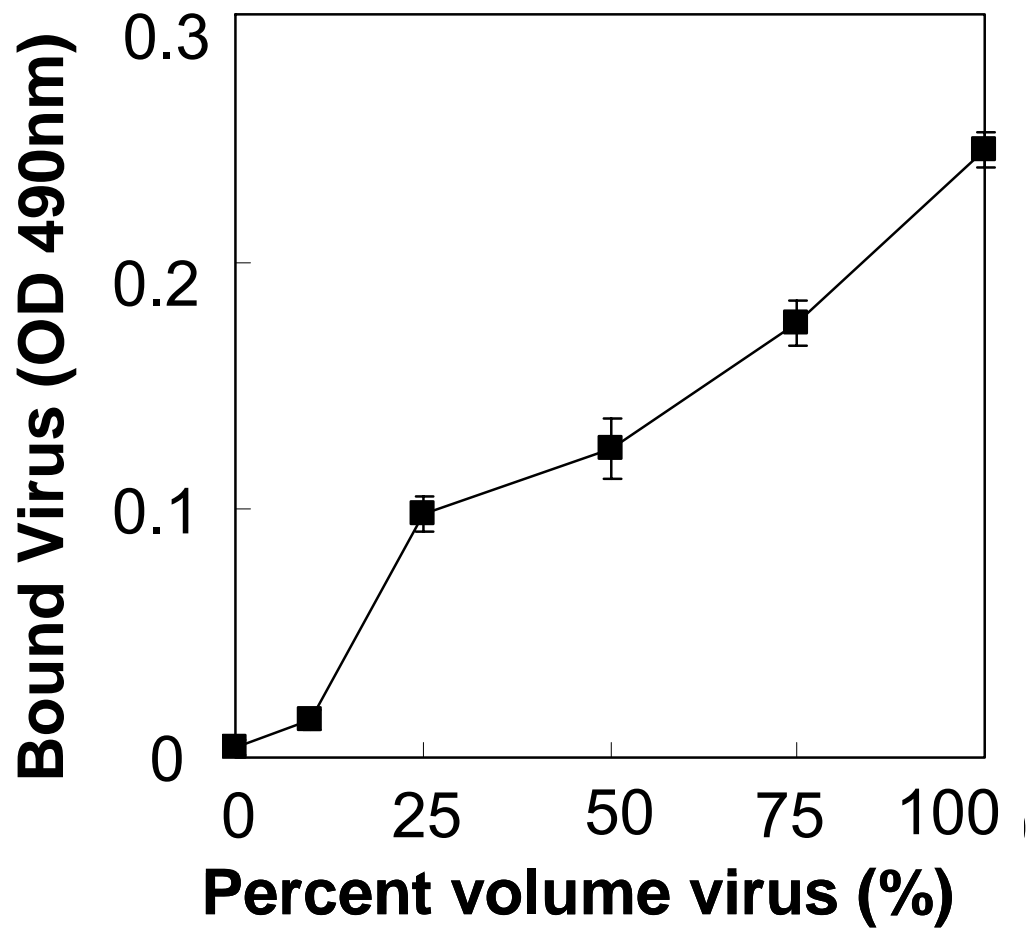


Figure 4.8 (A). Binding of virus particles to NIH 3T3 cells is not saturated at high concentrations of virus. NIH 3T3 cells were plated to confluence in 6 well plates. The next day different concentration of virus produced from TelCeB6 cells (virus producer cells) was incubated with NIH 3T3 cells at 4 °C for 2 hrs. The cells were washed twice with cold PBS, lifted from the wells using a cell scraper, centrifuged (800 x g for 5 min) and the pellet resuspended in lysis buffer. Cell lysis samples were then used to quantify virus protein using the p30 ELISA.

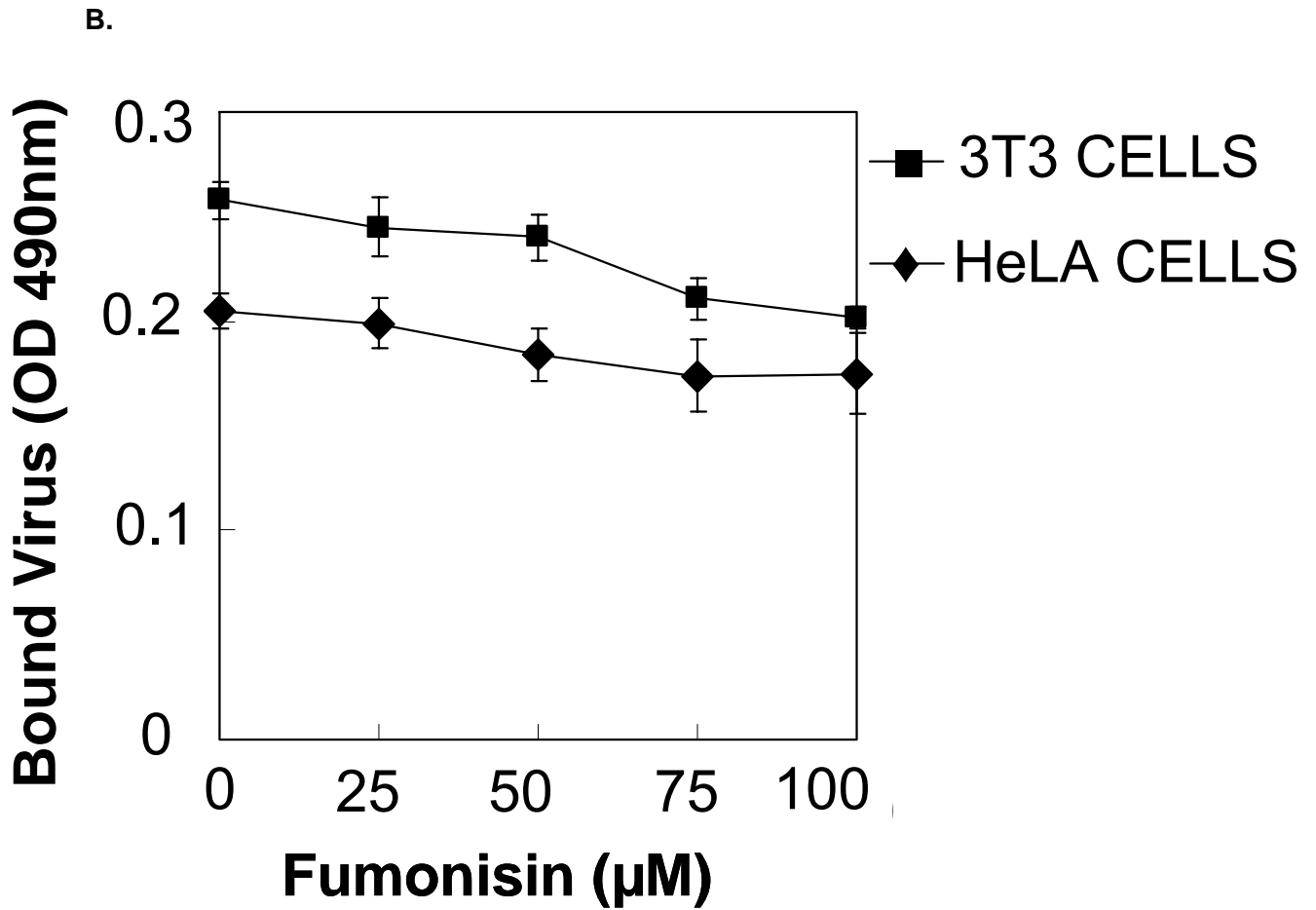


Figure 4.8 (B). Binding of virus particles produced from myriocin treated virus producer cells is not adversely affected. NIH 3T3 or HeLa cells were plated to confluence in 6 well plates. The next day virus produced after various concentrations of FB-1 treatment of virus producing cells, was applied to cells and incubated at 4 °C for 2 hrs. The cells were washed twice with cold PBS, lifted from the wells using a cell scraper, centrifuged (800 x g for 5 min) and the pellet resuspended in lysis buffer. Cell lysis samples were then used to quantify virus protein using the p30 ELISA.

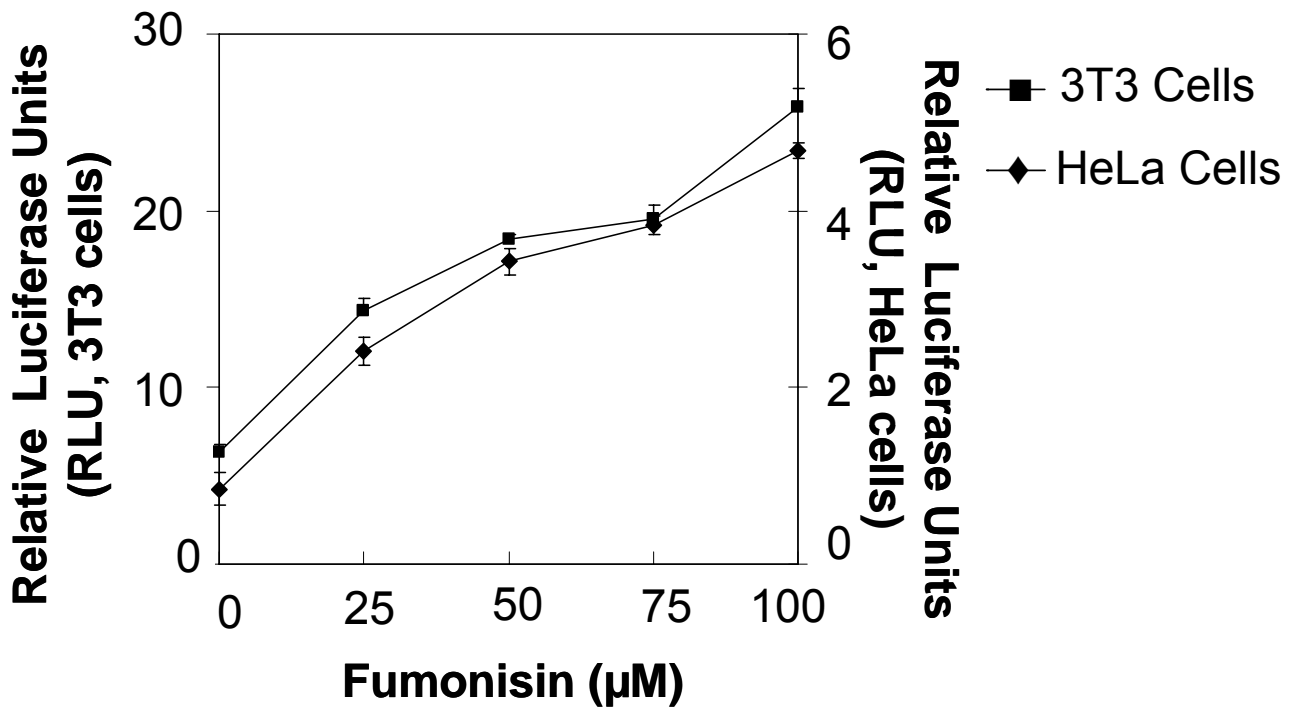


Figure 4.9. Virus particles produced by FB-1 treated cells fuse more efficiently with target cells. Telceb6-A cells were plated at approximately 80% confluency in 10-cm tissue culture dishes. The cells were transfected with 8 μg of pcDNA3-Nef-luc using Lipofectamine and added to the cells. The medium was replaced 6 hours later and replaced with DMEM/FBS. After 24 hours the supernatant was removed from the cells and replaced with media containing varying concentrations of FB-1. After 24 hrs of treatment, the virus-laden cell culture supernatant was harvested, filter sterilized (0.45-μm) and used to infect NIH 3T3 and HeLa cells. NIH 3T3 and HeLa cells were incubated with virus at 37 °C for 2 hrs on a rotating platform. After this, the cells were pelleted by centrifugation at 800 x g for 5 min, supernatant discarded, and the cell pellet washed twice in DMEM. The final cell pellet was resuspended in 0.1 mL of Luciferase Assay Buffer (Promega) and the luciferase activity was measured using a Turner Biosystems Modulus Microplate reader and expressed as relative luciferase units. This protocol is adapted from Saeed et al (20).

A.

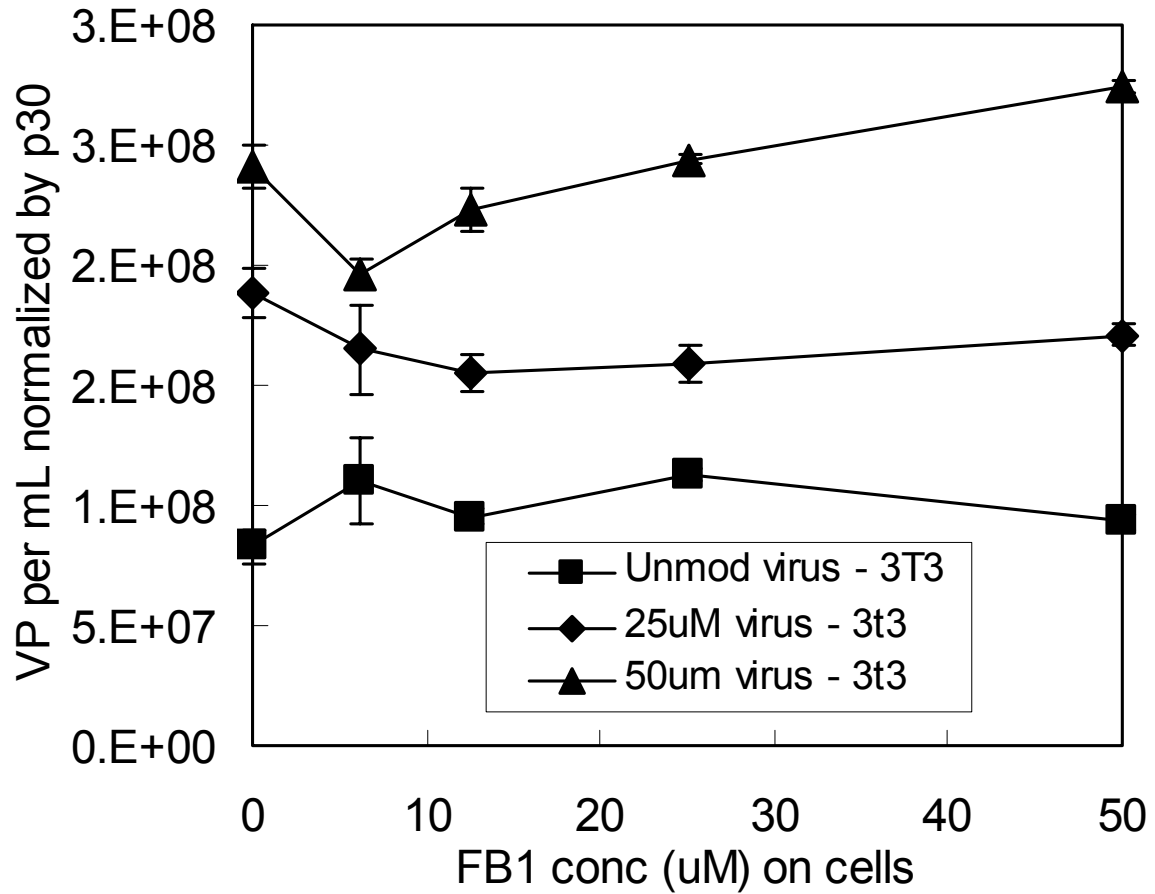


Figure 4.10 (A). Effect on virus infection after FB-1 treatment of NIH 3T3 cells. Virus was produced from the treatment of Telceb6 cells with FB-1 with concentrations of 0 μ M, 25 μ M and 50 μ M. After 24 hours the virus was harvested and diluted in a range of concentrations of FB-1, as indicated, and this mixture was used to transduce NIH 3T3 cells. NIH 3T3 cells had been plated at 5 000 cells per well of a 96 well one day earlier. Two days later, the ONPG assay was conducted to quantify the virus infection.

B.

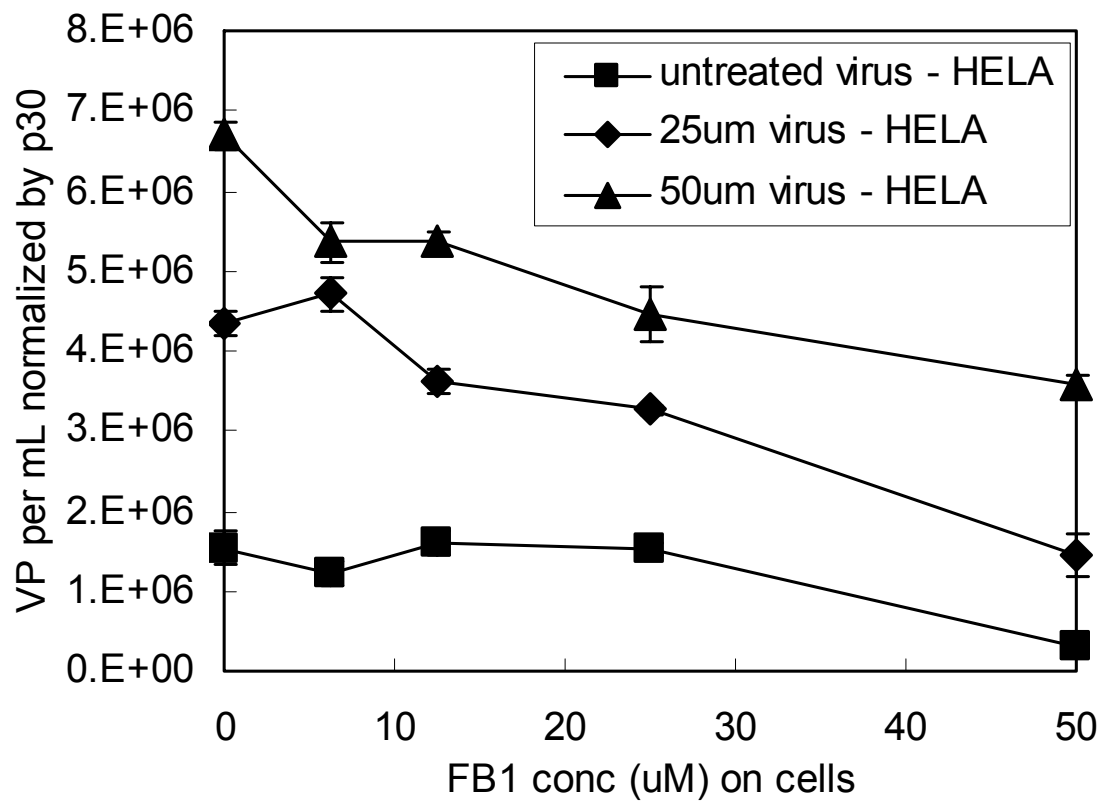


Figure 4.10 (B). Effect on virus infection after FB-1 treatment of HeLa cells. Virus was produced from the treatment of Telceb6 cells with FB-1 with concentrations of 0 μM , 25 μM and 50 μM . After 24 hours the virus was harvested and diluted in a range of concentrations of FB-1, as indicated, and this mixture was used to transduce HeLa cells. HeLa cells had been plated at 8 000 cells per well of a 96 well one day earlier. Two days later, the ONPG assay was conducted to quantify the virus infection.

4.5 Discussion

Previous studies have shown that inhibition of cholesterol synthesis in retrovirus producing cells or cholesterol extraction from target cells causes a significant decrease in virus production and infection. To test whether altering the levels of sphingolipids has a significant effect on MLV production and infection, we subjected virus producer cells to fumonisin B-1 (FB-1) treatment. FB-1 blocks de novo sphingolipid biosynthesis by inhibiting the synthesis of dihydroceramide, which is a precursor to all sphingolipid species, and by inhibiting the salvage pathway (19). First, we analyzed the effect of FB-1 treatment on the lipid composition of the cells. We found that there was significant reduction in the amount of sphingolipids in the FB-1 treated cells as compared to untreated cells. Specifically, reductions of 85% ceramide, 90% glucosylceramides, 60% sphingomyelin were observed. Furthermore, we purified and analyzed the virus particles from FB-1 treated cells and found that FB-1 treated virus particles exhibited a significantly reduced ratio of sphingolipids as compared to virus particles produced from untreated cells. Reductions of 30% in ceramides, 75% glucosylceramides, 30% sphingomyelin were observed for the different sphingolipids species. Since sphingolipids can have severe toxicity effects on cells, we measured cell viability of virus producing cells and the target cells used for infectivity assays (NIH 3T3 and HeLa cells) after they had been treated with FB-1. Our results indicated that cell viability was not affected by the treatment.

Next we analyzed the effect of FB-1 treatment on virus production and infection. Results from measuring virus capsid protein in stocks 24 hrs after FB-1 treatment indicate that FB-1 treatment of virus producing cells had a significant effect on virus production or release. At FB-1 concentration of 50 μ M, we observed 65% less production in virus capsid protein in the stock cultures. Furthermore, we observed a significant effect on specific infectivity of virus particles produced from FB-1 treatment.

Virus particles produced after 50 μ M FB-1 treatment showed a 2-fold increase in infectivity to HeLa cells and an increase of 3.6-fold infectivity in NIH 3T3 cells. Our results suggest there is a dose dependant increase in virus infectivity for both cell types.

Changing the lipid content of virus producing cells may also affect virus stability retroviruses are known to be enriched in specific lipid species, the removal of which makes virus particles inactive (such as cholesterol) (7, 17). For instance, depletion of cholesterol from virus particles or virus producing cells has shown to inactivate virus particles possibly by destabilizing the viral lipid bilayer (3). Our studies indicated that there was no difference in virus stability after FB-1 treatment and that both, viruses produced from untreated and treated cells decayed at similar rates. To further determine the increase in virus infectivity, we measured the effect of FB-1 treatment on virus binding to the target cells. Our results indicated that there is also no significant on the binding of virus particles. Lastly, we determined whether the increase in infectivity of virus particles occurred at the point where the virus membrane fuses with the target cell membrane. The results show that virus fusion increases as the dose of FB-1 treatments increased. These results indicate that depleting lipids from virus particles increased their infectivity by altering their ability to fuse with the target cell membrane.

Previous studies have suggested that virus budding sites are enriched in sphingolipids, such as sphingomyelin, thus disrupting sphingolipids synthesis may (7, 16). Thus, altering the synthesis in virus producing cells may alter virus capsid production or the production of virus envelope proteins, gp70. In our studies, we found that the production of p30 decreased as the dose of FB-1 treatment increased. Interestingly, the envelope protein production (gp70) increased with increasing doses of FB-1. This suggests that although there were fewer virus particles in the supernatant of virus producing cells, the virus particles after FB-1 treatment had greater number of gp70 proteins than viruses produced from untreated cells.

Retroviruses proteins have been shown to accumulate in intracellular vesicles, called multivesicular bodies (MVB) (8, 22). It has been implied that the MLV virus particles bud into MVB vesicles and then MVBs release the viral content to disseminate the virus particles. One theory is that viral Gag proteins, structural proteins of the viral nucleocapsid, are sorted directly from the Golgi where they interact with the envelope proteins via host cell effector proteins (such as TIP47) (1, 11). Interestingly, an alternate hypothesis to this theory is that retroviral proteins such as Gag and Env, all accumulate, assemble and bud from the plasma membrane. Recent studies by Jouvnet et al show time-lapse microscopy of HIV particles accumulating and budding from the plasma membrane (13, 14). These studies also showed that interfering with the endocytosis pathway of infected cells blocked the accumulation of HIV proteins in MVBs but did not interfere with virus release, further supporting the theory that retrovirus particles bud from the plasma membrane. Given our observations in the changes of virus producing cells after FB-1 treatment, it is possible that FB-1 treatment is interfering with the accumulation of viral proteins at the plasma membrane, and that although these proteins are produced by the cells, they are not able to bud as whole virus particles. Therefore, we examined the extent of the viral capsid protein production in virus producing cells after FB-1 treatment. Interestingly, our results indicated that FB-1 treatment interferes with the accumulation of viral proteins whether at the plasma membrane or in MVBs, and that although these proteins are produced by the cells, they are not able to bud as whole virus particles. Altogether, these results suggest that depleting sphingolipids using FB-1 from virus producing cells inhibits virus budding. Also, we found that blocking sphingolipid synthesis in virus producing cells affects virus production and fusion.

3.6 References

1. **Blot, G., K. Janvier, S. Le Panse, R. Benarous, and C. Berlioz-Torrent.** 2003. Targeting of the human immunodeficiency virus type 1 envelope to the trans-Golgi network through binding to TIP47 is required for env incorporation into virions and infectivity. *J Virol* **77**:6931-45.
2. **Brugger, B., B. Glass, P. Haberkant, I. Leibrecht, F. T. Wieland, and H. G. Krausslich.** 2006. The HIV lipidome: a raft with an unusual composition. *Proc Natl Acad Sci U S A* **103**:2641-6.
3. **Carmo, M., T. Q. Faria, H. Falk, A. S. Coroadinha, M. Teixeira, O. W. Merten, C. Geny-Fiamma, P. M. Alves, O. Danos, and A. Panet.** 2006. Relationship between retroviral vector membrane and vector stability. *J Gen Virol* **87**:1349-1356.
4. **Chan, R., P. D. Uchil, J. Jin, G. Shui, D. E. Ott, W. Mothes, and M. R. Wenk.** 2008. Retroviruses Hiv and Mlv Are Enriched in Phosphoinositides. *J Virol*.
5. **Chieco-Bianchi, L., M. L. Calabro, M. Panozzo, A. De Rossi, A. Amadori, L. Callegaro, and A. Siccardi.** 1989. CD4 modulation and inhibition of HIV-1 infectivity induced by monosialoganglioside GM1 in vitro. *Aids* **3**:501-7.
6. **Coffin, J. M., S.H. Hughes and H.E. Varmus.** 1997. *Retroviruses*. Cold Spring Harbor Laboratory Press.
7. **Hildreth, J. E., and Z. Liao.** 2001. Lipid rafts and HIV pathogenesis: Host membrane cholesterol is required for infection by HIV type-1. *AIDS Res Hum Retroviruses* **17**:1009.
8. **Hug, P., H. M. Lin, and J. M. Wang.** 2000. Glycosphingolipids promote entry of a broad range of human immunodeficiency virus type 1 isolates into cell lines expressing CD4, CSCR4, and/or CCR5. *Journal of virology* **74**:6377.
9. **Landazuri, N., and J. M. Le Doux.** 2004. Complexation of retroviruses with charged polymers enhances gene transfer by increasing the rate that viruses are delivered to cells. *J Gene Med* **6**:1304-1319.
10. **Landazuri, N., and J. M. Le Doux.** 2004. Complexation of retroviruses with charged polymers enhances gene transfer by increasing the rate that viruses are delivered to cells. *J Gene Med* **6**:1304-19.
11. **Lopez-Verges, S., G. Camus, G. Blot, R. Beauvoir, R. Benarous, and C. Berlioz-Torrent.** 2006. Tail-interacting protein TIP47 is a connector between Gag and Env and is required for Env incorporation into HIV-1 virions. *Proc Natl Acad Sci U S A* **103**:14947-52.
12. **Marandin, A., A. Dubart, F. Pflumio, F. L. Cosset, V. Cordette, S. Chapel-Fernandes, L. Coulombel, W. Vainchenker, and F. Louache.** 1998. Retrovirus-mediated gene transfer into human CD34⁺CD38^{low} primitive cells

capable of reconstituting long-term cultures in vitro and nonobese diabetic-severe combined immunodeficiency mice in vivo. *Hum Gene Ther* **9**:1497-511.

13. **Narayan, S., R. J. Barnard, and J. A. Young.** 2003. Two retroviral entry pathways distinguished by lipid raft association of the viral receptor and differences in viral infectivity. *J Virol* **77**:1977-1983.
14. **Nayak, S., H. Lee, J. Chmielewski, and L. A. Lyon.** 2004. Folate-mediated cell targeting and cytotoxicity using thermoresponsive microgels. *J Am Chem Soc* **126**:10258-10259.
15. **Ono, A., and E. O. Freed.** 2005. Role of lipid rafts in virus replication. *Adv Virus Res* **64**:311-58.
16. **Pickl, W. F., F. X. Pimentel-Muinos, and B. Seed.** 2001. Lipid rafts and pseudotyping. *J Virol* **75**:7175-83.
17. **Puri, A., R. Blumenthal, and A. Rein.** 2003. Modulation of entry of enveloped viruses by cholesterol and sphingolipids (review). *Molecular membrane Biology* **20**:243-254.
18. **Rawat, S. S., B. T. Johnson, and A. Puri.** 2005. Sphingolipids: modulators of HIV-1 infection and pathogenesis. *Biosci Rep* **25**:329-43.
19. **Riley, R. T., E. Enongene, K. A. Voss, W. P. Norred, F. I. Meredith, R. P. Sharma, J. Spitsbergen, D. E. Williams, D. B. Carlson, and A. H. Merrill, Jr.** 2001. Sphingolipid perturbations as mechanisms for fumonisin carcinogenesis. *Environ Health Perspect* **109 Suppl 2**:301-8.
20. **Saeed, M. F., A. A. Kolokoltsov, and R. A. Davey.** 2006. Novel, rapid assay for measuring entry of diverse enveloped viruses, including HIV and rabies. *J Virol Methods*.
21. **Smith, R. F.** 1994. *Microscopy and Photomicrography*, Boca Raton.
22. **Teissier, E., and E. I. Pecheur.** 2007. Lipids as modulators of membrane fusion mediated by viral fusion proteins. *Eur Biophys J* **36**:887-99.
23. **van Meer, G., D. R. Voelker, and G. W. Feigenson.** 2008. Membrane lipids: where they are and how they behave. *Nat Rev Mol Cell Biol* **9**:112-24.

CHAPTER 5

CONCLUSION AND FUTURE CONSIDERATIONS

5.1 Summary of results

In Chapter 2, we describe a new method for modifying the surfaces of retrovirus particles using lipid conjugates. The lipid conjugates consisted of a hydrophobic lipid anchor, 1,2-Distearoyl-*sn*-Glycero-3-phosphoethanolamine (DSPE), attached to a polymer linker, poly (ethylene glycol) chain which is covalently attached to the targeting functional group, biotin. These constructs, when mixed with a virus stock, associated with the virus surface in less than 2 hours. We used model replication-incompetent amphotropic retroviruses that encoded *lacZ* gene to investigate the characteristics of lipid conjugate modification containing biotin as a model cell-targeting group. We found that in less than 2 hours, the number of constructs that were associated with the particles reached a maximum. Even though the lipid conjugates were not covalently bound to the viruses, 25 % dissociated from the viruses after 8 hours of incubation at 37⁰ C in medium that contained 10% serum. Viruses modified with biotin conjugates bound to streptavidin-coated plates three-fold more than unmodified viruses. Importantly, virus titer experiments showed that the conjugates did not reduce the ability of the viruses to transduce cells.

In chapter 3 we investigated the use of fungal endotoxin, myriocin (ISP-1) to inhibit *de novo* sphingolipid synthesis in virus producer cells. We examine the effect on the lipid composition of virus producing cells and the virus particles produced from them. Since sphingolipids have been implicated in a variety of pathogens to help facilitate the entry process, we studied the effect of altering the lipid composition of virus particles on virus function. Our results suggest that the virus lipid composition can be significantly

altered by treating cells with ISP-1 and that these particles exhibit reduced infectivity in a cell-type dependant manner. Furthermore, the lipids of enveloped viruses play an important role in virus viral morphogenesis and infectivity, therefore we investigated different steps involved in the virus infection pathway and found that virus particles produced from ISP-1 treated cells are less fusogenic as compared to untreated cells. The implications of these results to improve gene therapy vectors and anti-retroviral therapies are discussed.

In chapter 4 we determined the effect of blocking sphingolipid synthesis by using fumonisin B-1 (FB-1) of virus producing cells and examined the effect on virus function. We found culturing virus producer cells in the presence of FB-1 leads to a drastic decrease in the levels of ceramide, sphingomyelin and glucosyphingolipids. Viruses produced with 50 μ M FB-1 treatment were observed to be as stable as, and bind to the same extent as viruses produced from untreated cells. Interestingly, virus from FB-1 treatment was 4 to 6-fold more infectious at doses of 100 μ M than controls virus particles. Interestingly, we found that FB-1 treatment interferes with virus budding and release from virus producing cells. Possible mechanisms for these observations are discussed.

5.2 Conclusions

In conclusion, we found that:

1. The surface of enveloped retroviruses can be altered with lipid conjugates. The modification is able to alter virus binding without reducing the ability of the viruses to infect cells.
2. Treatment of virus producer cells with ISP-1 decreased the concentration of sphingolipids in the lipid bilayers of the viruses they produced. The infectivity of these viruses was reduced in a cell-dependant manner.

3. The treatment of virus producer cells with fumonisin B1 decreased virus budding and increased the number of virus envelope proteins that were incorporated into the virus particles. The infectivity and fusogenicity of these viruses were higher than unmodified control viruses.

5.3 Future Considerations

In Chapter 2, we describe a novel strategy to alter the surface of virus particles using lipid-PEG conjugates tagged with biotin. We found that modified virus particles preferentially bound to a streptavidin-coated surface as compared to unmodified viruses and that the modification did not adversely affect virus infectivity. In Chapter 3 and 4 we investigated the role of lipids in virus binding and infection. We found that the treatment of virus producing cells with pharmacological agents can alter the composition of the virus lipid membrane, thereby affecting the ability of the virus' ability to fuse with cell membranes. Based on these findings on the role of lipids in virus function and targeting, we propose the following suggestions for future research:

1. First, future work should investigate the effect of changing the lipid anchor on the extent and stability with which lipid-conjugates associate with the virus surface. Virus particles should be modified using lipid anchors of different structure and length and visualized using electron microscopy to determine the effect on the physical interaction between the lipid conjugate and virus particles. Furthermore, some of our previous studies suggest that when modified viruses are incubated in the presence of human plasma (data not shown), the dissociation rate of the lipid conjugates from the virus surface was far greater than that in 10% serum in PBS. Therefore, this modification strategy will need to be adjusted for *in vivo*

applications and examining the effect of lipid type and structure of the lipid anchor will give insight into improving the lipid anchor design.

2. Second, future work should consider how the physical characteristics of the flexible linker would affect virus binding. One critical function of the flexible linker could be to shield the virus particle from binding to the membranes of non-target cell types. Since the first interaction of retroviruses with target cells is the non-specific adsorption of virus on the cell surface, possibly by via binding to proteoglycans and glycosaminoglycans on the cell surface, future work should investigate whether this PEG linker can be used to block virus particles from binding nonspecifically to these extracellular components. Virus modification using PEG coatings have been attempted before to provide a hydrophilic coat which increased blood circulation times and reduced the inflammatory response by the host immune system, without affecting the ability of viruses to infect cells. The effect of PEG chain length, and the use of branched PEG chains, should be explored and their effect on the extent of virus shielding investigated.

The effective length of PEG-chains and hence, the extent of shielding they provide, depends on the density of chains on the membrane surface and on the chain length. For instance, PEG₁₉₀₀ has a reported effective thickness of 6.5-7 nm at 9 mol% surface coverage, however at higher densities, 20 mol%, the PEG chains take on a fully-extend confirmation, with thickness of 15.8 nm. As stated earlier, the virus envelope protein extends approximately 10 nm from the virus surface and therefore, one would expect that using high coverage density may block the interaction between virus receptor and its cell receptor altogether. However, interestingly, *in vivo* tests have shown that adenoviruses pegylated with 20 kDa chains were able to successful infect cells, possibly because the

dynamic forces experienced by the particles *in vivo* is significantly different than *in vitro*. Therefore, it would be interesting to determine the extent of which nonspecific binding of virus particles can be blocked using the lipid conjugate, particularly *in vivo*.

3. For the future development of this strategy as a tool for creating targeted viruses, we must investigate the effect of using targeting moieties other than biotin. One potential strategy may be to use a ligand that preferentially delivers the viral vector to the site of diseased cells. For instance, new vessels in growing tumor tissue are formed by the secretion of collagen matrix to allow angiogenesis to occur. Previous studies have shown that viral vectors displaying the collagen-binding portion of the von Willebrand factor on their surface can selectively accumulate at tumors site *in vivo*. Although, this protein was originally known to facilitate adhesion of platelets to sites of injured epithelium, new insights into the biological process involved in tumor growth have led to its successful use in tumor tissue targeting. Thus far, three clinical gene therapy studies have shown partial responses and stabilization of the disease.
4. Treatment of virus producer cells with myriocin and fumonisin caused the production of virus with altered fusion properties. Our studies suggest that although virus particles are able to bind to cells, they become less fusogenic after myriocin treatment, and more fusogenic in response to fumonisin treatment. Thus, these results suggest that although both these pharmacological agents block de novo sphingolipid biosynthesis, the specific lipid species affected by these agents are different and thus elicit distinctly different responses in the virus producing cells.

Sphingolipid metabolism or catabolism in mammalian cells has many layers of complexity and many times, enzymes involved in these reactions are interconnected, regulating not only the levels of the individual bioactive sphingolipids species but also their metabolic intermediates. Many times, when a sphingolipid enzyme is implicated in a process, the direct product of this enzyme may not be the actual signaling effector. For instance, sphingomyelinase is an enzyme that converts sphingomyelin into ceramide as an immediate lipid product. Subsequent action of other enzymes such as ceramidase, sphingomyelinase synthase or glucosylceramide synthase can convert the ceramide signal to one that is mediated by sphingosine, diacylglycerol, or glucosylceramides, respectively. Therefore, it is difficult to implicate one specific lipid species. Therefore, in order to understand the specific mechanism behind the decreased fusigenicity after myriocin treatment, and increased fusigenicity after fumonisin treatment, we recommend that future work should investigate the effect on virus fusion and infection after exogenous addition of specific glycosphingolipids such as sphingomyelin.

5. Previous findings that used pharmacological agents to modify cellular lipid synthesis (such as methyl β -cyclodextrin, inhibitors of serine palmitoyltransferase, and other inhibitors of sphingolipid biosynthesis), showed that these agents can cause fluctuations in the intermediates involved in the lipid synthesis pathway, thereby affecting many different functions of the cell. Identification of lipid mediators involved in these functions has been difficult partially due to the hydrophobic nature of enzymes in sphingolipid metabolism and also because most of these sphingolipids are present at very low levels

inside the cell. To address these limitations, in these studies we use highly sensitive mass spectrometry methods for sphingolipid analysis. Furthermore, the poor solubility of sphingolipids for delivery of endotoxins or for exogenous addition into cells causes problems and many times delivery devices, such as albumin conjugates and cyclodextrin loading, must first be optimized and tested. Therefore, one suggestion to improve our current system of altering lipid content would be to use RNA interference.

6. We found that fumonisin treatment of virus producing cells increased the specific infectivity of retroviruses on NIH 3T3 cells and HeLa cells. Although there was a decrease in overall virus production, the infectivity of the virus particles produced from this treatment was significantly higher than viruses produced without fumonisin treatment. Since one of the major limitations with producing targeted retrovirus vectors is their decreased titer, future work should investigate whether treatment of virus producing cells with this pharmacological agent can be used to produce more fusogenic virus particles to increase virus infectivity for use in gene therapy protocols.

7. In the studies presented in this thesis (Chapter 3, Chapter 4), we observed a cell-type dependant effect of infectivity of virus with different lipid compositions. Future work should investigate whether this difference in infectivity can be used as a method of targeting viruses to one cell type versus another. One experiment of interest with the current system could be to co-culture NIH 3T3 cells and HeLa cells and determine whether the cell type dependant effect on infection is transferable when virus particles are exposed to both cell types. Initially, we hypothesized that the lipid composition of these two cell types might

differ significantly and that these differences might underlie the reason that the cell types differed in their susceptibility to infection by myriocin-treated viruses. Our lipid analysis suggests, however, that there were only slight differences in the levels of ceramides, glucosylceramide, and sphingomyelin present in the lipid bilayers of these cells. Therefore, future work should investigate the mechanism behind this cell type dependant decrease in infection, as exhibited by virus particles treated with myriocin, and whether this mechanism can be used to help produce viruses that are more infectious to clinically relevant cells types (such as hematopoietic stem cells, embryonic stem cells, breast cancer cells, neurons, etc.).

APPENDIX A.1

Experimental Protocol: Development of Biotin ELISA assay

Biotin-ELISA

1. Remove unreacted PEG chains
2. Make various dilutions of biotin-PEG-virus from a pre-determined conc of virus-titer.
3. Add samples to strep-avidan plates (96wells) with standard samples of specific concentration of biotin-PEG for **1hour, at 37°C.**

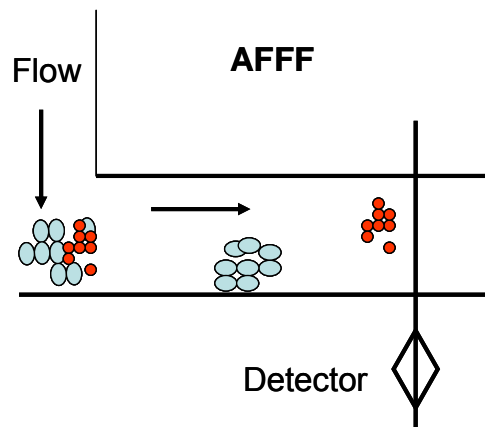
Make samples in Tris-buffered saline, TBS (pH 7.4) + 0.1% BSA.

4. Wash with 300ul TBS + 0.1% BSA + 0.05% Tween-20: wash 3x with 5 min incubation between washes at 15-25°.
5. Apply blocking buffer for **30min at 37°C;** 5% BSA + TBS
6. Incubate with anti-biotin POD Fab antibody at 1:1000 dilution for **1hour at 37°C.**
7. Wash plate with TBS + 0.1% BSA + 0.05% Tween-20; wash 3x with 5 min incubation between washes at 15-25°.
8. Add ABTS (Pierce)
9. Read at 405 nm on plate reader. May take 10-30 min to develop; add 0.5 % SDS for reliable endpoint measurement.

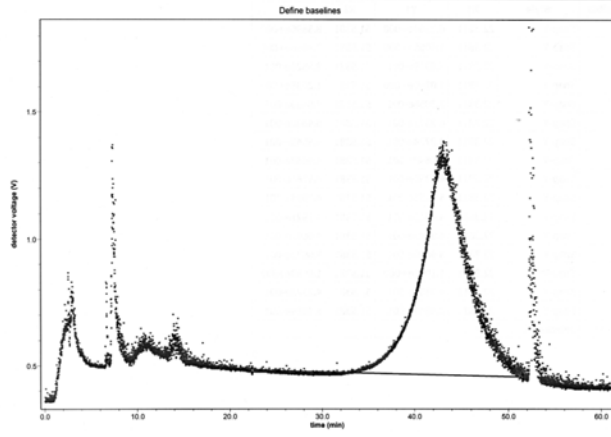
APPENDIX A.2

Radius of Gyration Approximations using Asymmetrical Field-Flow Fractionation

- We tried to approach this by measuring the radius of gyration using AFFF.
- In AFFF, a cross flow is used to push the colloids onto a membrane. Diffusion processes act against the external field so the colloids move towards the middle of the channel.
- An axial flow is then switched on allowing smaller particles to elute faster than the larger particles. A detector was set up to measure elution times and the radius of gyration was calculated. (SOFTWARE NAME)
- We took stocks of *lacZ* amphotropic retrovirus, mixed them with the lipid conjugate, and incubated for 2 hours at 4 deg. The unmodified control was incubated with TBS only.
- Polybrene was used to remove free lipid and the resulting pellets were analyzed using AFFF to measure radius of gyration, that is the radial distribution of mass of a particle. Elution time and focus flow rates were optimized to achieve good separation of the sample.
- Our data suggests that lipid modification increases radius of gyration.

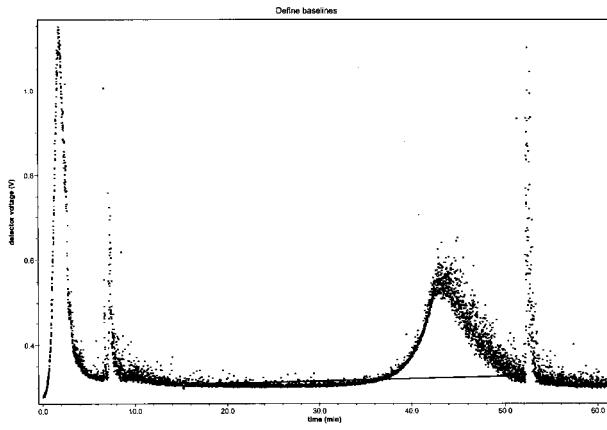


8-8-06.vaf\Procedures\Define baselines



$r_g = 89 \text{ nm}$

8-11-06.vaf\Procedures\Define baselines



$r_g = 98 \text{ nm}$

APPENDIX B

TECHNOLOGICAL INNOVATION: GENERATING ECONOMIC RESULTS (TI: GER®)

B.1 Project Description:

During my time at Georgia Tech, I had the opportunity to be admitted into the TI:GER program. This program is offered by the School of Management and is a collaboration between Georgia Tech and Emory University, School of Law. This is a one of a kind program that brings together PhD students, MBA students and Law students to create multifunctional teams to help them learn about the challenges of bringing their new technologies into the market. During this time, I had the opportunity to work with many talented students and meet many executives involved in different steps of the commercialization process. My team and I competed in three business plan competitions: New Ventures Business Plan Competition 2007 (2nd place winner), Lunar Ventures 2008 (1st place runner-up) and the Tyler New Ventures Business Plan Competition (3rd place winner). We had some success in raising funding and more importantly interest in this technology. Overall, this was a great opportunity to get first-hand experience in the challenges involved with start-up technologies.

B.2 Invention Description:

The present invention proposes a methodology for the manipulation of virus particles for their use in gene transfer, virus detection, virus targeting, evasion of the immune response, or any application which requires the modification of the surfaces of viruses.

The current invention uses retroviruses as the vehicle for gene transfer. Recombinant retroviruses are commonly used in gene therapy clinical trials because they can permanently integrate a therapeutic gene into the DNA of target cells, resulting in a long-term cure. Retroviral-mediated gene transfer can be used to treat inherited genetic disorders, complex genetic disorders, and infectious diseases, and has

numerous applications in tissue engineering. One major shortcoming of virtually all methods of gene transfer is the inability to strictly control their tropism, the types of cells to which they are able to transfer genes. For many applications, particularly for most in vivo gene therapies, the tropism of gene transfer vectors needs to be narrowed so that genes are transferred only to the cells and tissues of interest and to no others. For other applications, such as in cystic fibrosis gene therapy, the tropism of gene transfer vectors needs to be expanded so that genes can be transferred to the cell types of interest.

The current invention uses a novel tripartite system to increase the specificity with which viruses bind to target cells. First, a lipid based conjugate allows for quick and efficient integration into the virus surface, which is composed of a lipid bilayer. Second, the polyethylene glycol (PEG) linker allows for the increased biocompatibility of the virus such that the virus particles are able to evade a large immune response. Third, a specific ligand attached to PEG molecules allows for increased targeting capabilities such that the virus only interacts with cells that exhibit a complimentary receptor. This ligand will be disease dependant and may change depending on the desired dose of 'genes' that need to be delivered. This tripartite system, a lipid conjugated to a PEG molecule with a specific ligand, will be reacted with virus particles so the virus' tropism is affected.

B.3 Executive Summary:

ViraTag LLC is a start up venture and our goal is to bring our patent-pending technology into the viral diagnostic market to facilitate the rapid detection of human viral infections in plasma. ViraTag's first product launch will be a kit for diagnosing the HIV virus. Our patent pending technology will be incorporated into an HIV Diagnostic Kit that will set the standard for next generation HIV diagnostics.

As of today, doctors using HIV kits on the market are not able to diagnose a patient with HIV until six months after exposure to the virus. ViraTag's HIV Diagnostic kit will allow accurate detection of HIV four times faster, giving patients the ability to seek

treatment earlier, have a better quality of life, and stop the spread of HIV, while saving the healthcare industry billions of dollars. ViraTag provides an exciting investment opportunity for any potential investor.

- **The Opportunity:** Today, if a patient goes to the doctor a day after being exposed to the HIV virus, the doctor will tell them, “Come back in six months to be tested.” The use of ViraTag’s HIV diagnostic will allow a doctor to tell the patient “Come back in six weeks to be tested.” Currently, the HIV diagnostic kits in the market are not sensitive enough to detect HIV early in the infection cycle. Yet, patients need to learn of HIV infection early in the infection cycle in order to have a better quality of life and to avoid spreading the virus. As a result, doctors and commercial laboratories need the ability to diagnose individuals with HIV as early as possible, and they need the kits to be cost-effective. Moreover, governments, the healthcare industry, and insurance providers will reap the benefits of early detection. Studies show that early detection of HIV will save these parties billions of dollars.
- **ViraTag’s Solution:** ViraTag patent-pending technology can diagnose the presence of viruses like HIV with a 17-fold increase in sensitivity, a ten-fold reduction in costs, and an overall reduction in the time it takes to conduct the test from 6 – 8 days down to 30 minutes without the use of highly trained personnel. This means that ViraTag Diagnostic Kits can detect the HIV virus starting at **six weeks into the infection cycle**, while reducing costs from \$200 dollars per kit to \$10 per kit and saving labor costs associated with highly trained technicians.
- **The Competition:** ViraTag’s competition is relatively strong. Roche holds a dominant position with respect to molecular testing of HIV in the US at about 50% of the market. Chiron is also developing a molecular test for HIV but is currently available for use in a research setting only. Minor competitors include Abbott,

J&J, and Beckman Dickinson, with a combined 40% of market share. Affymetrix is a recent entry to the market. It has a proprietary technology called GeneChip which detects HIV strains. But Affymetrix's technology is only being used in a research setting, though we are watching it closely. Since a high degree of biological information can be gained from GeneChips, they are likely to have a major impact on the way HIV is clinically managed.

- **The Technology and ViraTag's Competitive Advantage:** ViraTag's diagnostic kits are based on a proprietary, patent-pending technology that specifically and accurately tags viruses so they can be identified if present in blood samples. The viruses are tagged with a fluorescent marker that is observable under a microscope. Our competitive advantage lies in the fact that we will be a first mover with enforceable intellectual property.
- **The Market:** ViraTag's target market is people who have potentially been exposed to the HIV virus. These people are typically between the ages of 18 and 49. We are initially targeting developed nations, including the U.S, Europe, China, and India, but will target developing nations as we expand our market share. In vitro Diagnostics is a \$45 billion market. Within this market, the HIV diagnostics market is worth \$8.57 billion and is rapidly growing at a Compound Annual Growth Rate of 17.79%. In the U.S., 60 million HIV tests were administered last year. Additionally, this is an ideal time for entry of an innovative HIV diagnostics product in the market because the patent on the current dominant technology has recently expired.
- **Marketing Strategy and Business Model:** In this industry, it is typical for emerging companies like ViraTag to a first partner with a global diagnostics company—an alliance partner—for regulatory navigation, manufacturing, and product distribution. Therefore, we will generate a prototype, and will outsource

manufacturing to a business partner. Based on this marketing strategy, we conservatively estimate our market penetration at 7% (partnering with Abbott), but we are optimistic that our target penetration will approach 50% (partnering with Roche). ViraTag shall follow this business model for the HIV kits. However, once ViraTag has a footing in the HIV market, we will manufacture our own diagnostic kits for viruses like Hepatitis C and B with the cash inflow generated from the HIV kits.

- **Risk and FDA Approval:** ViraTag's diagnostic kits fall into the Category II of FDA in vitro diagnostic kits, one category above items like band-aids. ViraTag will work with an alliance partner to complete the approval process in between nine to twelve months.